Technical Report Documentation Page

1. Report No.	2. Government Accession No.	3. Recipient's Catalog No.
TX-98/2968-S		

4. Title and Subtitle	5. Report Date
INNOVATIVE MATERIALS AND DESIGN OF SOUNDWALLS	October 1997
	6. Performing Organization Code

7. Author(s)	8. Performing Organization Report No.
Paul N. Roschke, H.-Y. Yeh, and Steven Esche	Research Report 2968-S

9. Performing Organization Name and Address	10. Work Unit No. (TRAIS)
Texas Transportation Institute The Texas A&M University System College Station, Texas 77843-3135	11. Contract or Grant No. Study No. 7-2968

12. Sponsoring Agency Name and Address	13. Type of Report and Period Covered
Texas Department of Transportation Research and Technology Transfer Office P. O. Box 5080 Austin, Texas 78763-5080	Project Summary: September 1995 - August 1997
	14. Sponsoring Agency Code

15. Supplementary Notes

Research performed in cooperation with the Texas Department of Transportation.
Research Study Title: Innovative Materials and Design of Soundwalls

16. Abstract

This report documents a study of the feasibility of using soundwalls constructed of recycled plastics in place of conventional building materials. Important considerations in selecting materials used in this study include: environmental impact, acoustics, aesthetics, performance, safety, and cost. Various recycled materials were solicited from commercial manufacturers and subjected to a number of laboratory and field tests. These tests include three-point bending tests, impact hammer excitations, and exposure to different types of weather. Based on those results, several of the most promising materials were selected for construction of a full-scale field installation of a test section of a soundwall. This field section was monitored for a period of one year for response to environmental factors such as wind and exposure to ultraviolet radiation. Analysis of the field structure includes system identification of dynamic characteristics, finite element simulation, and acoustic performance.

Results show that noise insertion loss of the soundwall is exceptional. Structurally, the prototype soundwall performed adequately over the course of the project with only a few members showing detrimental effects from the harsh thermal environment. System identification and experimental analysis of test data were successfully implemented and indicate that the prototype soundwall is moderately wind sensitive. A finite element model of the soundwall was developed to simulate both static and dynamic response to loads. Using methods of modal superposition and random response, deflection was predicted for the top of the wall due to application of a strong wind event.

17. Key Words	18. Distribution Statement
Acoustic, Fiberglass Reinforced Plastic, Finite Element, Noise Abatement, Plastic, Random Response, Reclaimed Material, Sound Barrier, Soundwall, Wind	No restrictions. This document is available to the public through NTIS: National Technical Information Service 5285 Port Royal Road Springfield, Virginia 22161

19. Security Classif.(of this report)	20. Security Classif.(of this page)	21. No. of Pages	22. Price
Unclassified	Unclassified	180	

INNOVATIVE MATERIALS AND DESIGN OF SOUNDWALLS

by

Paul N. Roschke
Associate Research Engineer
Texas Transportation Institute

H.-Y. Yeh
Associate Professor
Prairie View A&M University

and

Steven Esche
Graduate Research Assistant
Texas Transportation Institute

Research Report 2968-S
Research Study Number 7-2968
Research Study Title: Innovative Materials and Design of Soundwalls

Sponsored by
Texas Department of Transportation

October 1997

TEXAS TRANSPORTATION INSTITUTE
The Texas A&M University System
College Station, Texas 77843-3136

IMPLEMENTATION STATEMENT

This report summarizes results of a research program that evaluates use and performance of recycled materials in a full-scale sound barrier. Opportunities for implementation of this research are as follows:

1. The Texas Department of Transportation (TxDOT) could contract for a recycled material manufacturer to construct a soundwall for a trial installation along a state highway in Texas. While this installation was built and tested at the Riverside Campus of Texas A&M University for a period of one year, there was little response from the public regarding aesthetics and acoustic effectiveness of the noise barrier. An evaluation of the performance and feasibility of its use could be made after two years of field observation by citizens, TxDOT engineers, and local officials. If in-service performance is judged to be satisfactory, the prototype soundwall design could be upgraded to the status of being an acceptable alternative to conventional soundwall designs that use masonry and concrete.
2. A set of design procedures could be developed that allow the selection of foundation sizes, dimensions of structural members, and material properties based on the projected height of the soundwall as required by acoustic and environment considerations of the site. Wind load provisions are expected to control the design. Focus of soundwall design procedures could be placed on limiting deflection of the recycled plastics in the barrier. To answer concerns related to wind sensitivity of the soundwall, a relatively sophisticated method of analysis such as finite element modeling could be integrated into the design procedure. Parametric tests could also be conducted with the finite element model to estimate dynamic response of the soundwall to design wind events.
3. A full-scale crash test could be conducted to determine the degree of effectiveness in resisting penetration by an errant vehicle.

ACKNOWLEDGMENT

This study was conducted under a cooperative program between the Texas Transportation Institute, the Texas Department of Transportation, and the Federal Highway Administration. The comments and suggestions of Melissa Montemayor and Rebecca Davio, who worked closely with the researchers, are highly appreciated.

Researchers are especially grateful for use of a plot of land at the National Geotechnical Site at the Riverside Campus of Texas A&M University. Access to a water supply, electricity, trailer storage, and an impact hammer was generously supplied by Prof. Jean-Louis Briaud. Material suppliers that donated material include Plastic Pilings, Lee Composites, and Pelletech, Inc.

Special thanks also goes to Dr. Jer-Nan Juang of NASA Langely Research Center who supplied software and worked with the researchers on system identification of the soundwall structure and to Prof. Kishor C. Mehta, Prof. Douglas A. Smith, and the Wind Engineering Research Center at Texas Technological University who provided wind data.

TABLE OF CONTENTS

TABLE OF CONTENTS (CONTINUED)

TABLE OF CONTENTS (CONTINUED)

TABLE OF CONTENTS (CONTINUED)

TABLE OF CONTENTS (CONTINUED)

LIST OF FIGURES

LIST OF FIGURES (CONTINUED)

LIST OF FIGURES (CONTINUED)

LIST OF FIGURES (CONTINUED)

LIST OF TABLES

1. INTRODUCTION

1.1 BACKGROUND

Sound barriers, or soundwalls, exist primarily to reduce noise detected by people living and working near roadways that have high-volume or high-speed traffic. As structural elements, these barriers must exhibit both durability of materials and safety for motorists, while maintaining their capability to reduce noise. Materials such as wood, concrete, and masonry block are currently used in noise abatement systems throughout the United States (Armstrong 1996). Figure 1 demonstrates an example of the use of masonry concrete in a sound barrier in Jersey Village, Texas.

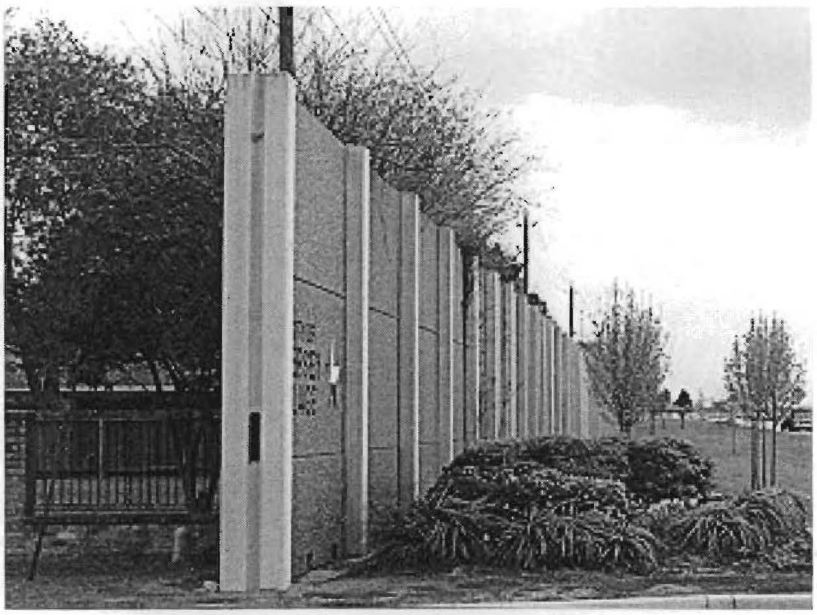

Figure 1. Typical Texas Soundwall

In recent years, motivation for finding new, recycled materials to construct these structures has increased due to decreasing space for landfill. This dilemma has spawned an industry that produces a variety of innovative materials. More specifically, the notion of using recycled plastic in place of more traditional materials such as concrete and steel appears to be a possible solution to the growing waste problems that society faces today. To the extent that recycled materials can be manufactured into an effective and economical

barrier that meets noise reduction standards and aesthetic requirements, an opportunity exists for transportation agencies to decrease landfill requirements and increase living standards for people who live or work near a roadway.

Aesthetics of sound barriers is an important concern. Figure 2 shows a portion of a soundwall that is observed from a residential neighborhood. Although motoring traffic sees a pleasant wall surface, this view does not necessarily provide an appealing sight for the permanent residents. Ideally, aesthetic concerns need to be considered for viewers on both sides of the wall.

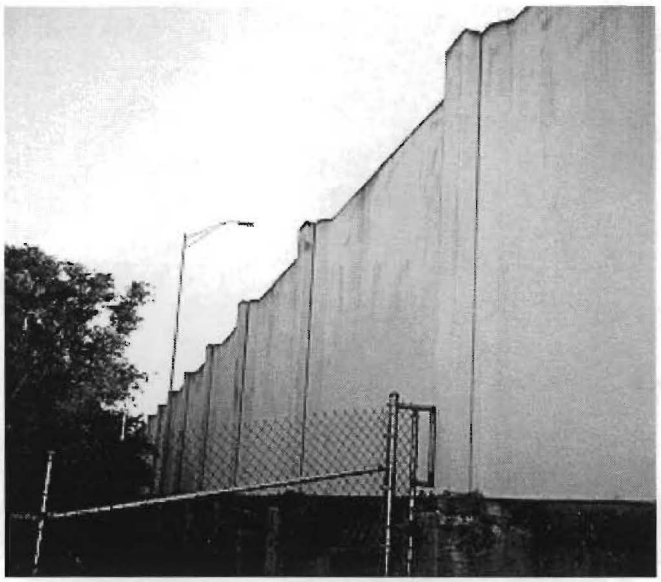

Figure 2. View of Backside of Masonry Soundwall

Many previous attempts to use recycled plastic materials as major structural members have failed due to unfavorable viscoelastic properties. Creep, splitting, and excessive bending are several issues related to structural performance that need to be considered. Introduction of new recycled materials in recent years has produced a variety of improvements that now allow them to be candidate materials for application in road signs, traffic barriers, and absorption systems (Bligh et al. 1995; Hag-Elsafi et al. 1996; Roschke et al. 1995). Complex polymers are being mixed with high-strength materials such as steel and fiberglass to improve mechanical properties. This reduces problems generally associated with semi-flexible plastics.

The aim of this research project is to conceptualize, design, build, and test a soundwall that incorporates a significant amount of recycled materials. Moreover, this system needs to be structurally resilient to both wind loads and long-term weathering. To the extent that it is successful, the public will have an alternative type of sound barrier that substantially reduces noise in residential and commercial neighborhoods and is aesthetically pleasing.

1.2 SCOPE OF STUDY

This project can be subdivided into a number of individual tasks. Initial efforts are to review archival literature and survey current approaches of governmental agencies related to the use of recycled materials in sound barrier design. A number of recycled materials manufacturers are also contacted to procure sample materials. Viable candidate materials for sound barrier construction in Texas are then chosen based on their material properties, constructabiliy, and cost. After suitable materials and structural designs are obtained, full-scale sections of the soundwall are built for testing in the laboratory and in the field.

The review of archival literature serves two purposes. First, it summarizes current advances made in recycled material soundwall design as well as changes in design and testing guidelines. Second, it also allows the researchers to focus on areas lacking detailed investigation, especially those affiliated with performance of recycled materials in sound barriers.

The design phase of this project applies laboratory and field tests to determine the working behavior and modes of failure of recycled materials in sound barriers that are selected as having a high potential for successful application. Fundamental properties such as modulus of elasticity, density, and material composition are gathered for each of the materials from their respective manufacturers. After an initial screening process, materials are solicited from manufacturers for static and dynamic testing. These tests include three-point bending tests and impact hammer excitations. Exposure to high temperatures and ultraviolet rays also serves to disclose any propensity for thermal warping. Initial designs

for the prototype soundwall are based on mechanics of materials bending formulae in which environmental loads are taken from the ASCE 7-95 "Minimum Design Loads for Building and Other Structures" (1995) and AASHTO "Guide Specifications for Structural Design of Sound Barriers" (1989). Design criteria focus on limiting deflection due to lateral wind loading.

Culmination of the design phase was construction of a full-scale field model at the Texas A&M Riverside Campus that incorporates combinations of promising materials (see Figure 3). The prototype barrier is 3.66 m (12 ft) tall and 29.28 m (96 ft) long. The structure is monitored for almost one year while a number of acoustic and dynamic tests are performed to determine weatherability, wind sensitivity, and acoustical effectiveness of the barrier.

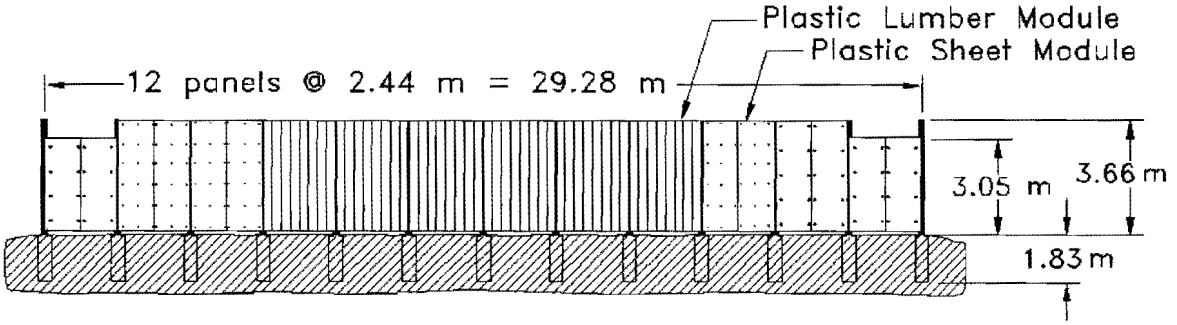

Figure 3. Elevation View of Prototype Soundwall and Foundation

2. REVIEW OF LITERATURE

2.1 BRIEF HISTORY

Environmental specialists, transportation officials, and engineers have focused a great deal of attention on the environmental impact of pollution caused by highway-generated noise. In an attempt to contain this type of sound pollution, national and state agencies have implemented systematic construction of noise barriers.

It is estimated that in 1995 over 183 km (114 miles) of noise barriers, or soundwalls, were constructed at a total cost of $141,000,000 (Armstrong 1996). Although this type of construction first became prominent in the late 1980s, noise barriers were actually introduced in the early 1970s. There was steady advancement in barrier innovation as engineers, architects, and contractors relied on local building codes and "Standard Specifications for Structural Supports for Highway Signs, Luminaires, and Traffic Signals" for specification and design criteria (AASHTO 1975). In an effort to summarize expertise gained during this period, the National Cooperative Highway Research Program published "Synthesis of Highway Practice 87 - Highway Noise Barriers" (Cohn 1981). In 1985, "Review of Structural Design Criteria for Noise Walls" was introduced to review structural design criteria and practices of that period (Basu and Akhter), while the first true standard for soundwall design was promulgated in 1989 when AASHTO developed "Guide Specifications for Structural Design of Sound Barriers."

2.2 RESEARCH TOPICS

Concomitant with increased construction of noise barriers, the early 1990s spawned a new industry that produced structural members that contained significant amounts of recycled plastic materials. Only in the past few years have these materials been considered for use in noise barriers. This review focuses on application of recycled plastics in construction of sound barriers. Products made from rubbers are of less interest because they have been known to leach toxic chemicals into the environment and are much heavier

than typical plastics. Recycled glass, on the other hand, lacks resiliency to abrasion and impact forces that are associated with transportation related systems.

Several research interests associated with the use of recycled plastics in sound barriers include acoustic behavior, aesthetic potential, structural integrity, and constructibility of recycled plastic soundwalls. Figure 4 shows an example of a recycled plastic soundwall tested by the Oregon Department of Transportation. With respect to constructibility, it was concluded that recycled plastics are heavier than typical lumber and that wall panel boards with shiplap joints may not lock sufficiently to prevent bowing. The project report did not mention aesthetic or acoustic potential of the barrier.

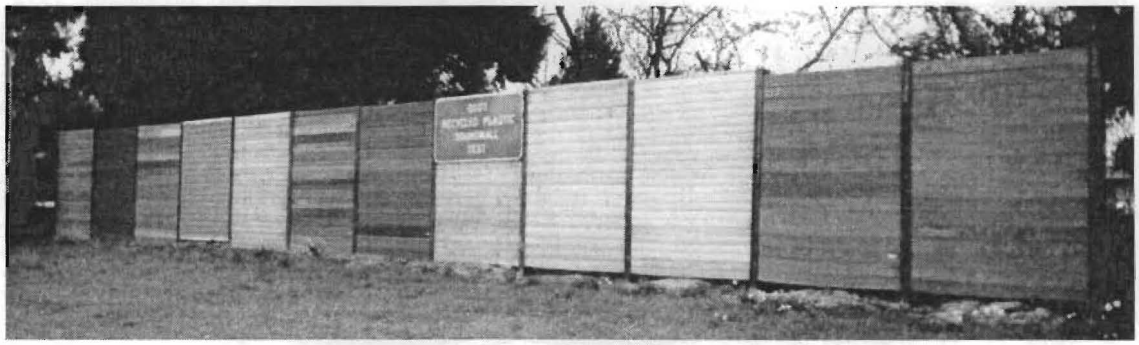

Figure 4. Recycled Plastic Soundwall in Oregon

Other sound barriers have also been developed by private companies that incorporate varying amounts of recycled materials (Freudenrich 1996). Figure 5 shows a recycled composite soundwall in Las Vegas, Nevada, constructed by Carsonite International, Inc., located in Carson City, Nevada. Many of these systems utilize concrete or steel columns and wall components fortified by metal casings. In contrast, a prototype soundwall was developed by this project that utilized 99% recycled materials, including the columns, with the exception being a modest number of metallic connections.

Figure 5. Conventional Soundwall Incorporating Plastic Materials

2.2.1 Acoustics

Clearly, from its appellation an important function of a soundwall is its ability to reduce noise transmission between a source and a receiver. The performance of a sound barrier, often measured by its insertion loss, is known to be affected by the geometry, locations of the receiver and source, ground cover, and many other factors (Fyfe and Harrison 1995). Insertion loss is a quantitative measure of reduction in noise level due to installation of a noise barrier. Basic guidelines are set by each state on the manner in which traffic noise analysis is to be performed. Texas Department of Transportation (TxDOT) adopted "Guidelines for Analysis and Abatement of Highway Traffic Noise" for highways in Texas (1996). This document includes a discussion of sound and traffic noise fundamentals and the overall traffic noise analysis process. It also specifies that compliance with Title 23, Code of Federal Regulations, Part 772 (1982) and FHWA's "Highway Traffic Noise Analysis and Abatement Policy and Guidance" (1995) are prerequisites for granting federal-aid highway funds for construction or reconstruction of a highway. Other documents that are also helpful in understanding soundwall acoustics and methods used to analyze properties associated with sound include: "Sound Procedures for Measuring Highway Noise: Final Report" (Bowlby 1981), "Roadside Noise Abatement" (1995), and "FHWA Highway Traffic Noise Prediction Model" (Barry and Regan 1978). Most recently, "Measurement of Highway-Related Noise" was published by the United

States Department of Transportation (Lee and Fleming 1996). This document reflects substantial changes and improvements in noise measurement technologies since the 1981 FHWA publication "Sound Procedures for Measuring Highway Noise: Final Report." Methods of acoustic analysis were taken from the document "Measurement of Highway-Related Noise" and ASTM E-90 standards specified in "Guidelines for Evaluating the Performance of Highway Sound Barriers" (1996).

Acoustic analysis of noise barriers is further refined when special applications are considered. The noise abatement performance of a soundwall can be enhanced by applying absorptive treatments or special geometrical configurations to a barrier. For example, details of applying a specially shaped top to a barrier are given by Cohn and Harris in an article entitled "Improving the Performance of Highway Soundwalls" (1993). In most applications these products are, in general, not composed of recycled materials. For this reason, specially shaped tops are not incorporated into the prototype soundwall design.

2.2.2 Aesthetics

As pointed out by Tang and Lindeman, "Noise wall aesthetics is one of the most important aspects of a noise barrier next to its noise abatement capability" (1996). Improperly designed walls not only disgust residents living nearby, but also have adverse effects on drivers as they travel past the wall. Aesthetic quality of a barrier can increase or decrease the property value of neighborhoods that are adjacent to the barrier. The subject of noise barrier aesthetics is addressed frequently in pertinent literature (Storey and Godfrey 1994). Aesthetic appeal is primarily related to the geometry, layout, and landscaping of the structure. As shown in Figure 6, options that are often used in walls constructed with conventional materials include coloring schemes, texturing, and engraving of wall segments (Simpson 1976; Farnham and Beimborn 1990; Bendtsen and Schou 1991).

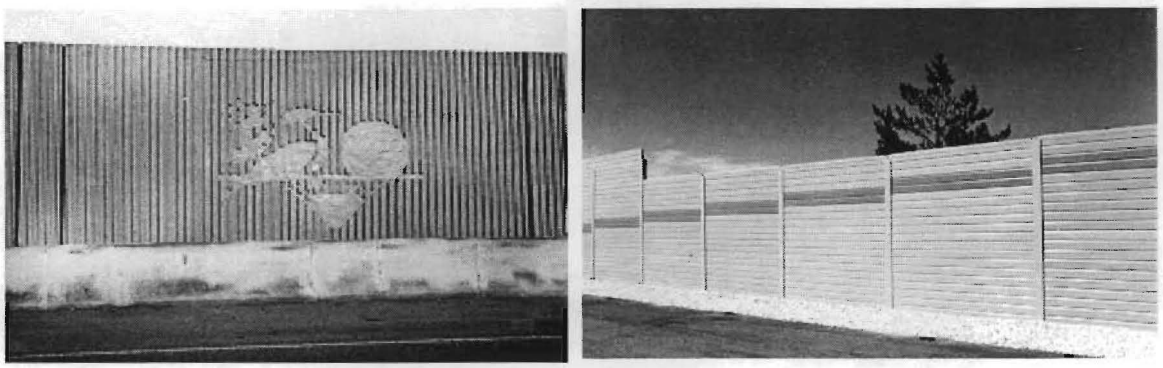

Figure 6. Attractive Noise Barriers

Aesthetics of recycled plastic soundwalls is an important consideration because texturing and geometric variations are not always available due to manufacturing processes and limitations of the material. "Developments of Standards for Noise Barriers Using Recycled-Plastic Lumber" proposes various geometric layouts of wood and steel-framed systems that incorporate plastic lumber (Hag-Elsafi et al. 1996). An Oregon report entitled "Recycled Plastics in Highway Construction and Maintenance – Construction Report" does not directly address the issue of aesthetics, but includes several pictures of a soundwall (see Figure 4) that was designed and constructed with plastic lumber (Hunt 1993).

2.2.3 Design and Construction

In addition to acoustics and aesthetics, a third area of interest in soundwall design is structural integrity. Over the years there have been many specifications for the design of barriers that utilize conventional materials such as wood, concrete, metal, or masonry (AASHTO 1989). Only recently have specifications for walls built with recycled plastic materials been submitted. In 1993, the Research and Development Branch of the Ontario Ministry of Transportation published "Development of Specifications for Plastic Lumber Use in Highway Applications - Phase 1" (Mota et al. 1993). As the title states, this document focuses on the use of recycled plastic lumber in highway applications, but it lacks detail in the area of soundwall design. The New York State Department of Transportation published "Development of Standards for Noise Barriers Using Recycled-Plastic Lumber" (Hag-Elsafi et al. 1996). As mentioned previously, this report incorporates design tables that provide structural information on designing wood and steel

frames that support the wall and allow attachment of plastic lumber to the surface. The design tables also include information on choosing sizes of column footings.

Most recently, a noise barrier design utilizing hollow recycled plastic panels was proposed in a document entitled "Sound Barrier Applications of Recycled Plastics" (Saadeghvaziri and MacBain 1998). Here, researchers followed guidelines set forth in "Guide Specifications for Structural Design of Sound Barriers" (AASHTO 1989) and "Noise Barrier Design Guidelines" (Farnham and Beimborn 1990) to construct a small prototype by stacking hollow panels, or cells, in a vertical fashion. Not much information is given on how panels would be joined to create a long span or how the wall would be supported by a foundation.

2.2.4 Structural Dynamics

There has been very little published research in the area of the dynamic behavior of soundwalls. Finite element analysis and system identification are two approaches that can be used in predicting dynamic behavior of structures. Finite element modeling makes it possible to predict behavior of an actual system to various loadings such as wind, impact, or earthquakes. A report entitled "Effective Noise Barrier Solutions for TxDOT: A First-Year Progress Report," briefly mentions development of a finite element model of a section of a soundwall system (Klingner et al. 1996). It includes application of a static wind load in an attempt to determine deflection and strength of a proposed design, but results are still pending as the final report for this project is not yet published. A second document, "Sound Barrier Applications of Recycled Plastics," uses finite element analysis to predict static deflection for two span lengths of 0.6-m (2-ft) high panels upon application of a wind pressure force. No information is given with regards to dynamic behavior. In the area of system identification of the dynamic characteristics of a soundwall, no sources of literature are available. This report gives information related to these two subjects.

3. MATERIALS

3.1 SELECTION PROCESS

Finding alternative materials for use in soundwalls that can reduce life cycle cost is a high priority. Concomitant with increasing material costs, environmental factors are also encouraging the use of recycled materials. Application of materials that are durable and possess the required performance criteria not only benefits the environment but also reduces the burden being placed on landfills. In this study, a comprehensive investigation into identification of suitable recycled plastics is given special emphasis.

A variety of recycled plastic materials and plastic shapes are available from a multitude of manufacturers as outlined in "Recycle Texas: A Reuse and Recycling Directory" (1995). Of particular interest to this project are plastics that have a composite nature in that they are reinforced with steel, fiberglass, or fiberglass rods. Since these materials are available in many sizes, shapes, and colors, requests for customized materials are generally limited only by the capabilities of a particular manufacturer.

3.2 ACQUISITION

A multitude of manufacturers were contacted by telephone concerning their recycled products that are suitable for use as structural members. While some materials were purchased at a full price, others were donated to the project with the only expense being that of shipment. Several products were obtained for experimentation and testing in the laboratory. Those that were deemed suitable for further evaluation and complemented the overall design were obtained in larger quantities for construction of the full-scale soundwall. It is noted in passing that several companies produce and construct complete sound barrier systems. Although use of recycled materials in those structures was investigated, the design and construction of the prototype soundwall for this project was entirely independent of existing commercial barrier systems to the point that any similarity in design is merely coincidental.

Table 1 lists commercial manufacturers that were contacted and the products they supply. Material properties that are listed are derived from literature from the manufacturer and previous research (Roschke et al. 1996). Specific gravity of each material is included

so that a rough estimate of its weight can be calculated. The modulus of elasticity is also included so that stiffness of the material can be estimated.

Table 1. Manufacturers of Recycled Materials

Manufacturer	Note	Composition	Specific Gravity	Modulus of Elasticity (MPa)
American Ecoboard, Inc.	1	HDPE	--[a]	--[a]
Carsonite International	2, 3	Fiberglass-reinforced thermoplastic, Rubber tire core	1.70	17,300
Enviro	1, 3	80% HDPE, 20% loose fiberglass	0.70 - 0.80	3,100
Durawood® by International Plastics, Corp.	1	HDPE, LDPE, PP	0.93	--[a]
Trex™ by Mobil Chemical Co.	1	50% HDPE, 50% waste wood	0.96 - 0.99	1,209
Pellatech, Inc.	1	HDPE	--[a]	--[a]
Plastic Pilings, Inc.	1	HDPE, LDPE, PP	--[a]	3,109
TriMax™ by Polymerix, Inc.	2, 3	80% HDPE, 20% loose fiberglass	0.70 - 0.80	3,109
Lexan® by Quilite International	2	Nonrecycled polycarbonate	1.20	234
Timbrex® by Rec. Plastic Products, Inc.	1, 4	50% HDPE, 50% waste wood	0.96 - 0.99	1,154
Recywall® by Sanders Enterprises, Inc.	2	--[a]	0.92 - 0.93	141
Seapile™ by Seaward International, Inc.	1	HDPE (Duralin®)	0.88 - 1.01 (skin), 0.54 - 0.75 (core)	517 (no reinforcement), 3,178 (fiberglass rods), 9,673 (steel rebar)
Sound Fighter Systems, Inc.	2	HDPE	0.91 - 0.97	--[a]

1. Applications such as marine construction, fencing, decking, traffic-related barriers or signs, and piling.
2. Developed as a commercial soundwall system.
3. Used in conjunction with steel or fiberglass which may account for an increase in the elastic modulus.
4. Timbrex® is identical to Trex™ by Mobil Chemical Co.

Notation: HDPE = high-density polyethylene, LDPE = low-density polyethylene, PP = polypropylene
--[a] = Not available

Materials listed in Table 2 (and shown in Figure 7) were obtained from selected manufacturers given in Table 1. Items not listed in the table include a large bag of coarse "crumb" rubber and several square-shaped plastic tubes that were considered as potential members. Another preliminary concept included inserting "crumb" rubber into the interior of the soundwall, but reports of potentially toxic chemicals related to the rubber product leaching into the ground led to elimination of the concept.

Table 2. Soundwall Materials

Quantity	Material	Dimensions (m)
4	Black recycled plastic columns with four #8 steel rebar	0.20 × 0.20 × 5.49
4	Black recycled plastic columns with four #4 steel rebar	0.20 × 0.20 × 5.49
5	Black fiberglass-reinforced columns	0.20 × 0.20 × 5.49
30	Unreinforced plastic spacers	0.10 × 0.20 × 4.66
20	White sheet panels	1.22 × 3.66 × 0.01
4	Gray sheet panels	1.22 × 3.66 × 0.02
23	Green unreinforced plastic timbers	0.05 × 0.23 × 3.66
23	Brown unreinforced plastic timbers	0.05 × 0.23 × 3.66
23	Black fiberglass-reinforced plastic timbers	0.05 × 0.23 × 3.66
69	Tan fiberglass-reinforced plastic timbers	0.05 × 0.23 × 3.66

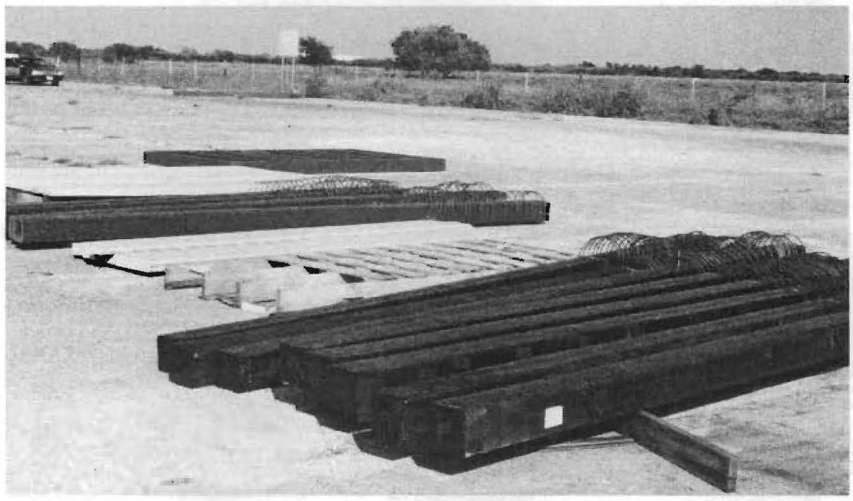

Figure 7. Materials Assembled to Construct Full-Scale Soundwall

3.3 TESTING OF PROPERTIES

Products manufactured from recycled plastics are known to be nonhomogeneous and to have inconsistencies and imperfections. Quality is controlled by the production technique and quality control of the manufacturer. Many studies have been and are

currently being performed on recycled materials to determine which products are suitable for structural application (Bligh et al. 1995; Roschke et al. 1995). The goal of this project is not to carry out extensive testing on properties of the multitude of reclaimed materials; rather, primary effort is placed on designing and constructing a soundwall that makes extensive use of existing recycled products. Ultimately, behavior in the field of the component materials and structure as a whole is of critical importance.

3.3.1 Three-Point Bend Test

A #8 steel-reinforced column and a fiberglass-reinforced column were obtained from Plastic Pilings, Inc. and Enviro Special Products, Inc., respectively (see Figure 9). A three-point bending test was performed on each type of column to determine stiffness characteristics. These characteristics are important because design of the soundwall is governed by deflection, and it is expected that the stiffness of the columns will provide the primary resistance to deflection.

The columns were set up as simply supported beams and loaded with an actuator so that force-displacement plots could be developed. Tests were performed using an LVDT (see Section 7.4) to measure displacement and Labview® data acquisition software to record force and transducer magnitudes (see Figure 8).

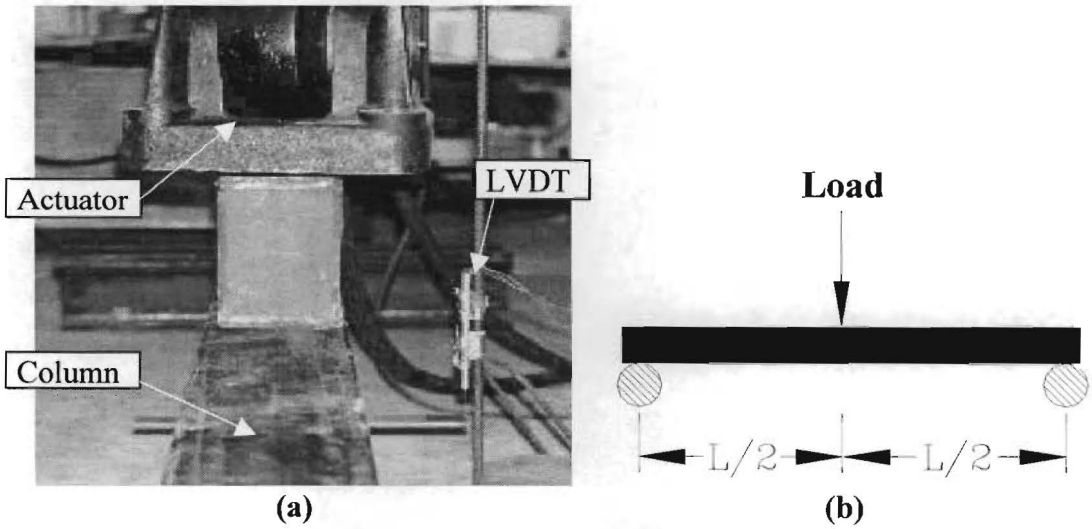

Figure 8. Setup for Three-Point Bending Test: (a) Experiment; and (b) Load Configuration

Stiffness of each column is found by rearranging the deflection formula for a simply supported beam with concentrated load at the center (Boresi et al. 1993):

$$Stiffness = EI = \frac{PL^3}{48\Delta_{MAX}} \tag{1}$$

where P is magnitude of the concentrated load (N), L is the unsupported length of the beam (m), and Δ_{MAX} is the maximum deflection measured by the LVDT at the midspan.

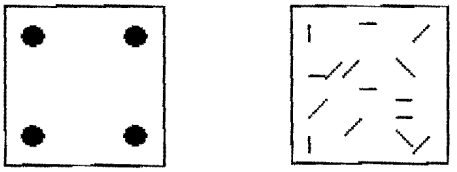

(a) (b)

Figure 9. Cross-Sections of Columns: (a) #8 Steel-Reinforced; and (b) Fiberglass-Reinforced

Data from a test on each of the two columns is shown in Figure 10. Using Equation (1) with an unsupported length of 3.5 m, bending stiffness of the steel-reinforced and fiberglass-reinforced columns are approximately 717.7 kN-m^2 and 510.4 kN-m^2, respectively. Even though the steel reinforcement provides superior stiffness at higher loads, the fiberglass column is sufficiently stiff such that it will be included in the design of a section of the prototype sound barrier.

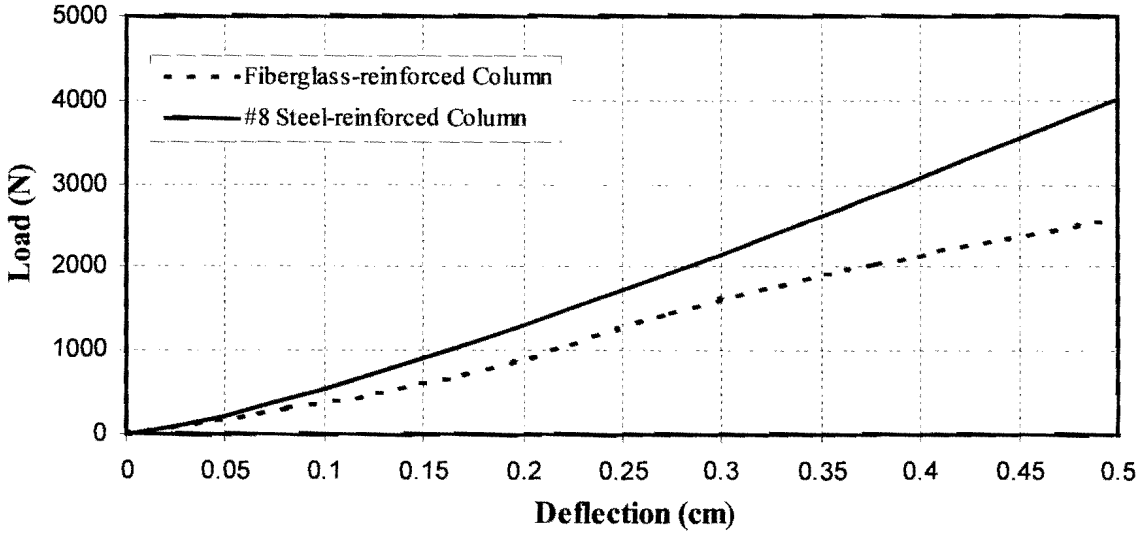

Figure 10. Force-Deflection Curve for Columns

3.3.2 Heat Exposure

As a simple auxiliary test of the response to direct sunlight, two recycled plastic members were inclined against a wall at an angle of approximately 10° from the vertical position (see Figure 11). One member was reinforced with fiberglass and the other was unreinforced plastic. Within several days of exposure, the geometry of the unreinforced lumber was noticeably curved, while the reinforced sample remained straight.

This simple test displayed the susceptibility of the unreinforced plastic members to warping due to extreme heat. Based on this information, the researchers decided that a majority of the members that would be exposed to direct sunlight should be fiberglass-reinforced. However, a short section of the prototype soundwall would be designated to be covered by unreinforced plastic members so a comparison of performance could be made between the two types of members as they were exposed to long-term weathering (see Chapter 6).

Figure 11. Sag of Fiberglass-Reinforced and Unreinforced Plastic Lumber

4. DESIGN OF FULL-SCALE SOUNDWALL

4.1 INTRODUCTION

Recycled plastic soundwalls have previously been developed that incorporate steel, I-shaped columns into their designs. This allows multiple boards to be oriented horizontally and placed between adjacent posts (Hunt 1993). A wall can be built as high and as wide as desired since the lengths and widths of the columns or boards can be adjusted. Warping is one consideration in using these lumber members in particular and recycled materials in general. Impact safety is another consideration in these designs because the steel columns protrude from the surface of the panel. Upon impact, an errant vehicle could deform the plastic lumber and cause a vehicle to snag on the rigid column.

Recognizing such limitations, the conceptual design proposed for this project takes into account the following major concepts:

- Encapsulate the columns within the wall for reasons of aesthetic and roadside safety.
- Resist the likelihood of warping of wall materials.
- Improve the aesthetics in comparison with previous recycled plastic soundwall designs by replacing the patchwork of vertical and horizontal lines with either vertical lines or, ideally, no lines at all.
- Maximize the use of recycled materials in the structure.

Most wall systems with recycled plastic content incorporate steel columns or frames in their design. With the exception of a modest number of metal connections, steel reinforcing bars, and concrete drilled shafts, the prototype soundwall in the current study utilizes 100% recycled products.

4.2 CONCEPT

Similar to construction with precast concrete tilt-up panels, columns in this soundwall are placed prior to arrival of the wall panels. Individual wall panels, called modules, are transported to the field by a flatbed truck where they are placed between the columns with hoist, crane, or forklift (see Figure 23). The modules have overhanging

edges that allow them to slide over the columns, thus encapsulating the columns. Each module can be prefabricated at a convenient site as compared to on-site construction. The manufacturer needs to know the desired span and height so material properties and structural members can be adjusted to accommodate the desired geometry. Figure 12 is a model of a prototype soundwall designed by researchers of this project. In the figure, the interior frame is shown for each module so the variety of configurations can be examined. The modules are supported against lateral forces by the columns which, in turn, are supported by footings.

4.2.1 Modules

Structurally, the modules are designed to withstand strong winds and damage from small objects such as rocks or hail. Primary structural support comes from an inner frame composed of vertical and horizontal members (see Chapter 5). A major requirement of each module is that it maintain its rectangular form for easy insertion between columns. If desired, holes could be cut into the base of each module for water drainage.

Aesthetically, two themes are developed and embodied in the prototype soundwall. One alternative is that plastic lumber be used in "vertical line" designs so that adjacent wall panels blend in with each other. Another alternative uses plastic sheets to create "smooth" panels with flowing lines. Texturing, etching, and coloring schemes can then be applied to enhance appearance of the wall.

The modular system allows aesthetics for both sides of the wall to be custom designed. Smaller patterns, or textures, can be placed more closely on the side of the homeowner, while larger etchings can be spaced further apart on the side of passing motorists.

4.2.2 Columns

The columns provide primary support against wind load acting on the surface of the wall. Weight of the modules is not supported by the columns since the modules rest on the

ground. With this in mind, a design procedure was followed so that appropriately sized columns could be selected to resist wind load deflection (see Section 4.3).

4.2.3 Foundation

Large footings mandated by AASHTO standards to support columns in the ground are not necessarily required by structures that utilize recycled plastic. Although recycled plastics are by no means lightweight materials, their density is less than metals and precast concrete.

Recognizing this, the 13 columns of the prototype structure were encased in 1.8-m (6-ft) deep concrete footings that are 46 cm (18 in.) in diameter. Steel reinforcement with a pitch of 7.6 cm (3 in.) was included to confine the concrete. In comparison, a 4.27-m (14-ft) tall precast concrete soundwall is located near Beltway 8 in Harris County, Texas, that has 4.57-m (15-ft) deep shafts each with a diameter of 0.76 m (30 in.) ("Plans of Proposed State Highway Improvement" 1995). Potential savings in both time and labor could be made through the use of smaller albeit more closely spaced footings.

As mentioned previously, the modules constructed for this study rest directly on the ground. Ideally, a concrete mat would be constructed so that the modules rest on a clean, level surface.

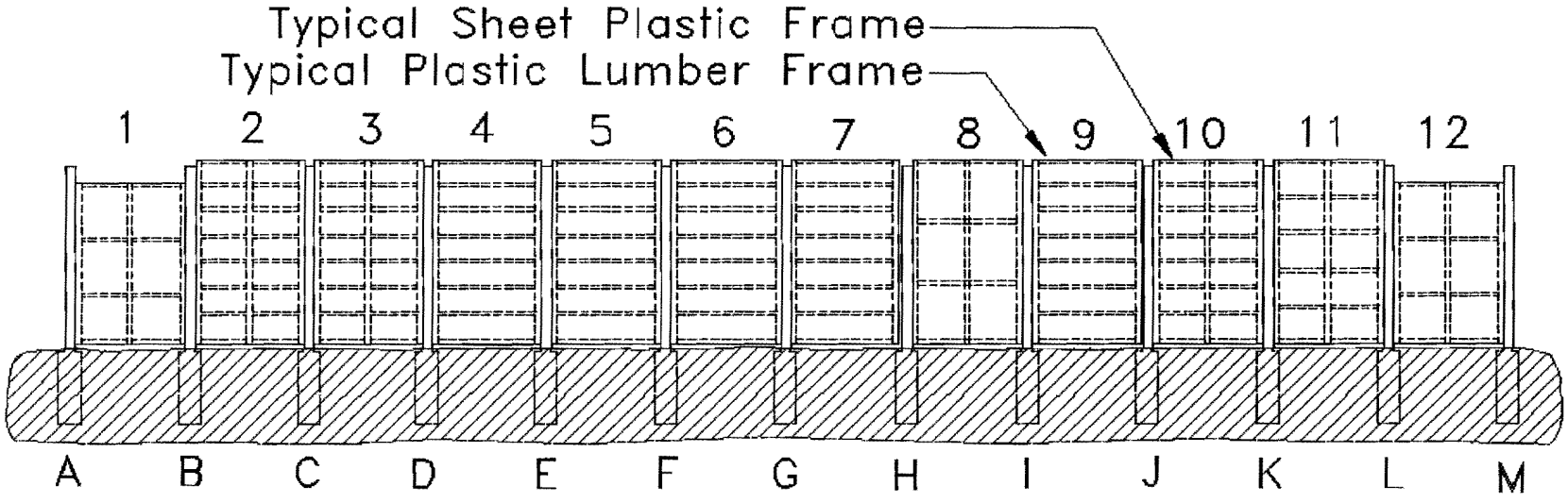

Figure 12. Prototype Soundwall and Identification of Various Components

4.3 LOAD CASES

A sound barrier undergoes dead, wind, and impact loads during its service life. The soundwall in this project was explicitly designed to resist lateral deflection due to wind pressure load. Since plastic is not as stiff as masonry or precast concrete materials, it is difficult to design an acoustic barrier that doubles as a vehicle impact barrier. This issue was not overlooked as the facade of the soundwall was designed to redirect an impacting vehicle so that it is not snagged by the columns. Nevertheless, the primary goal of the design process was to select structural members that would limit lateral deflection of the wall due to wind loading.

With this in mind, the ASCE 7-95 "Minimum Design Loads for Buildings and Other Structures" (1995) and the AASHTO "Guide Specifications for Structural Design of Sound Barriers" (1989) were used to develop design wind loads that result in deflection of the soundwall in the transverse direction. For purposes of simplification, the wind pressure is applied to a tributary area of the wall and the resulting force is applied to the columns.

4.3.1 ASCE Wind Load Criteria

According to ASCE 7-95 (1995), wind velocity pressure is determined by the following formula:

$$q_z = 0.613 K_z K_{zt} V^2 I \tag{2}$$

where q_z is wind pressure in Pa (psf), K_z is an exposure coefficient, K_{zt} is a speed factor for hills and escarpments, V is wind speed in m/sec (mph), and I is an importance factor of the structure.

For the purpose of this study, the soundwall is taken to be a Category II structure which implies that failure of the soundwall structure would pose a moderate hazard to human life or potential for damage to property if it were to fail (see ASCE, Table 1-1). Exposure Type C is chosen since the soundwall site is an open terrain with scattered obstructions having heights less than 9.1 m (30 ft) (see ASCE, Section 6.5.3). K_z is taken as 0.85 (see ASCE, Table 6-3 and Table 1-1), K_{zt} is 1.0 (see ASCE, Section 6.5.5), V is 45

m/sec (see ASCE, Figure 6-1), and I is taken as 1.0 (see ASCE, Table 6-2). The wind speed is based upon a 50-year mean recurrence interval.

Substitution of these values results in a wind velocity pressure of 1,055 N/m^2. The force per unit height, w, is 2,638 N/m of each column for a 2.44-m (8-ft) panel width. To more accurately model pressure distribution of wind on the wall surface, the constant pressure distribution is converted to a linear distribution. Here, pressure is assumed to be zero at ground level and to increase to $2w$ at the top of each column so that overall force of the constant pressure distribution is maintained (see Figure 57). It is then possible to determine the maximum deflection, bending moment, and stress for a variety of columns from the following formulae (Boresi et al. 1993):

$$\Delta_{\max} = \frac{11 w_o h^4}{120 EI} \qquad \sigma_{\max} = \frac{M_{\max} c}{I} \qquad M_{\max} = \frac{w_o h^2}{3} \tag{3}$$

where Δ_{max}, σ_{max}, and M_{max} are the maximum deflection, bending moment, and stress, respectively. The variable, w_o, is equal to $2w$, or the magnitude of the linearly distributed load at the top of the column. The distance from the neutral axis to the extreme fiber of the column cross-section is designated as c and is equal 10.2 cm (4 in.), while the height of each column, h, is 3.66 m. Here, I is the transformed moment of inertia about the major bending axis and is equal to 1.42×10^4 cm^4 (341.3 in.^{4}).

Deflections, stresses, and costs were parameters used to determine whether to include or exclude a particular type of column in the prototype soundwall. For example, a 3.66-m (12-ft) tall, fiberglass-reinforced column ($E \approx 3.1 \times 10^9$ N/m^2) with cross-sectional dimensions of 20.3 cm × 20.3 cm (8 in. × 8 in.) and fixed base was estimated to have a maximum deflection of 19.7 cm (7.8 in.) in a 45 m/sec (100 mph) windstorm. The maximum stress was also predicted to be less than the yield stress of the composite material; therefore, this comparatively inexpensive and commercially available column was selected for use in the soundwall.

4.3.2 AASHTO Wind Load Criteria

In order to check the selection of column dimensions suggested by a design approach that follows ASCE 7-95 (1995), a second set of calculations was performed using AASHTO criteria. The wind pressure is determined by the following formula:

$$P = 0.00256(1.3V)^2 C_d C_h \tag{4}$$

where P is the wind pressure in English units of lb/ft^2, V is the wind speed in mph, C_d is a drag coefficient, and C_h is a combined height, exposure, and location coefficient.

Similar to ASCE criteria, location of the structure plays a role in calculation of the wind pressure. For a wall with a height to its centroid that is less than 4.27 m (14 ft), C_h is taken to be 0.37 if it is placed in Category B1 and 0.59 if placed in Category B2. Category B1 is defined here as a residential area within a distance 457 m (1,500 ft) that is upwind from a soundwall installation, and Category B2 is a soundwall installed in an area with mostly open terrain. Design wind speed is determined from Figure 1-2.1.2.A of the 1989 AASHTO specification. For central Texas, V is found to be 31.5 m/sec (70 mph), and C_d is taken to be 1.2.

As shown in Appendix A, deflection, moment, and stress and are calculated for a variety of columns for Categories B1 and B2. In the calculations, design wind speed varies from 31.5 m/sec (70 mph) to 49.5 m/sec (110 mph). Cross-sectional dimensions and modulus of elasticity of the columns also vary; however, all columns have the same height. Overall, estimated deflection varies from 14.1 cm (5.6 in.) to 28.7 cm (11.3 in.).

4.4 LIMITATIONS

Limiting factors that affected design and construction of the prototype barrier for this research project included material costs and an available field-site. Many of the materials acquired for testing and construction were donated to the project with the only charge being that of shipment. Due to the density and large volume of recycled materials, interstate delivery by truck was relatively expensive. In the end, economic constraints for the project limited the overall length of the wall to 29.3 m (96 ft).

A second limiting factor was availability of a field site that was readily accessible to the researchers. Even though there is no regular traffic by the installation site at the Riverside Campus of Texas A&M University, this location was chosen over several other sites that were considered so that a variety of module configurations could be installed and removed without disruption of normal traffic. Of course, lack of traffic noise required an artificial means for generation of noise that enabled testing of acoustic properties of the barrier (see Section 10.5).

5. CONSTRUCTION

5.1 INTRODUCTION

A full-scale prototype soundwall was installed at the Riverside Campus of Texas A&M University in September and October 1996 (see Figure 13). The barrier consists of 13 columns that are 5.49-m (18-ft) long and 12 modules that are 2.44-m (8-ft) wide. Total length and height dimensions of the wall are 29.3 m (96 ft) and 3.66 m (12 ft), respectively.

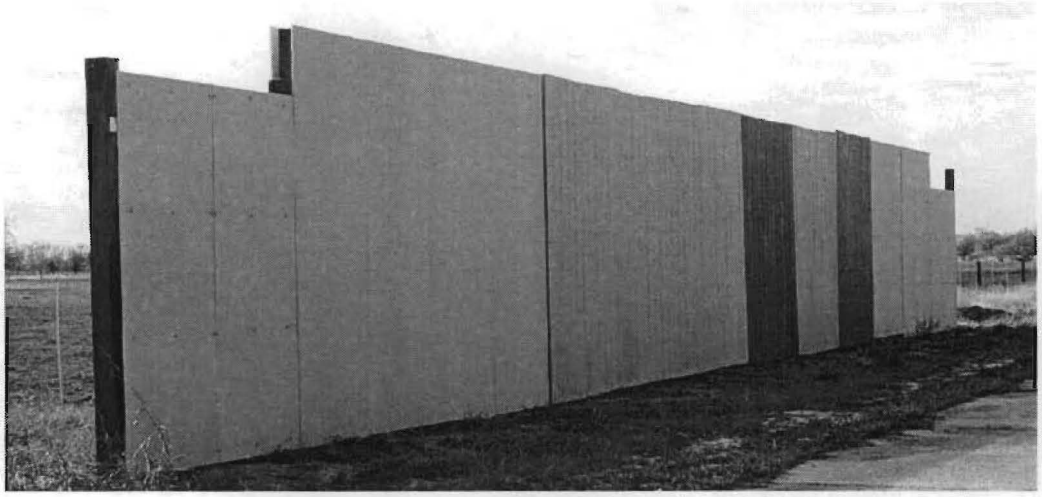

Figure 13. Full-Scale Prototype Soundwall

As previously mentioned, a module is a self-contained unit that spans the space between two columns. Each unit is composed of an inner frame that provides structural integrity and an exterior facing. For this project, six of the modules have flat panels of plastic sheeting on the exterior surfaces, while the other six modules incorporate plastic lumber for facing (see Figure 3). The exterior face of each module is designed to encapsulate adjacent columns so that the exterior of the sound barrier appears as one continuous surface. As described in Section 5.3, materials and configuration of the inner frames varies from one module to the next to accommodate different connections and surface materials (see Figure 12).

Construction of the soundwall began with assembly of several prototype modules in the Structures Laboratory at Texas A&M University. Efforts focused on constructability of recycled materials with special interest being given to methods of connecting various structural members. After initial construction and tests, researchers moved these modules

and subsequent construction operations to the National Geotechnical Experiment Site at the Riverside Campus of Texas A&M University. Experience gained from construction of early prototype modules was used to build additional modules that are more aesthetic, stronger, and have a higher potential for field implementation.

5.2 CONNECTIONS

A number of factors including safety, strength, aesthetics, and cost were considered in selecting connections. Attachment devices that were investigated included bolts, nails, screws, adhesives, and a PVC welding unit. Table 3 lists several advantages and disadvantages associated with each type of connection. In addition, daisy bolts were considered but not implemented, and a PVC welder was used unsuccessfully to bond several plastic members.

Table 3. Summary of Module Connections

Connection	Advantages	Disadvantages
Bolts [1]	1. High strength 2. Small quantities required 3. Stripping or pullout alleviated 4. Modules can be repaired	1. Aesthetically unappealing 2. Very expensive (even in bulk) 3. Difficult to insert in warped materials 4. Protruding bolt poses danger
Hex-head and Phillips-head screws [2]	1. Medium strength 2. Aesthetically appealing 3. Ease of installation with drill 4. Pullout alleviated	1. Stripout in soft materials 2. Moderately expensive in large quantities 3. Small surface projections can snag an errant vehicle
Smooth and ring-shank nails [3]	1. Low to medium strength 2. Aesthetically appealing 3. Inexpensive 4. Easy installation with nail gun	1. Possible pullout 2. Large quantity needed 3. Time consuming without nail gun
Glues, epoxies, adhesives [4]	1. Aesthetically appealing 2. Easy installation with roller 3. Corrosion resistant 4. Joint flexibility	1. Degrades over time 2. Affected by temperature 3. Flexibility 4. Hazardous vapors during construction

1. Bolts are used only on sheet plastic modules where a small number of attachment locations are needed.
2. Hex-head screws worked well, while Phillips-headed screws were stripped by the drill bit. Tapered Phillips-headed screws may perform well because they can be countersunk.
3. Ring-shank nails grip much better than smooth nails to the extent that smooth nails should not be considered.
4. Four pairs of high-density polyethylene coupons were individually bonded with two types of glue. Some samples had smooth sides bonded to smooth sides, while others were primed by sanding. Use of a screwdriver separated all of the samples indicating that neither of the two bonding agents was satisfactory.

The first module constructed utilized 22.9-cm (9-in.) long bolts. The bolts were sufficiently strong but proved to be aesthetically unattractive. Another disadvantage of the bolts is their high cost, even when purchased in large quantities. The advantage of a bolted system is that it can be disassembled; however, reassembly may be difficult if the recycled materials warp, expand, or contract.

Large screws that are 15.2-cm (6-in.) long were also used as the primary means of connection. They were found to be excellent connectors for most of the recycled materials, although striping did tend to occur in softer recycled plastics. This problem can be remedied through use of larger screws with bigger threads.

Initial attempts at employing ordinary smooth nails were discontinued when some plastic boards on a module dismembered due to nail pullout. Smooth nails were replaced with ring-shank nails that performed markedly better. It is difficult to drive ring-shank nails into harder plastic; however, it is expected that use of a nailgun would prevent bending of the nails associated with poor hammering technique. Time would also be saved in the construction process through use of a nailgun. Major advantages in using ring-shank nails are that they are inexpensive and not visible from a distance, making a wall constructed with nails visually more appealing. However, it is important to remember to use appropriate corrosion protection with all metallic connections.

Labeling on commercially available epoxies, glues, and adhesives warned that they are not suitable with "certain types" of plastics. Recycled materials are often composed of many types of plastics making it difficult to ascertain the compatibility of a bonding agent with recycled plastic material. E-6100® and E-6000® adhesives, by Eclectic Products, Inc., were tested on several recycled plastic coupons. In the end, these bonding agents provided insufficient bond strength between the plastic members to which they were applied. Some surfaces were roughened, but this preparation made little difference in bond strength. In fact, it was observed that the bonding agent adhered to the smooth surface instead of the rough surface in some instances.

A final connection investigated was by means of a PVC welder. Using a jet of hot air, the welder joins PVC piping through localized melting. The welder was shown to have unpredictable results when used on various recycled plastic coupons. Some samples

caught fire, while others melted. Filler material used by the PVC welder is polyvinyl chloride which appears to be incompatible with the polyethylenes and polypropylenes to which it was applied.

5.3 ASSEMBLY OF MODULES

Dimensions for the first two prototype modules were initially set at 2.44-m (8-ft) wide by 3.05-m (10-ft) high. Widths of less than 2.44 m (8 ft) were considered impractical because too many columns would be required for a typical barrier. Alternatively, wider spans would inhibit transportation of the modules by truck to a construction site. Transportation and sound engineers at TxDOT recommended increasing the height of the structure to 3.66 m (12 ft). Therefore, final dimensions of the remaining 10 modules were chosen to be 2.44-m (8-ft) wide by 3.66-m (12-ft) high as shown in Figure 14.

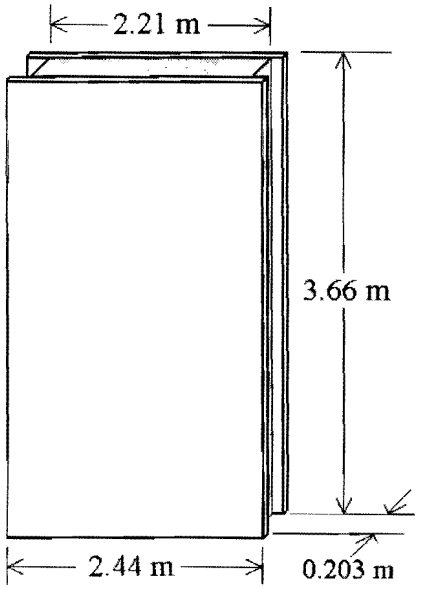

Figure 14. Dimensions of Module

The concept behind modular construction is to have prefabricated modules slide down between columns that have previously been installed at a site. Each module is designed to overlap one-half of the faces of two adjacent columns. The exterior surface of the module has a width of 2.44 m although the interior frame of the module must be smaller to allow insertion between the columns. The outside width of the inner frame is calculated by subtracting one-half the width of the column on each side of the module. To

account for material imperfections and errors in construction an additional gap of 1.27 cm (0.5 in.) is included. Columns used for this project had nominal widths of approximately 20.3 cm (8 in.); consequently, inner frames were 2.21-m (7.25-ft) wide.

The surface material, either sheet plastic or plastic lumber, of each module overhangs the edges of the frame by 11.4 cm (4.5 in.). This overhang is used to secure the module to two adjacent columns. It is important that the overhang on the module be securely fastened to the column in a permanent fashion since this is the primary connection in the out-of-plane direction between a module and column. Secure connections were not made for the prototype wall in order to allow modules to be readily removed for testing (see Chapter 6).

5.3.1 Plastic Sheet

This section describes construction of the first module that incorporated plastic sheeting. Although it has a height of 3.05 m (10 ft), five more modules with a similar design were fabricated at a height of 3.66 m (12 ft).

Construction of the short sheet plastic module requires four plastic sheets measuring 1.22-m (4-ft) wide × 3.05-m (10-ft) tall × 1.27-cm (0.5-in.) thick. Three recycled plastic boards, or "spacers," with a nominal cross-sectional area of 10.2 cm (4 in.) × 20.3 cm (8 in.), are placed vertically to provide bending stiffness (see Figure 15). In taller modules, several fiberglass-reinforced boards are placed horizontally to provide additional support; these boards have nominal cross-sectional dimensions of 3.8 cm (1.5 in.) × 20.3 cm (8 in.) (see Figure 17).

Figure 15. Interior Frame of Sheet Plastic Module

Construction of the short module described herein is unique in that it is assembled with 16 steel bolts that are 22.9-cm (9-in.) long and 1.3 cm (0.5 in.) in diameter (see Figure 16). The module is built by laying two of the four sheets side by side on a flat surface and placing the remaining two sheets on top. In this way, precisely aligned bolt holes can be drilled in the top and bottom sheets. Spacers are then placed on the top of the sheets in a lengthwise fashion along each outside edge and down the center. Along the center, one-half of the spacer rests on one sheet and one-half rests on the other sheet; on the outer edge of the module, the spacers are inset 11.4 cm (4.5 in.) to create an overhanging lip. The lip enables the module to slide over the column.

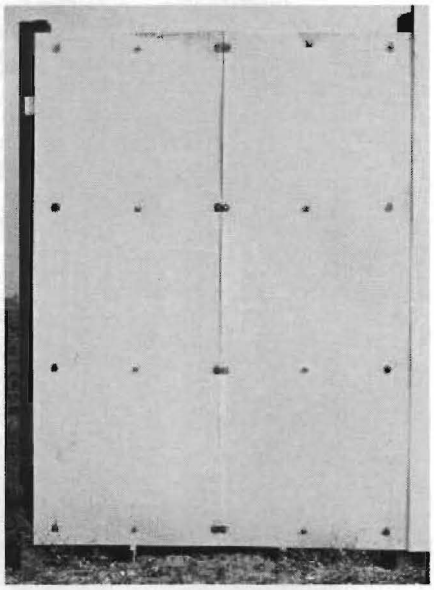

Figure 16. Bolted Sheet Plastic Module

Holes are drilled in the spacers starting 10.2 cm (4 in.) from the bottom and progressing at 84.7-cm (33.3-in.) intervals. The middle spacer has two holes drilled at every interval because two sheets frame into it. After drilling is complete, one layer of sheets is removed and placed on top of the spacers so that the bolts can be inserted and tightened.

This type of module was found to have a weak link along the middle crease. Each sheet panel overlaps the middle spacer by 3.8 cm (1.5 in.) leaving very little edge clearance for the bolt. Additional rotation occurs about the center frame member since the joint is

not extremely rigid. Two short modules lacked horizontal boards used in taller module designs and thus exhibited increased flexure along this crease. In taller modules, horizontal boards are wedged in between the vertical spacers with screws, nails, or bolts to help resist rotation. The number of horizontal boards depends on the type of connection being used. As shown in Figure 17, modules constructed with screws and nails have eight horizontal members; as can be deduced from the bolt pattern in Figure 16, bolted modules have only four horizontal members.

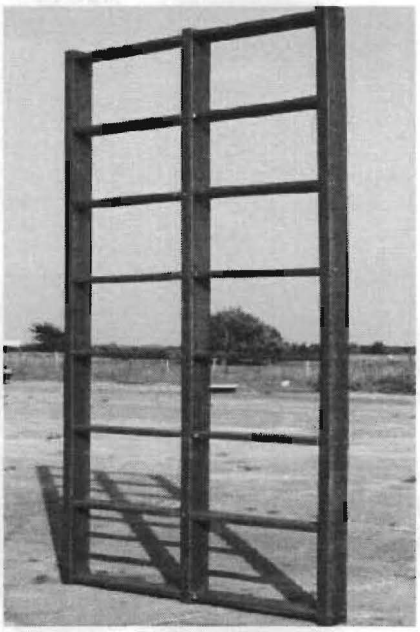

Figure 17. Typical Sheet Plastic Frame

5.3.2 Plastic Lumber

Plastic boards, similar to those used in the lumber industry, are also produced by recycled plastics manufacturers and are used here as exterior members for construction of six modules. Materials required to build a plastic lumber module include two vertical spacers, a multitude of the fiberglass reinforced boards used for horizontal support, and 22 tongue-and-groove boards. Connections include #8 ring-shank nails and screws that are 15.2-cm (6-in.) long and 1.0-cm (0.375-in.) in diameter. Bolts are not a viable option due to the vast quantity that would be required. The frame of a plastic lumber module differs from a sheet plastic frame only in exclusion of the middle spacer.

Once again, the number of plastic boards placed horizontally in the frame depends to some extent on how many nails or screws one wants to use to connect each exterior board to the inner frame. In the frame shown in Figure 18, an exterior board is attached at up to eight locations along the height of the module.

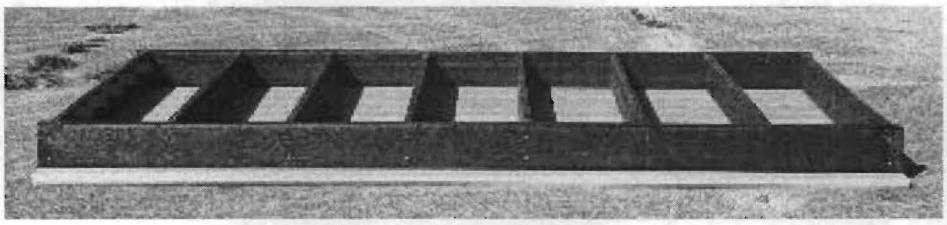

Figure 18. Typical Plastic Lumber Frame

A relatively simple way to build a frame for a plastic lumber module is to cut all horizontal spacers to the same length. Each frame has an overall width of 2.21 m (87 in.). After subtracting the width of two vertical spacers from the overall width, each horizontal board needs to be cut 2.0 m (79 in.) long. The first horizontal board is placed between the two vertical spacers and flush with the ends. Two 15.2-cm (6-in.) long screws having a 1.0-cm (0.375-in.) diameter are driven into each end of the horizontal board from the outside of the vertical spacers. Work proceeds on the other horizontal boards that are distributed evenly along the long frame member until the last horizontal board is placed at the other end of the frame.

Next, tongue-and-groove boards are connected to the interior frame. Because one module will eventually slide next to another, it is important to avoid excessive board overhang that may impede insertion of adjacent modules. The first tongue-and-groove board should be aligned so that it hangs over the edge of the frame 11.4 cm (4.5 in.) and is flush with the bottom of the frame. After securing the board at the bottom with a screw or nail, the overhang of the top is adjusted and secured. Material inconsistencies may cause the lip to overhang more or less than the specified 11.4 cm (4.5 in.) in middle sections which have yet to be connected. This is the reason for the 1.3 cm (0.5 in.) of "play" that was included in determination of size of the inner frame. If the board warps excessively, it must be forced to the correct shape so that the first board overhangs the appropriate amount.

As a next step, the adjacent tongue-and-groove board is aligned so that the tongue of the first board is inserted in the groove of the second board as far as possible. After making sure that the bottom edge is flush with the bottom of the frame, the second board is tacked down in the same manner as the first board. This is the procedure used to connect all of the remaining boards. The last board was often found to overhang the edge of the frame by more than 11.4 cm (4.5 in.) and was therefore trimmed with a saw.

Tongue-and-groove boards are generally produced in a variety of standard sizes. In this case, sizes used lead to an uneven number of boards per face. For a large-scale project, manufacturers should be able to reduce the size of the plastic lumber they produce so that specified widths of modules will have an exact overhang for a certain number of boards. This will lead to more consistent construction of wall modules. Alternatively, frame configurations or column sizes could be altered to accommodate the overhang of a set number of standard-sized tongue-and-grove boards.

5.4 STRENGTHS AND WEAKNESSES OF MODULES

5.4.1 Fiberglass-Reinforced Plastics

Of the six plastic lumber modules that were constructed, four have surfaces with fiberglass-reinforced tongue-and-groove boards. Most interior frames have a combination of fiberglass-reinforced plastics and unreinforced plastics. The fiberglass-reinforced lumber members are more structurally sound than unreinforced timbers because they have more precise dimensional tolerances and higher stiffnesses. This leads to an increased rigidity in the modules which is obviously preferable. Another advantage in use of fiberglass material is that the screws do not strip their holes as easily, and heat does not noticeably deform fiberglass-reinforced lumber.

5.4.2 Connections

While the bolts used as connections are adequate, ring-shank nails and screws proved to be the only aesthetically acceptable connectors. Screws, with their large threads, grip the inner-framework better than ring-shank nails. One drawback of using screws is that they can strip their holes if the internal member is not fiberglass reinforced. However, as shown in Figure 19, not even bolts were immune to accidental damage by a forklift

during construction. Finally, regardless of which type of connection is chosen, care must be taken to use corrosion protection.

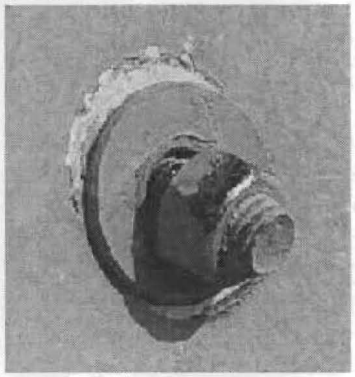

Figure 19. Damaged Bolt

5.4.3 Sheet Panel Thickness

A total of six sheet panel modules were constructed for use in the prototype soundwall. Three modules used bolts and eventually manifested serious warping of the panels as shown in Figure 20. A 1.9-cm (0.75-in.) thick panel was utilized on the final

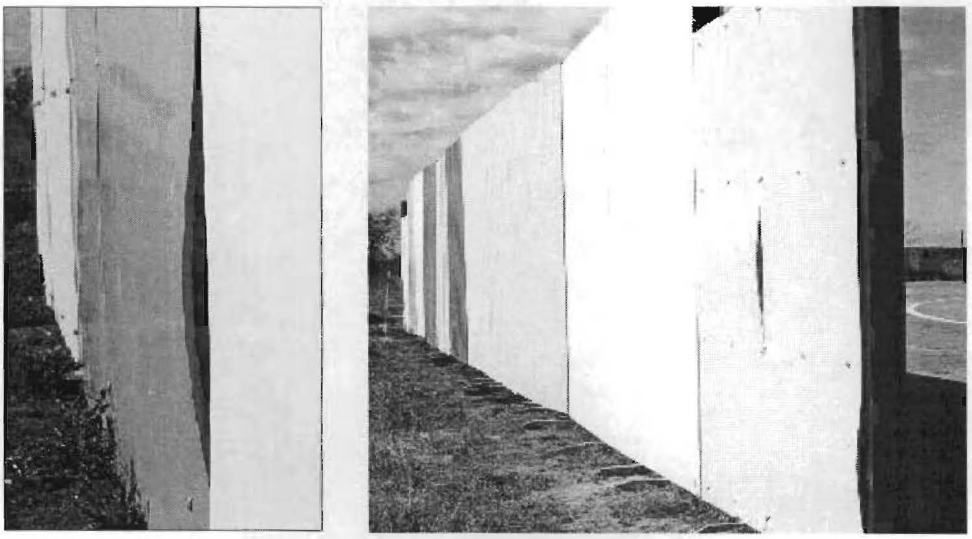

Figure 20. Warped Sheet Panels

module instead of the usual 1.3-cm (0.5-in.) thick panel, but the additional material made little difference as the panel on the exterior still warped. Clearly, connection spacing and clamping force are important for prevention of warping. Bolts that have a higher clamping

force and are spaced 1.22 m (4 ft) apart may contribute to warping. However, there was little warping in the three modules with nails or screws spaced at 0.61 m (2 ft). Six screws were placed along each outer edge and on two rows up the middle. Screws or nails were placed in several other locations on the interior portions of the panel surface. Altogether, each module contains approximately 60 screws and nails.

5.4.4 Frame Configuration

Two types of frames were constructed depending on whether the module had plastic sheets or plastic lumber on the outside surface. Frames used with plastic lumber modules are easier to build and require fewer connections. When attaching surface materials, it is also easier to see where screws or nails are to be placed because the inner frame is not covered (as is the case with the sheet plastic).

An advantage of the frames used with sheet plastic modules is that there is a third vertical member in the center of the frame that provides added bending stiffness; however, the frame is less stiff in the horizontal direction due to the lack of continuity across the middle provided by horizontal boards. For more information on module rigidity see Section 6.3.

5.4.5 Aesthetics

The majority of the people who visited the site agreed that the six plastic lumber modules were the most aesthetically pleasing sections of the soundwall (see Figure 21 [b]). One particular lumber module is especially attractive because it has different colored lumber (see Figure 21 [c]). Vertical lines of the lumber modules also make the transition from module to the next almost indistinguishable.

Three bolted, sheet plastic modules manifested local warping that made them unattractive. The other three modules with sheet plastic that utilized nails or screws appeared to be in good condition after almost a year of exposure to temperature fluctuations of winter and summer (see Figure 21 [a]). Visually, they are rather plain; however, several designs with Texas themes were created so they could be engraved into

the smooth plastic sheet panels (see Appendix E). Only one manufacturer reported successful etching of a design into the plastic; unfortunately, no evidence was presented to the researchers.

Figure 21. Modules: (a) Tan Sheet Plastic; (b) Tan Plastic Lumber; and (c) Multicolored Plastic Lumber

5.4.6 Potential Design Improvements

Vertical members used in the interior frame are composed of unreinforced recycled plastic. As stated previously, these materials are not as stiff as fiberglass-reinforced plastic. Screws strip and nails pull out more easily in unreinforced plastic. For this reason, future construction of recycled plastic soundwalls would do well to incorporate members that have fiberglass reinforcement in the interior frame.

When the project began, maximum available width of plastic sheets was 1.22 m (4 ft). Two sheets were placed side by side to build a module that is 2.44 m (8 ft) wide. Manufacturers now produce sheets that span the full 2.44-m (8-ft) width. These wide panels would affect the design of a sheet plastic module because the vertical spacer in the middle would no longer be necessary. Consequently, the type of frame that is used for the plastic tongue-and-groove lumber could also be used for the sheets.

Another alternative is to build a module that is 3-m (9.84-ft) wide instead of the 2.44 m (8 ft) that is presently used to achieve a standard English width of 8 ft (2.44 m). Design of the frame could easily be adjusted to accommodate new dimensions.

5.5 PREPARATION OF COLUMN FOUNDATION

On September 26, 1996, TxDOT drilled 13 holes at the Riverside Campus of Texas A&M University (see Figure 22). Holes ranged in depth from 1.83 m (6 ft) to 2.44 m (8 ft) with each hole having a diameter of 0.46 m (18 in.). Holes were drilled 2.44 m (8 ft) center to center such that the overall length of the wall was 29.26 m (96 ft). The diameter of the hole was chosen to allow researchers to place a smooth, #3 steel reinforcement spiral with a 7.6 cm (3 in.) pitch around each of the columns in order to confine the concrete. A sand matting was placed at the bottom of each hole to reduce settlement of the structure in the muddy clay soil. Columns were placed in the holes and surrounded by concrete that has a compressive strength of 3.45×10^7 Pa (5,000 psi). All columns were ordered with nominal cross-sectional dimensions of 20.3 cm (8 in.) × 20.3 cm (8 in.).

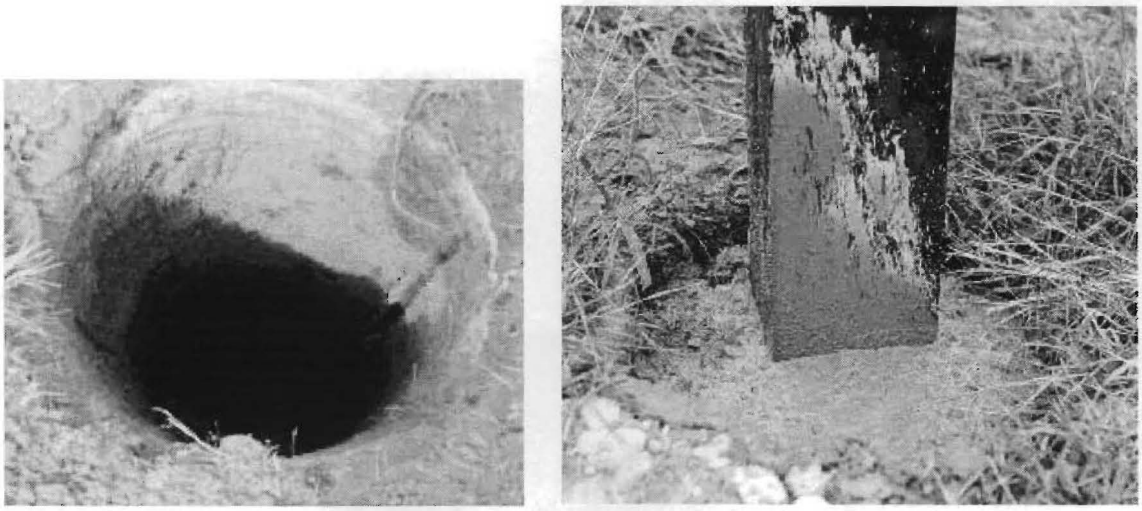

Figure 22. Column Hole and Recently Placed Column Footing

Of the 13 columns, four columns had 1.3-cm (0.5-in.) diameter steel reinforcement bars near each corner and were 5.18-m (17-ft) long. Four more columns had 2.5-cm (1.0-in.) diameter steel reinforcement near each corner of the cross-section and were 5.18-m

(17-ft) long. The remaining five were made from fiberglass-reinforced plastic with a length of 5.49 m (18 ft). The location of these columns are A-D, E-H, and I-M, respectively, as shown in Figure 12 and visually apparent in Figure 24.

5.6 INSTALLATION OF MODULES

Concrete was placed for the foundation for 13 columns and allowed to cure for two weeks. Instead of lifting the modules with a crane as originally planned, the modules were strapped to a forklift and lifted into place (see Figures 23 [a] and [b], respectively). Time to insert all 12 modules was approximately three hours. Installation of all of the modules was relatively easy. A minor problem was encountered in sliding the last module between its columns. This was the first module that was built and the internal frame members were constructed slightly too wide.

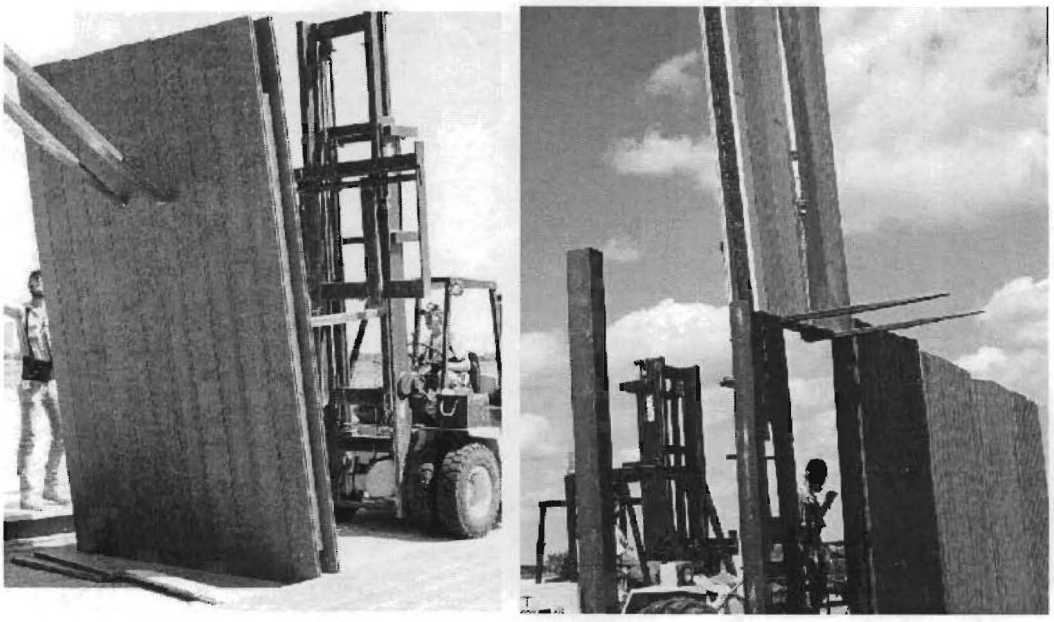

(a) **(b)**

Figure 23. (a) Attachment of Module to Forklift; and (b) Module Insertion

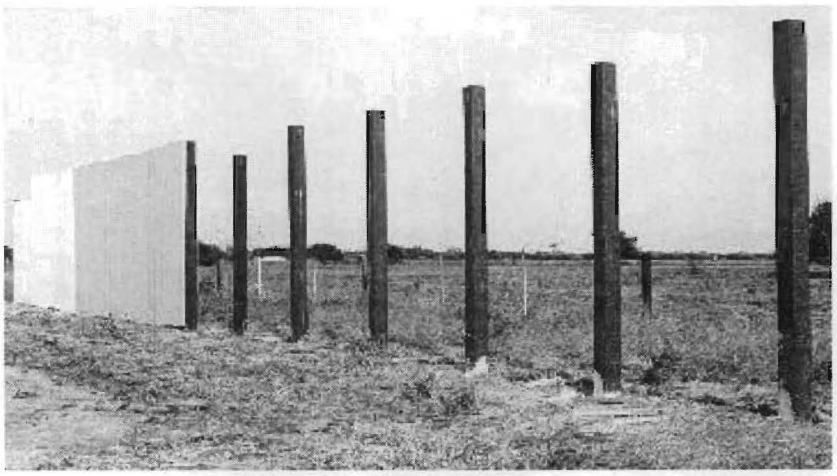

Figure 24. Columns and Partially Constructed Soundwall

5.7 OVERVIEW

A modularized form of design allowed the researchers to create a variety of modules that had uniquely different characteristics. Visual attractiveness of the prototype wall was hindered by this conglomeration of types of wall panels, but it is expected that an aesthetic design could be formulated that would be acceptable both structurally and aesthetically. A potential improvement for future installations could include the addition of a cap along the top of the wall to give the structure a finished appearance.

Construction of the 12 wall panels was completed by a crew of four people in approximately two months. Many refinements could be made in the construction process if a long wall were to be produced by a contractor with more extensive manufacturing capabilities.

Smaller footings were used for the columns than those generally associated with soundwalls of this magnitude, partially because of the light weight of the wall compared to that of a masonry soundwall. A method of determining the appropriate footing size for a soundwall of this type could be developed similar to that proposed in "Development of Standards for Noise Barriers Using Recycled-Plastic Lumber" (Hag-Elsafi et al. 1996).

6. STATIC AND ENVIRONMENTAL TESTS

6.1 MOTIVATION

Static load tests were performed on three types of columns and five types of modules. Columns were tested to determine their stiffness, while several modules were tested to determine the structural rigidity of each combination of frame and surface materials. Results from these tests make it possible to calibrate analytical and finite element simulations and ascertain which frame configurations optimize structural rigidity.

In addition to static test results, effects of temperature change and ultraviolet radiation on the soundwall are discussed in this chapter. Based on observations of the soundwall being exposed to almost one year of extreme weather conditions, conclusions are made with regard to durability, or weatherability, of the recycled plastic structure.

6.2 COLUMN STIFFNESS

A schematic of the three types of column cross-sections is shown in Figure 25. To determine the stiffness of each column, a horizontal concentrated load was imposed at the top of the column with a pulley system. Horizontal displacement was measured at a distance x from the top of the column with a linear-variable differential transformer (LVDT) as diagramed in Figure 26.

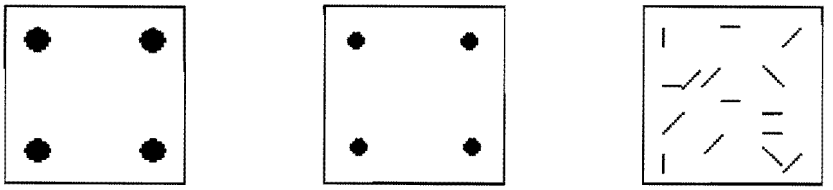

(a) (b) (c)

Figure 25. Cross-Section of Columns: (a) #8 Steel-Reinforcement; (b) #4 Steel-Reinforcement; and (c) Fiberglass-Reinforcement

Deflection of a cantilever column with a concentrated load at the end is given by (Boresi et al. 1993):

$$\Delta = \frac{P}{6EI}(2L^3 - 3L^2x + x^3) \tag{5}$$

where E is modulus of elasticity (N/m^2), I is the moment of inertia (m^4), P is an applied load (N), L is height of the column (m), and x is the distance from the load to the point of measured deflection (m).

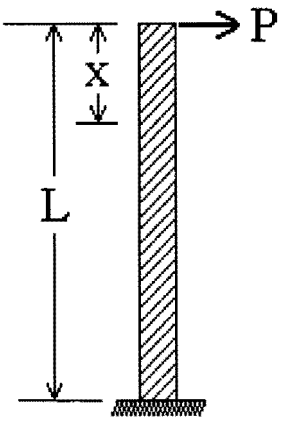

Figure 26. Cantilever Column with Concentrated Load at Free End

Column height is assumed to extend from the free end of the column to the top of the concrete footing; therefore, estimation of a length to equivalent fixity, which might be associated with a pylon in a soil foundation, is unnecessary. Equation (5) can be rearranged and combined with experimental load-deflection data to determine the stiffness, EI, of the three types of columns. Results from the tests are summarized in Table 4.

A horizontal load of 274 N (62 lb) induced a deflection of 0.9 mm (0.035 in.) in the #8 steel-reinforced column resulting in a calculated stiffness of 714.9 kN-m^2 (249,000 ksi). The column with the #4 steel-reinforcement deflected more than the other two columns and correspondingly had the lowest stiffness, 236.5 kN-m^2 (84,000 ksi). Meanwhile, the fiberglass-reinforced column outperformed the #4 steel-reinforced column by allowing a deflection of only 1.6 mm (0.062 in.). The approximate stiffness of the fiberglass-reinforced column is 1.8 times that of the #4 steel-reinforced column.

The #8 steel-reinforced column is unquestionably the most rigid of the three types of columns, but improved stiffness comes at a cost of $74.90/meter. In comparison, the fiberglass column costs $57.80/meter making it economically favorable compared to either of the steel-reinforced columns (see Table 4).

Table 4. Stiffness of Columns

Column Type	P (N)	L (m)	x (m)	Δ (m)	Stiffness (kN-m^2)	Cost ($/m)
#8 steel-reinforcement	274	3.19	1.89	0.0009	714.9	74.90
#4 steel-reinforcement	271	3.18	1.96	0.0024	236.5	65.60
Fiberglass-reinforcement	265	3.53	2.24	0.0016	429.3	57.80
Conversion: kip-in.^{2} = 2.87 N-m^2						

6.3 MODULE RIGIDITY

As shown in Figure 27, five modules were removed from the test section of the full-scale prototype soundwall and placed on wooden supports. Masses were sequentially applied at the center of each module until a total of 738 N (166 lb) was reached. Deflection was measured with an LVDT located near the point of load application. Simple supports were placed along two parallel edges of the modules when testing transverse rigidity as diagramed in Figure 28 (b).

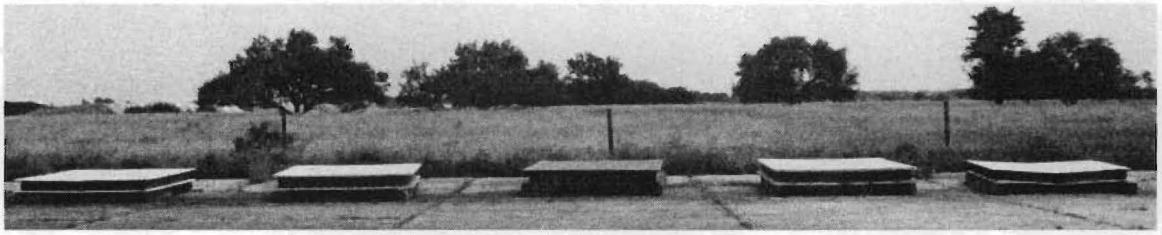

Figure 27. Modules Removed for Static Testing

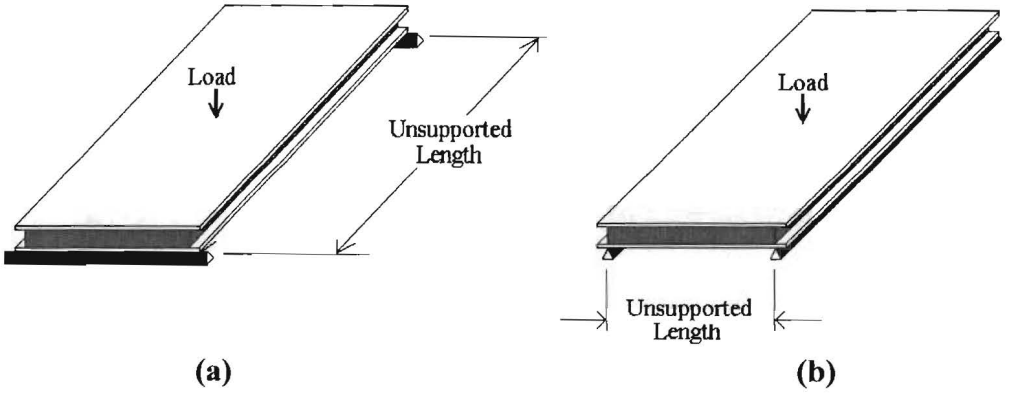

Figure 28. Support Locations for (a) Long Span; and (b) Short Span

Force-deflection data from the tests are shown in Figure 29. The relationship between force and deflection is not always linear due to viscoelastic behavior of the recycled plastic material. When supports are placed along the short dimension of each

module, plastic lumber modules allow less deflection than sheet plastic modules. The sheet plastic modules have three continuous members in the interior frame compared to only two members in lumber modules; these continuous members provide stiffness to resist bending (see Figures 17 and 18, respectively). Tongue-and-groove boards that are 5.08-cm (2-in.) thick on the plastic lumber modules provide more rigidity against bending than modules with the 1.27-cm (0.5 in.) thick sheets that have an extra vertical spacer. An unreinforced plastic lumber module, which is also more rigid than a sheet plastic module, is not as rigid as the fiberglass-reinforced lumber modules. This is expected since fiberglass-reinforced plastics are stiffer than unreinforced plastics.

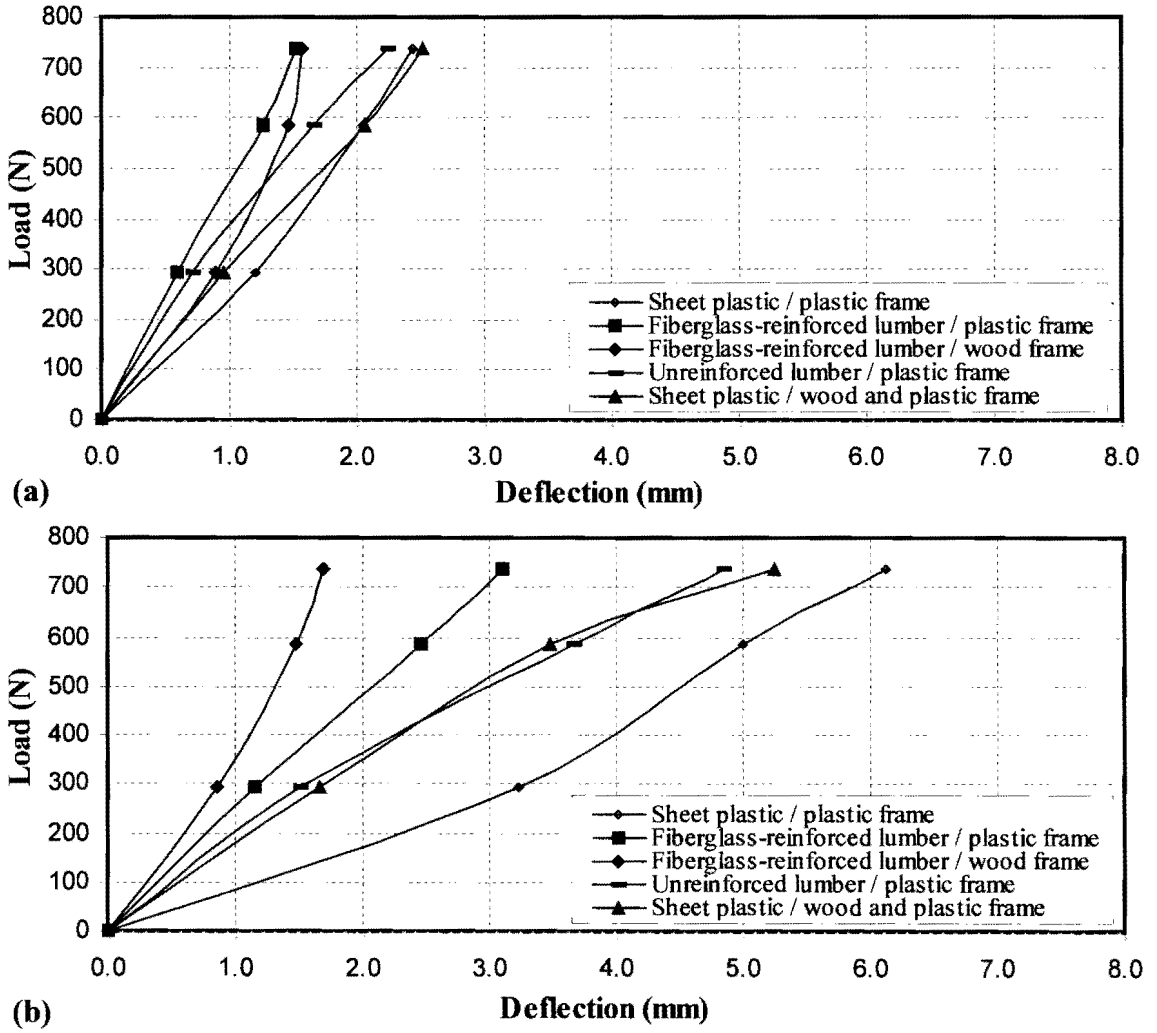

Figure 29. Force-Deflection Curves: (a) Short Span is Unsupported; and (b) Long Span is Unsupported

Plastic lumber modules also perform better than the sheet modules in resisting bending in the short span direction (i.e., supports are placed along the long dimensions) due to the fact that horizontal members of the interior frame are continuous across the entire width of the module. In sheet plastic modules, insertion of a vertical spacer in the middle of the frame results in discontinuity of the horizontal boards. Attachment of these short boards to the long center frame member is not truly rigid and allows additional rotation (see Figure 17).

6.4 EFFECTS OF TEMPERATURE

A simple monitoring system was devised for the prototype wall to measure horizontal motion of the top of each column relative to its base. The purpose is to reveal creep, bowing, or settlement of the structure. A plumb bob was hung from a screw that was embedded in the top of each of the 13 columns. By measuring the distance of the plumb bob from a defined point at the base of the column, it was possible to measure two orthogonal components of displacement that lie in a plane that is parallel with the ground (see Figure 30). This method assumes that the base of the column is relatively "fixed" and does not undergo rotation or displacement.

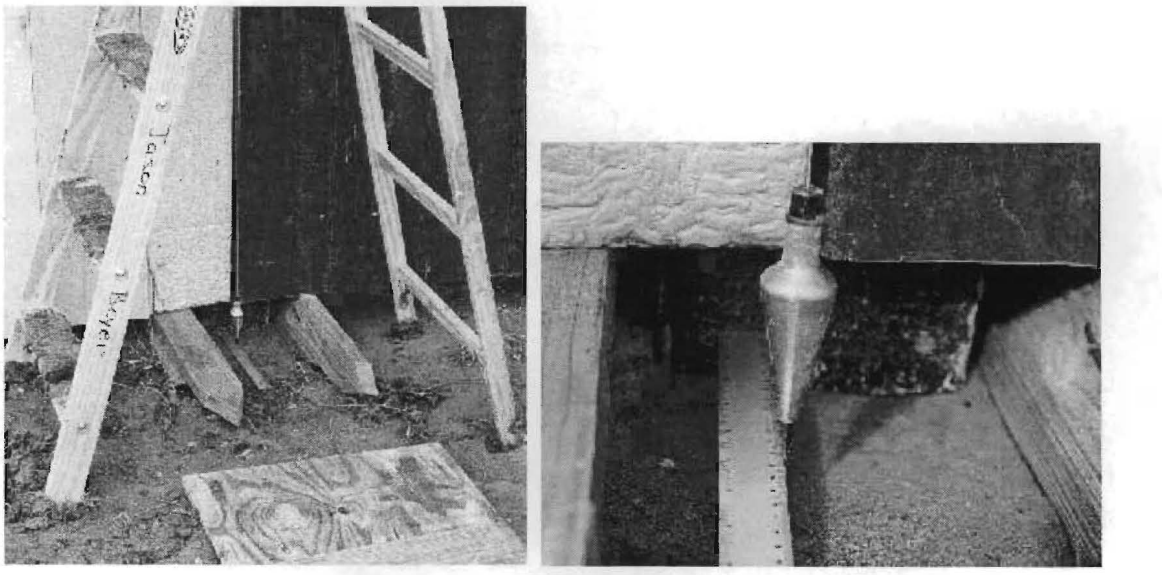

Figure 30. Plumb Bob: (a) Setup; and (b) Measurements

Measurements were taken approximately once a month for six months after the wall was constructed. Displacements of columns in the direction of the length of the wall were

small compared to displacements normal to the plane of the wall and are neglected in what follows. An elevation view of the wall in Figure 31 illustrates deflection during each reporting period. Dates of measurement and weather conditions are also listed in Table 5. Measurements taken on the first date are taken as a datum for comparison with later readings. Maximum recorded deflection was 28 mm (1.1 in.) which occurred on the 117th day after construction when the weather temperature was freezing. Trends in wall movement were irregular; evidently, the temperature at which measurements were taken played an important role in affecting the measured values. On one occasion, measurements were taken every 30 minutes for two hours as a simple check on repeatability. Deflections changed less than 3 mm over the course of these five readings.

Table 5. Dates and Weather Conditions of Plumb Bob Measurements

Reporting Period	Days after Construction	Weather Conditions
1	0	Late afternoon, hot, dry, breezy
2	27	Early morning, mild, dry, windy
3	58	Late morning, cold, soaked, windy
4	89	Late morning, chilly, damp, calm
5	117	Late afternoon, freezing, damp, calm
6	149	Late morning, mild, dry, breezy

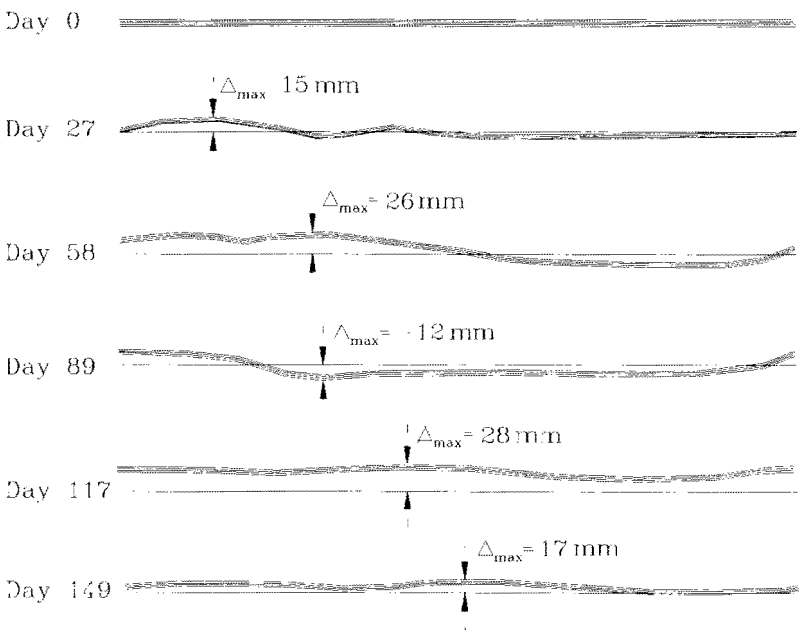

Figure 31. Measured Displacement at the Top of the Prototype Soundwall

On a relatively hot day in August 1997 measurements of displacement at the top of columns C, G, and K (see Figure 12) were taken every two hours with a plumb bob. Displacement versus temperature was recorded to determine the effect of thermal expansion of the recycled plastic materials due to intense heat of the sun (see Figure 32). Columns C, G, and K contain #4 steel reinforcing bars, #8 steel reinforcing bars, and fiberglass, respectively. Temperature was measured with an outdoor thermometer that was attached to the middle of the outside surface of the module so that the approximate surface temperature of the plastic materials could be recorded as they absorbed solar heat. The bulb of the thermometer was covered from exposure to direct sunlight. Measurements were taken at 7:15 a.m., 9:05 a.m., 11:15 a.m., 1:15 p.m., and 3:15 p.m. and the corresponding temperatures were 26 °C, 36 °C, 42 °C, 44 °C, and 40 °C, respectively. Maximum deflection at the top of the columns relative to the base during the recording period was 6 mm (0.2 in.) which occurred near noon when the temperature was 44 °C (110 °F) on the surface of the plastic. At 1:15 p.m., velocity of the wind increased and the temperature inside the wall cooled causing the tops of the columns to move back toward their position at the beginning of the recording period.

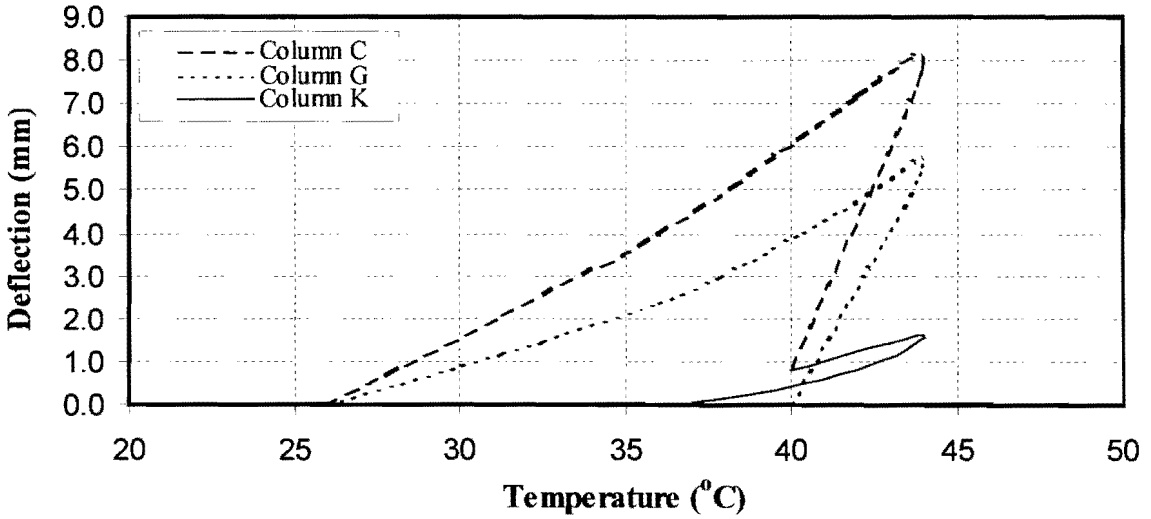

Figure 32. Wall Position Versus Temperature

From these measurements, it is clear that the top of the columns continuously change position throughout the day; however, the magnitude of change in position of the

top of the wall relative to the base is imperceptible to the human eye. Only approximate deflection was measurable by this simple technique; large deflections did not occur over the six-month period. Long-term deflections of the wall over a long period of time were deemed to be within acceptable limits and not likely to affect serviceability of the structure.

6.5 SUMMARY

Performance of the steel- and fiberglass-reinforced columns under static and thermal loads showed that they provide a viable option to traditional materials for support of low- to mid-height recycled plastic soundwalls. Plastic columns reinforced with steel have an advantage in that additional steel can be included to increase stiffness; unfortunately, increasing the amount of steel significantly adds to cost.

With respect to design of modules, fiberglass-reinforced lumber modules were shown to have higher stiffness in both the short and long-span directions compared to sheet plastic modules. Use of plastic lumber on the exterior surface provides more stiffness to resist bending about an axis parallel with the base of the wall compared to sheet plastic. Also, in the short span direction, lumber modules are stiffer because horizontal members in the frame are continuous in the horizontal direction. Performance of sheet plastic modules could be improved by removing the weak section along the center (see Figure 15). After the prototype soundwall was completed, one manufacturer stated that sheet plastic is now available in 2.44-m (8-ft) widths. In this case, the middle spacer of the interior frame would be unnecessary and the frame used to build the lumber modules could also be used with the sheet plastic modules.

After observing the soundwall for a period of nearly one year to see if it could withstand the extreme weathering conditions associated with winters and summers in Texas, it is concluded that the recycled plastic soundwall is suitable for trial installation. Localized bowing did occur on some of the sheet plastic modules, but the plastic lumber modules and the soundwall as a whole showed few effects from weathering and ultraviolet radiation exposure. There was also no noticeable change in the orientation of the soundwall.

7. DYNAMIC TESTS

7.1 INTRODUCTION

Knowledge of fundamental dynamic properties of a structure, including natural frequencies, damping ratio, and mode shapes, adds insight as to how a system will respond under environmental loads such as wind and impact. These dynamic characteristics are also important in evaluating the long-term durability and serviceability of a soundwall. Three methods that can effectively be applied in the dynamic analysis of a soundwall are system identification, experimental analysis, and numerical simulation. The former two methods are taken up in this chapter. The primary objective in following discussion is to aid in determination of the degree to which the prototype soundwall is sensitive to oscillatory wind loadings. Numerical analyses of the structure are discussed in the following chapter.

7.2 SYSTEM IDENTIFICATION

System identification is the process of developing or improving a mathematical representation of a physical system using experimental data (Juang 1994). For the present application, the physical system of interest consists of a soundwall as well as the column and module subcomponents. Once the salient dynamic properties of the soundwall are determined, reasonably accurate predictions of dynamic behavior can be made for strong wind events.

One branch of system identification for structures is modal parameter identification, which is generally referred to as modal testing. In modal testing, measurement of signals produced by a dynamically excited structure that is assumed to behave linearly allows modal parameters such as damping, frequencies, mode shapes, and modal participation factors to be identified. Originally, modal testing and parameter identification techniques were independently developed in fields of structural testing and automatic control, respectively; however, they are currently becoming unified due to interaction of the two fields.

Another approach through which modal parameters can be identified concentrates on analyzing experimental data in the time and frequency domains. Curve-fitting procedures can be invoked to compute frequency response functions (FRFs) before extracting modal parameters. Some of these procedures include single degree of freedom (SDOF) curve-fitting methods, multiple degree of freedom (MDOF) curve-fitting methods, and multi-curve fitting methods (Ewins 1984).

After the 1960s, time-domain approach techniques began to gain more attention. Most of these algorithms derive from the complex exponential method. The first important procedure of this type is known as the Ibrahim time-domain method (ITD) (Pappa and Ibrahim 1981). Since then, two other major approaches have been developed in the time-domain arena: the polyreference method (Vold et al. 1982) and the eigensystem realization algorithm (ERA) (Juang and Pappa 1988). The latter method was developed by control theorists for modal parameter identification and model reduction of dynamic systems using test data (Juang 1997). A recent development in the time-domain approach to system identification uses state-space system realization with correlation of input and output data. This approach can be implemented with a software package of MATLAB routines known as SOCIT (Juang et al. 1996).

SOCIT, an acronym for System/Observer/Controller/Identification Toolbox, is a collection of MATLAB® files that implement a variety of modern system identification techniques containing both time and frequency-domain algorithms. These algorithms are based on linear state-space formulations. They use sampled pulse and impulse system response histories for discrete and continuous systems, respectively, that are known as Markov parameters. Time-domain or frequency-domain data are curve fitted by determination of certain parameters. An eigensystem realization algorithm (ERA) is then used to obtain a state-space model, and system parameters can be extracted by finding the eigenvalues and eigenvectors of the realized state matrix. A brief description of three algorithms in SOCIT that perform these functions is as follows:

1. **SRIM.m** - forms a matrix from what is termed an "information matrix" that is determined from input and output data in the time domain. It outputs frequency and damping values (see Appendix C).

2. **IDENGINE.m** - uses an observer/Kalman filter identification technique to directly identify a discrete model from arbitrary input and output time histories.

3. **FRF2SS.m** - identifies a state-space model from a frequency response function.

7.3 EXPERIMENTAL ANALYSIS

As mentioned above, many methods have been developed for identification of modal parameters in the fields of structural testing and control system identification. Traditional experimental techniques also exist by which modal parameters can be extracted from test data. In this study, a single degree of freedom (SDOF) peak-amplitude method in the frequency domain is adopted to analyze data collected from the soundwall structure. Results of this approach are directly compared with results obtained via the system identification software, SOCIT.

The peak-picking method assumes that in the vicinity of a resonant frequency the response of the structure is dominated by the mode whose natural frequency is closest to the resonant frequency. This method generally works adequately for a structure that has a frequency response function (FRF) that exhibits well-separated modes and possesses a moderate level of damping. Although these requirements may limit applicability of the method, it is still useful in obtaining an initial estimate of the required parameters such as frequency and damping. An outline of the method is as follows (Ewins 1984):

1. Individual resonance peaks are detected on a Bode plot of the FRF, and the frequency at maximum response amplitude is taken as the natural frequency of the mode (ω_r);

2. The frequency bandwidth of the mode with a response level of $1/\sqrt{2}$ of the peak amplitude is determined ($\Delta\omega$). The two points in the frequency domain, ω_1 and ω_2, are deemed half-power points;

3. Damping of the mode is estimated from the following formula especially for inertance FRF functions where the input is force and the output is acceleration:

$$\varsigma_1 = \frac{\omega_1(\omega_2 - \omega_1)}{2\omega_1\omega_2} \tag{6}$$

4. The unscaled mode shape can be obtained by comparing both the ratio of the peak amplitudes and the phase angles of different FRFs at the same natural frequency.

This peak-amplitude method is implemented with a MATLAB® algorithm entitled "**MODEL.m**" (see Appendix C). The algorithm computes natural frequencies, damping ratios, and unscaled mode shapes from given input and output time histories.

7.4 INSTRUMENTATION

Input and output data needed by the system identification method includes impact hammer forces and acceleration responses. Data needed for wind simulations in Chapter 9 include time-histories of wind speed and direction. These data were acquired from the prototype soundwall with a data acquisition unit and other standard measurement devices as outlined in the following description.

Data acquisition was performed with hardware from National Instruments™ in conjunction with its companion LabVIEW® virtual instrument software. The hardware includes a SCXI-1000 chassis that holds four conditioning units, generally SCXI-1121, 4-channel isolation amplifiers (see Figure 33). Each conditioning unit is connected to a SCXI-1321 terminal block that collects up to four channels of data. All of the data are directed to a high performance, software-configurable, 16-bit data acquisition board (AT-MIO-16E) containing a 16-bit, 10 μsec sampling analog-to-digital converter.

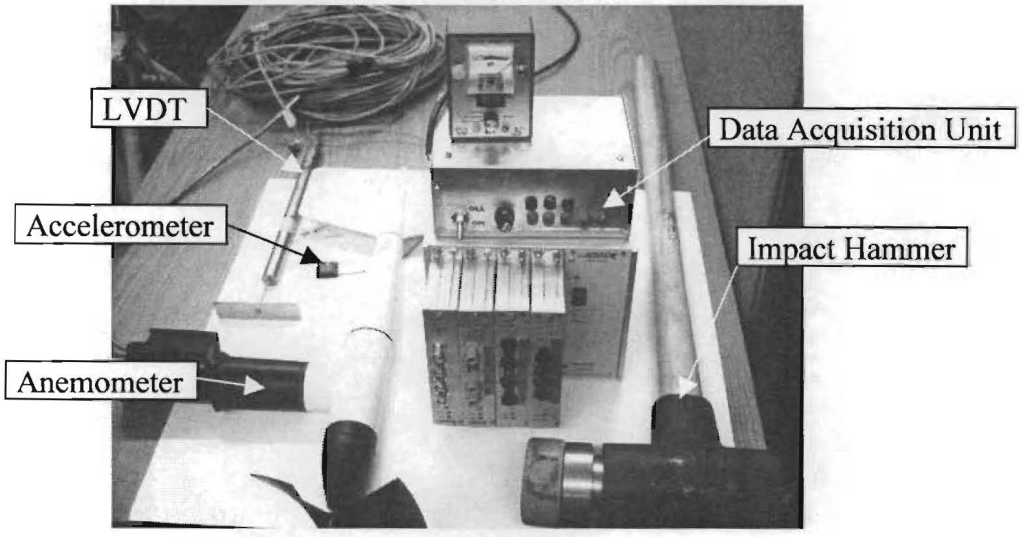

Figure 33. Measurement Devices

Eleven Endevco variable capacitance accelerometers that have a maximum range of ±10 g (model 7290A-10) were used to measure acceleration response of columns and

modules in the prototype soundwall (see Figure 33). Primarily, accelerometers were used to record accelerations induced by an impact hammer and strong winds.

Several direct current linear variable differential transformers (LVDTs) manufactured by Schaevitz Engineering™ (model 2000DC-D) were used to measure displacements (see Figure 33).

A Lixie impact hammer with a piezo conditioner (SN 9314) and load cell (SN 3304) was used to impart motion to the structure and develop a time history of the impact force for various components of the soundwall (see Figure 33). It was necessary to collect data at a rate higher than 100 Hz to obtain an accurate record of the impulse imparted by the impact hammer.

An anemometer manufactured by Young, Inc., was used to collect wind data (see Figure 33). The instrument was calibrated in a wind tunnel and was used to measure wind speed and direction. A MATLAB file entitled **WINDTOOL.m** was developed to convert wind speed and rotation into a wind pressure force acting orthogonal to the soundwall.

7.5 THEORY

The full-scale soundwall is composed of columns and modules made from a variety of materials and arranged in several geometric orientations. This variety leads to complications in dynamic analysis. To simplify investigation of the system, an impact hammer was used to impart transient excitation to individual columns, individual modules and, finally, to the entire soundwall.

Time histories of input and output data are gathered from a structure that is set into motion by loadings from the impact hammer. A frequency-domain method of dynamic analysis of the structure can be implemented through use of a Fourier transform that is defined as (Lutes and Sarkani 1997):

$$\tilde{f}(\omega) = \frac{1}{2\pi}\int_{-\infty}^{+\infty} f(t)e^{-i\omega t}dt \qquad (7)$$

where $\tilde{f}(w)$ represents the transformed function in the frequency domain, ω is frequency, t is the time, $f(t)$ is a function describing the load history in the time domain, and i is the unit imaginary number. This operation is performed on a set of numerical data using an efficient computation known as the fast Fourier transform (FFT):

$$X(k) = \sum_{j=1}^{N} x(j)\omega_N^{(j-1)(k-1)} \tag{8}$$

where $X(k) = fft(x)$ are the transformed vectors of length N and:

$$\omega_N = e^{\frac{-2\pi i}{N}} \tag{9}$$

is an N^{th} root of unity.

An FFT can be implemented on a single set of numerical data, such as an input or output time-history, to transform data into the frequency domain. However, other useful information can be gained through use of a harmonic transfer function, which is a ratio of the Fourier transform of the acceleration response to the Fourier transform of the input excitation:

$$\ddot{H}(i\omega) = \frac{\ddot{x}(i\omega)}{F(i\omega)} \tag{10}$$

where $\ddot{x}(i\omega)$ is the Fourier transform of the acceleration response and $F(i\omega)$ is the Fourier transform of the excitation. An advantage of using an FFT is that many mathematical software packages are readily capable of performing this operation.

Complex arithmetic is introduced through application of an FFT; therefore, it is necessary to convert to polar notation for easy recognition. Polar notation consists of a real amplitude and phase angle. The real amplitude is the square root of the sum of the squares of the real and imaginary components:

$$A(\omega) = \sqrt{R(\omega)^2 + I(\omega)^2} \tag{11}$$

where $A(\omega)$ is the real amplitude, $R(\omega)$ is the real component, and $I(\omega)$ is the imaginary component.

The phase angle is the inverse tangent of the ratio of the imaginary component to the real component:

$$\theta(\omega) = \tan^{-1}\left(\frac{I(\omega)}{R(\omega)}\right) \tag{12}$$

7.6 TEST RESULTS

7.6.1 Impact Excitation on Columns

Impact hammer tests were conducted on three types of columns used to construct the prototype wall: #8 steel-reinforced plastic, #4 steel-reinforced plastic, and fiberglass-reinforced plastic. An accelerometer was placed at the top of each column and an impact hammer was used to strike each column at approximately midheight (see Figure 34). The peak-amplitude method and SOCIT were then used to determine natural frequencies and damping of each column.

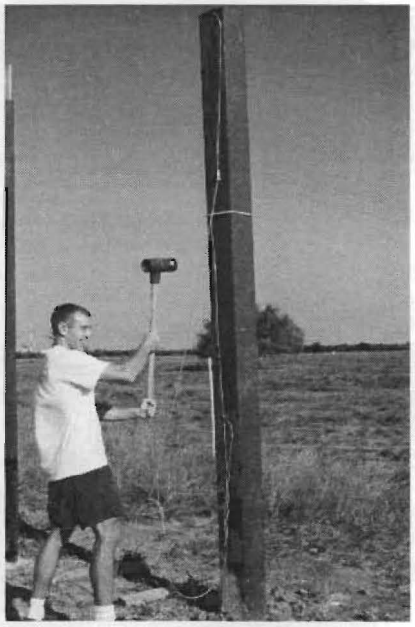

Figure 34. Impact Hammer and Column

Typical time-history and frequency-domain representations of the impact force from the hammer are shown in Figures 35 (a) and (b), respectively. Figure 35 (c) shows the corresponding phase angle versus frequency. MATLAB algorithms used to carry out these numeric operations are listed in Appendix C (see **TRANSFER.m** and **FFT.m**).

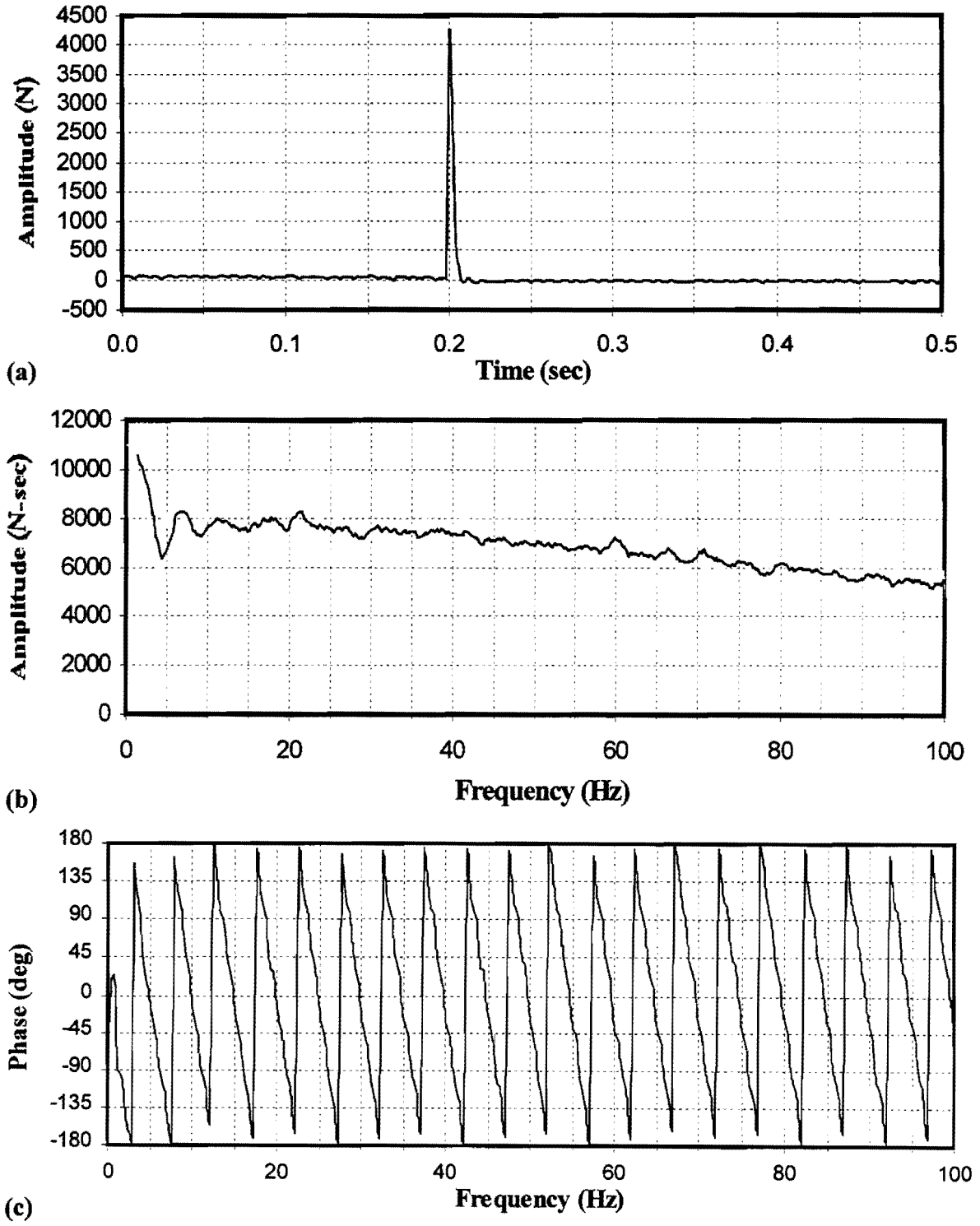

Figure 35. Typical Impact Hammer Excitation: (a) Time-History of Force; (b) FFT Amplitude; and (c) FFT Phase Angle

The frequency-domain counterpart of an ideal impulse load is termed "white noise," and it has constant amplitude over the entire frequency domain. The goal is to excite all possible modes of vibration without any truncation caused by incomplete frequency content of the input. A time-history of the acceleration response along with the amplitude and phase angles of transfer functions as computed by Equations (11) and (12), respectively, are shown in Figures 36-38 for each type of column. Predictions of the first three modal frequencies and corresponding percent critical damping ratios are computed by the peak-amplitude method (see Equation 6) as well as by SOCIT and are listed in Table 6.

Table 6. Frequencies and Damping of Columns

Type of Column	Method of Identification	1st mode		2nd mode		3rd mode	
		ω_1 (Hz)	ξ_1 (%)	ω_2 (Hz)	ξ_2 (%)	ω_3 (Hz)	ξ_3 (%)
#8 steel-reinforced column	Peak-amplitude	6.10	1.86	33.94	2.86	80.08	3.92
	SOCIT	6.07	1.87	33.53	2.83	79.41	3.74
#4 steel-reinforced column	Peak-amplitude	4.40	2.54	25.88	2.09	68.85	3.48
	SOCIT	4.46	2.65	25.99	3.15	68.18	3.46
Fiberglass-reinforced column	Peak-amplitude	4.88	3.36	30.03	2.51	81.79	2.46
	SOCIT	4.96	3.40	29.76	2.41	81.04	2.87

The first modal frequency (ω_1) of each column is clearly evident from the plot of the transfer function. Consequently, the peak-amplitude method and SOCIT had little trouble determining the frequency (ω_i) and damping (ξ_i) associated with each mode. Results from both the SOCIT package (using the **SRIM.m** algorithm in Appendix C) and the peak-amplitude method are in good agreement. While damping is small for all of the columns, the highest value of 3.4% occurs for the fiberglass-reinforced column in the first mode. Damping contributions for the 2nd and 3rd modes decreased for the fiberglass column, but increased for the two steel-reinforced columns in the 2nd and 3rd modes.

Several factors affect results obtained for each individual column. One factor is the height of the column. None of the three columns was exactly 3.66 m (12 ft) in height as proposed in the prototype soundwall design; however, it is assumed that a minor difference in height would result in only slight changes in natural frequencies. Another simplifying assumption made for the freestanding columns is that there are no effects from flexibility of the soil and the concrete footing.

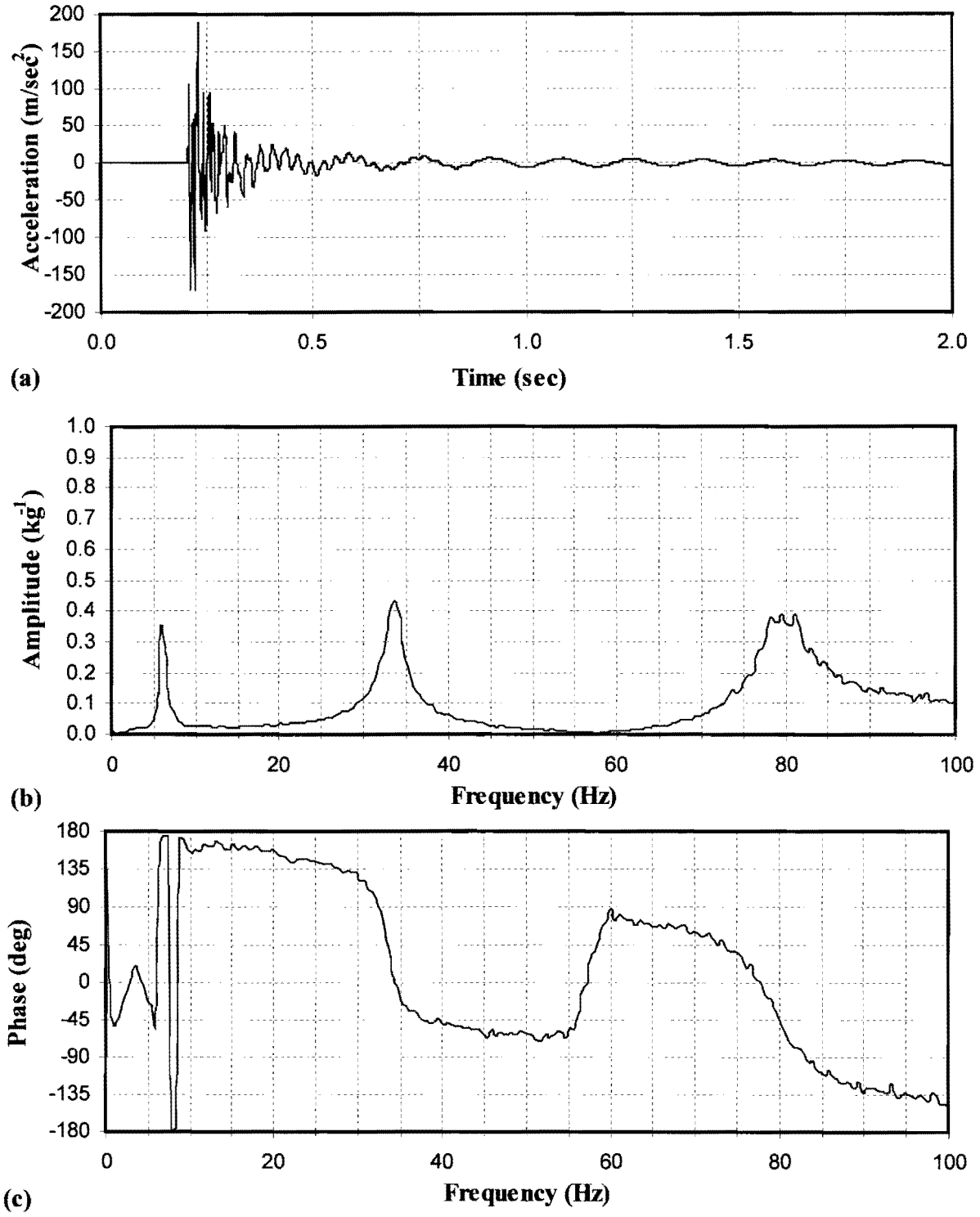

Figure 36. #8 Steel-Reinforced Column Response to Impact: (a) Time-History of Acceleration; (b) Transfer Function Amplitude; and (c) Transfer Function Phase Angle

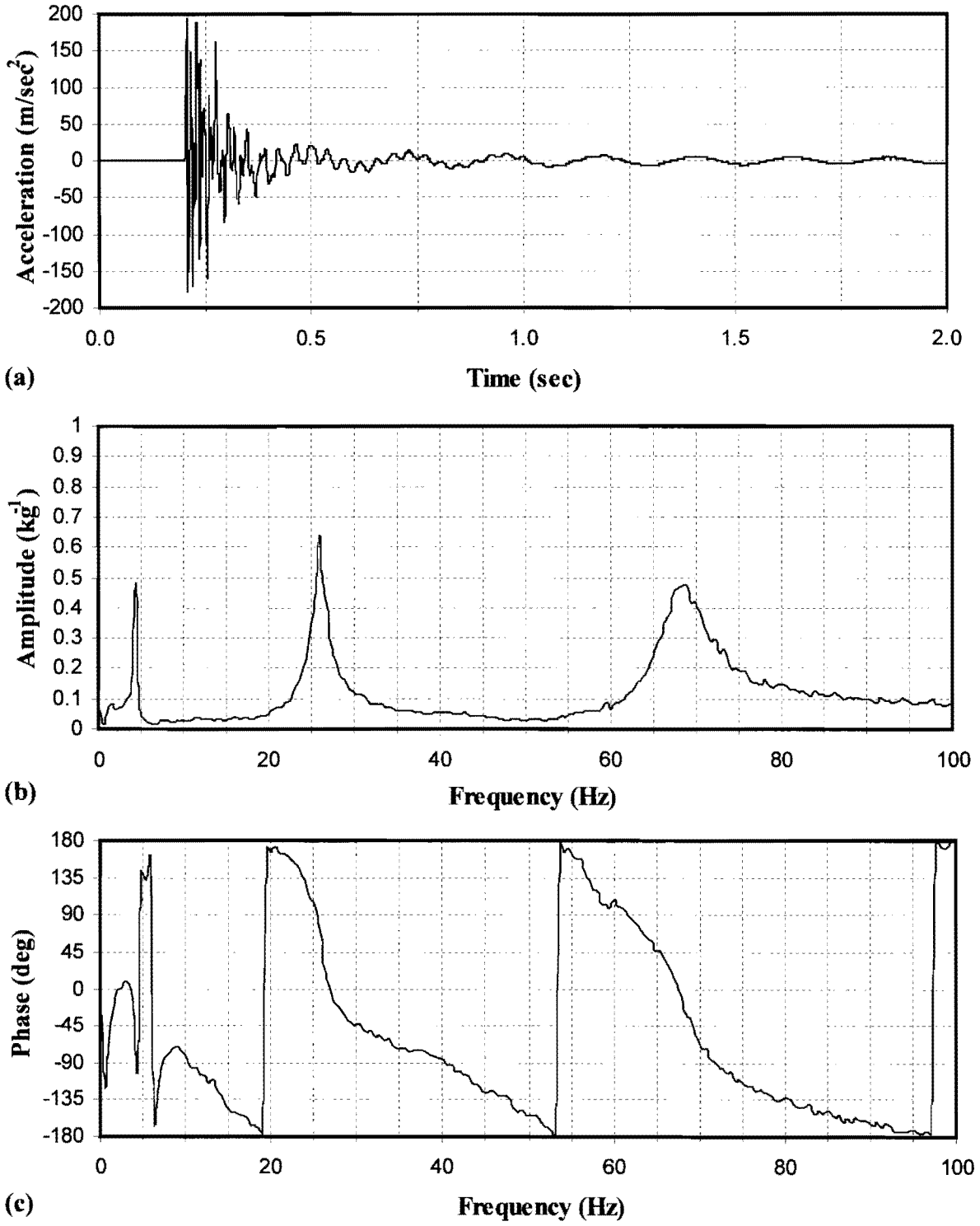

Figure 37. #4 Steel-Reinforced Column Response to Impact: (a) Time-History of Acceleration; (b) Transfer Function Amplitude; and (c) Transfer Function Phase Angle

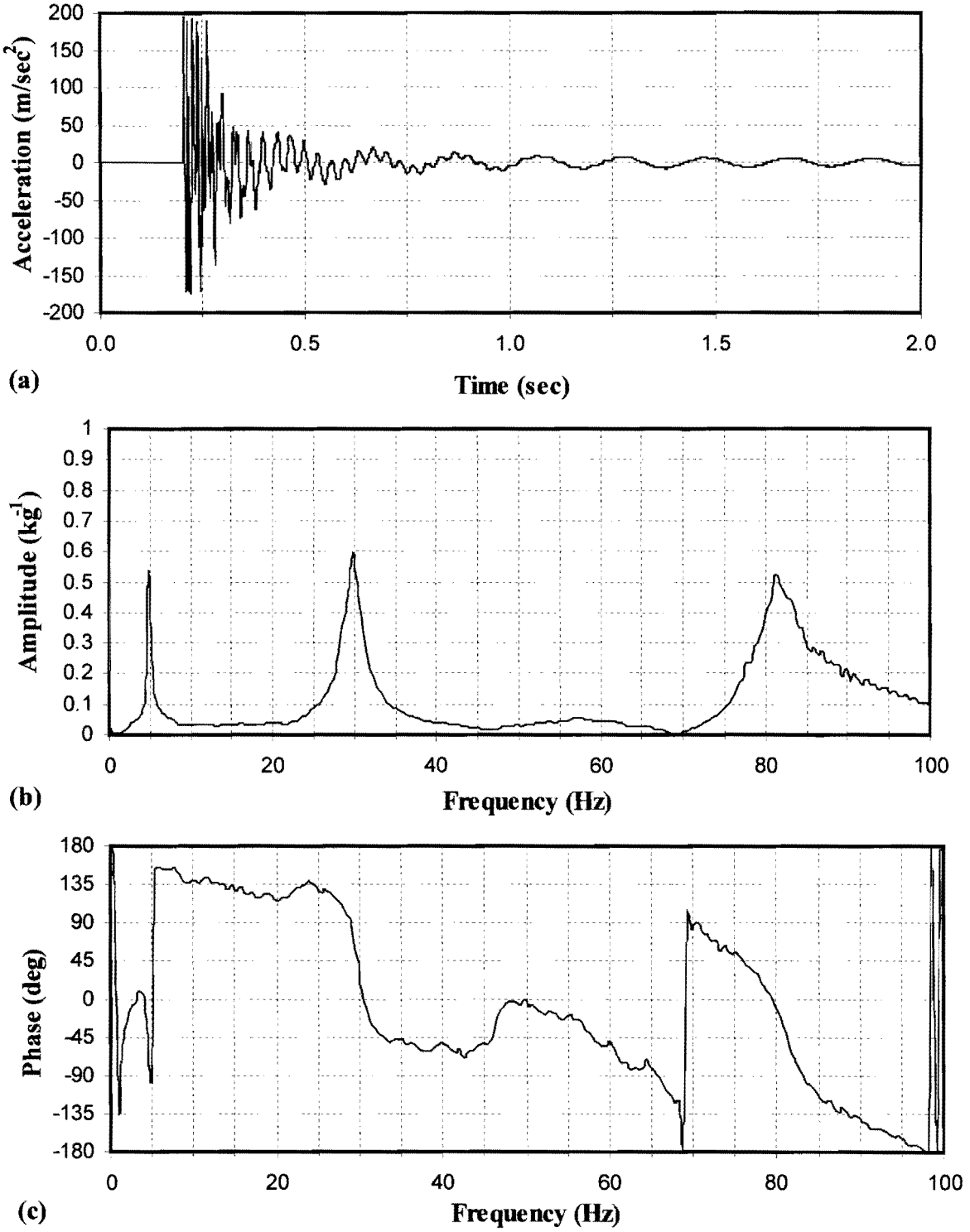

Figure 38. Fiberglass-Reinforced Column Response to Impact: (a) Time History of Acceleration; (b) Transfer Function Amplitude; and (c) Transfer Function Phase Angle

7.6.2 Data Acquisition for Two Modules

As an intermediate step in determination of dynamic properties of the entire soundwall, two adjacent modules and their supporting columns were isolated and tested so that a comparison could be made between dynamic properties of a short and long span of wall. As shown in Figure 39, modules 1-4 and 7-12 were removed from the structure and modules 5 and 6 were supported by three columns. An accelerometer was placed at the top of module 5 and instead of using the impact hammer, modules 5 and 6 were excited into harmonic resonance through rhythmic pushing on the column between the two modules. Once the structure was in resonance, pushing was discontinued and acceleration response was recorded (see Figure 40 [a]). No input force was recorded.

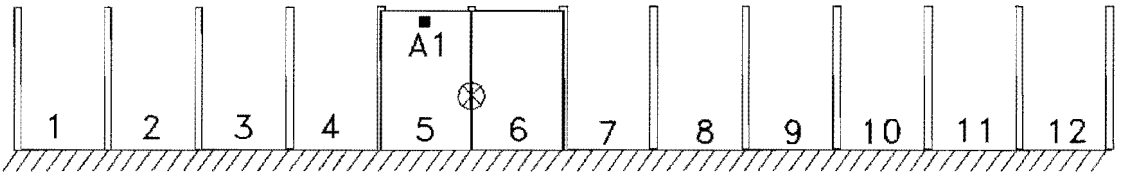

Location of Accelerometer
Location of Loading

Figure 39. Accelerometer Placement on Two Modules

Acceleration data were transferred to the frequency domain by an FFT (see Figure 40 [b]). It is not possible to execute SOCIT algorithms on the data that was collected since system identification methodology requires both input and output data. However, the peak–amplitude method is applied to determine natural frequencies and damping for the two module subsystem (see Table 7). The first three natural frequencies of the two module system were determined to be 2.33, 9.47, and 11.85 Hz.

Table 7. Frequencies and Damping of Two Adjacent Modules

Structure	Method of Identification	1st mode		2nd mode		3rd mode	
		ω_1 (Hz)	ξ_1 (%)	ω_2 (Hz)	ξ_2 (%)	ω_3 (Hz)	ξ_3 (%)
Two Modules	Peak-amplitude	2.33	3.53	9.47	5.65	11.85	6.57

The most important feature of these results is that the first resonant frequency is much lower than frequencies associated with the columns (see Table 6), while damping for the two module system is notably higher for the second and third modes in comparison with damping values obtained from tests on single columns.

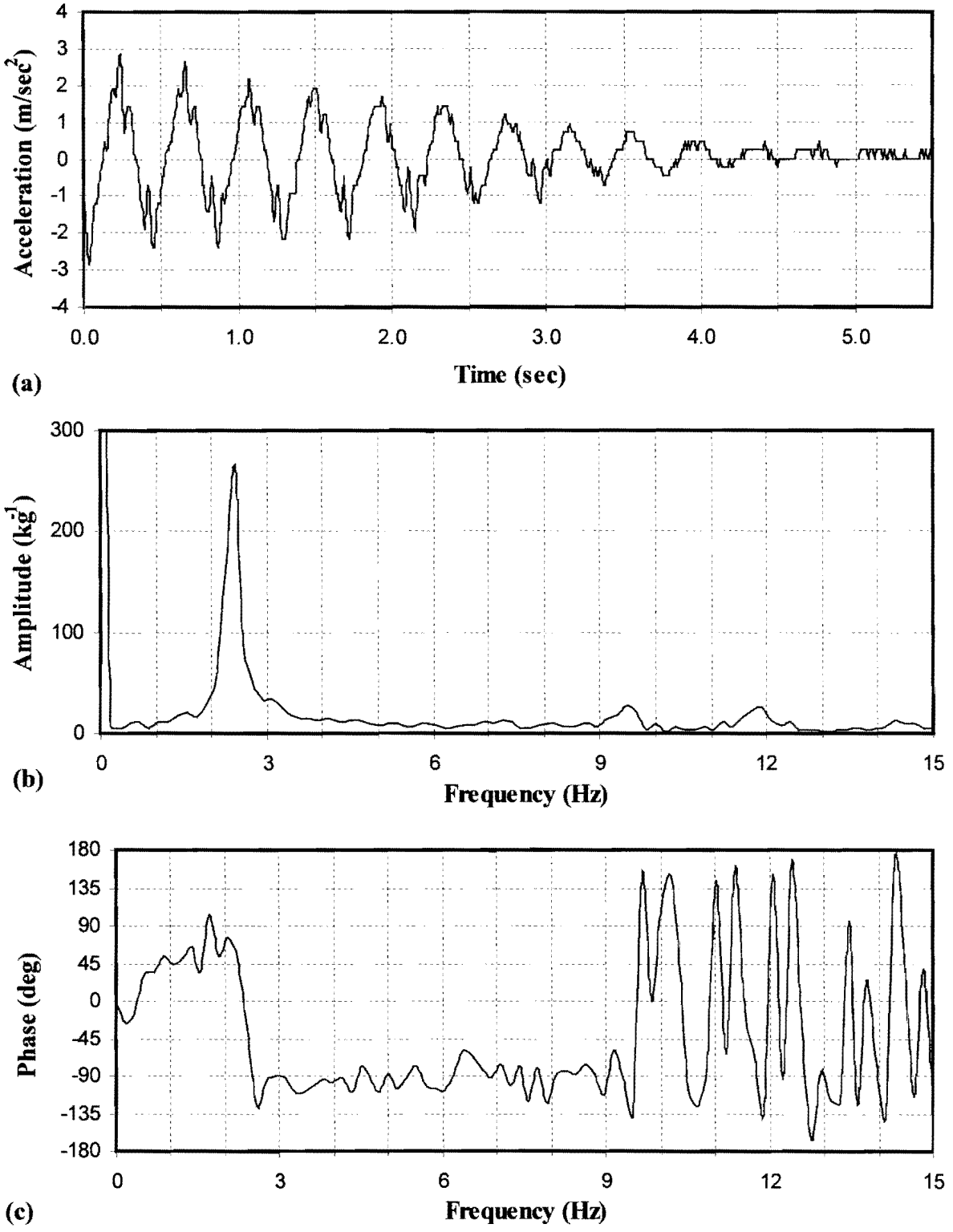

Figure 40. Response of Two Modules to Harmonic Pushing: (a) Time-History of Acceleration; (b) FFT Amplitude; and (c) FFT Phase Angle

7.6.3 Data Acquisition for Twelve Modules

Nine accelerometers were placed at the top of modules 2 through 10 as shown in Figure 41, and the impact hammer was used to strike the wall at a location near the top of column F (see Figure 12). A typical acceleration response time-history, transfer functions, and histories of phase angles are shown for six of the nine acceleration responses in Figures 42 (a), (b), and (c), respectively.

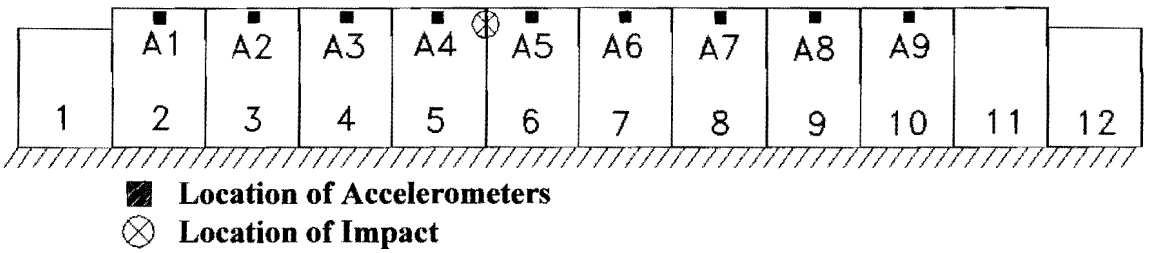

Figure 41. Accelerometer Placement on the Soundwall

The peak-amplitude method indicates that the first and second natural frequencies of the prototype soundwall are 1.88 Hz and 2.71 Hz, respectively (see Table 8). By examining phase angles of all nine transfer functions at the first natural frequency of 1.88 Hz it is seen that all are positive and of the same magnitude. Displaced shape of the soundwall when excited at this frequency is similar to the simple bending of a cantilever plate. For visualization purposes, a displaced shape as predicted by a finite element model of the soundwall is shown in Figure 54 (a). While not entirely evident from Figure 42 (c), close examination of phase angles of transfer functions at the second natural frequency shows that approximately one-half of the wall has positive phase angles and one-half of the wall has negative phase angles. A displaced shape of the wall for this mode also obtained by FEA is shown in Figure 54 (b).

Table 8. Frequencies and Damping of the Soundwall

Method of Identification	1st Mode		2nd Mode	
	ω_1 (Hz)	ξ_1 (%)	ω_2 (Hz)	ξ_2 (%)
Peak-amplitude	1.88	5.99	2.71	5.24
SOCIT	--[a]	--[a]	2.73	8.72

Note: --[a] = Not available

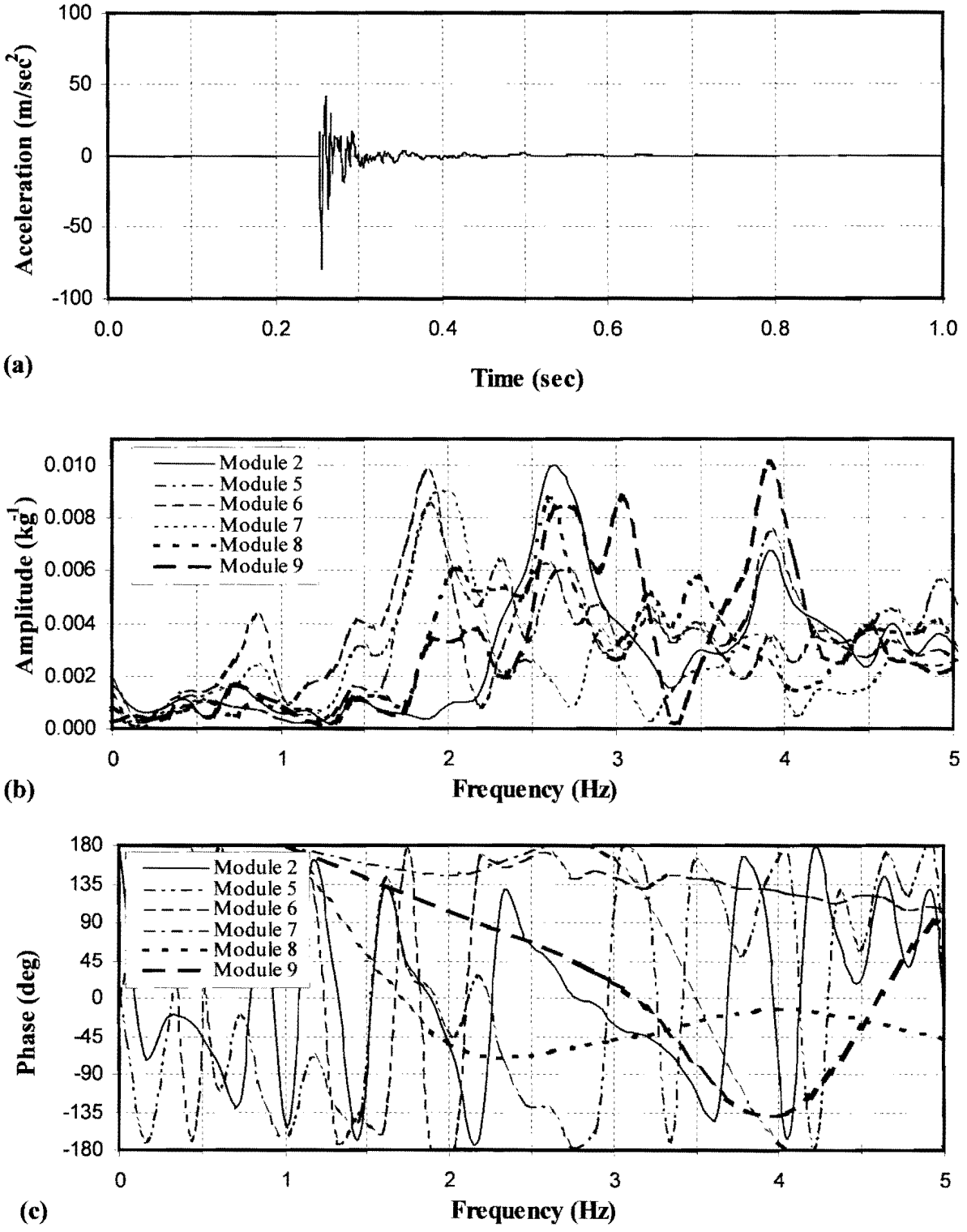

Figure 42. Response to Impact Hammer Excitation on the Soundwall: (a) Time-History of Acceleration; (b) Transfer Function Amplitude; and (c) Transfer Function Phase Angle

At 1.88 Hz, the entire soundwall has a lower first natural frequency than that of the isolated two-module section of soundwall (see Tables 7 and 8). As the length of the wall increases, it is expected that increased mass of the soundwall structure concomitantly results in lower natural frequencies. The prototype soundwall structure is very complex and somewhat irregular in material and geometry which makes it difficult to predict exact system characteristics. Recycled plastics are, in general, nonhomogenous, anisotropic, and nonlinear materials. Different module configurations, connection conditions, and effects of local vibration also add to complexity of the system. Nevertheless, first and second natural frequencies of the prototype wall are assumed to be known along with damping and deflected shapes.

7.7 SUMMARY

Two methods were successfully used to determine modal parameters of the soundwall: system identification and the peak-amplitude method. Both worked well for determination of higher natural frequencies; however, SOCIT sometimes failed to give lower frequencies that were clearly shown by the inertance transfer functions. SOCIT algorithms use curve-fitting techniques in the time or frequency domain and accuracy of the fitted curve near the origin is greatly affected by the sampling rate. To take full advantage of the SOCIT package, a slower form of excitation such as a sinusoidal signal could be implemented.

SOCIT was developed by control specialists and, therefore, potential users need to have a thorough understanding of the theory of linear system identification to enable results gathered from various algorithms to be correctly interpreted. The peak-amplitude method is simple and effective, but it should not be used alone for evaluation of a complex structure.

For a structure excited by strong winds, low frequencies are of primary concern. A low frequency for the 1^{st} mode indicates a necessity for checking the structure with respect to wind sensitivity. In conjunction with dynamic properties determined through analytical and numerical analysis (Chapter 8) and development of the characteristics of wind (Chapter 9), it is possible to make a quantitative analysis of this issue.

8. DYNAMIC ANALYSIS

8.1 INTRODUCTION

Analytical and numerical methods for identification of dynamic properties of the prototype soundwall are presented in the form of a classical energy formulation (the Rayleigh method) and finite element analysis (FEA), respectively. Results obtained using these methods, along with those gathered from system identification and experimental testing (see Chapter 7), are summarized and compared in the final section of this chapter.

8.2 ANALYTICAL DERIVATION

Since the predominant range of frequencies of wind is rather low, it is expected that only the first few modes of vibration of the soundwall make significant contributions to the dynamic response. For this reason, frequencies corresponding to the first two modes of vibration are investigated using the Rayleigh method (Clark 1972). Components of the actual structure are made of different materials and have a variety of geometries. Although these differences add complexity to the analysis, approximate estimates of dynamic properties can still be obtained by using assumptions of homogenous material and secure connections.

In the closed-form analysis that follows, a soundwall is assumed to be attached to a rigid, semi-infinite half-space. The wall has finite height and length designated by b and ℓ_w, respectively (see Figure 43). Elements of the structure include discrete columns that are spaced at a distance denoted by a and thin plates that are rigidly attached to the columns. The bottom edge of each plate is taken to be simply supported by the half-space.

For a freely vibrating, conservative system, energy oscillates between potential energy (i.e., strain energy of the structure) and kinetic energy. Total energy remains constant if the system is undamped. By assuming a reasonable function that closely approximates geometric and force boundary conditions of the mode shape for each subcomponent of a structure, the frequency of vibration for a specific mode can be calculated. Because the assumed shape of deformation imposes additional conditions of

constraint, the structure is stiffer and calculated frequencies are higher than actual values. Thus, Rayleigh's method gives an upper bound for the magnitude of the frequency of interest.

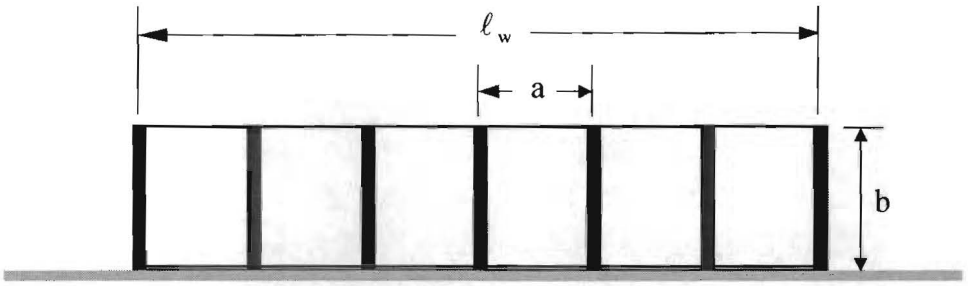

Figure 43. Simplified Analytical Model of the Soundwall

8.2.1 Rayleigh's Method

The prototype soundwall is deemed to consist of a multitude of thin plate and beam elements in the following sections. The contribution of each type of element to the total bending energy of the structural system is considered separately and then the results are superimposed. Axial and shear deformation are neglected.

First, consider the case of free-vibration of a beam bending element that has a constant cross section (see Figure 44 [a]). It is assumed to have the following mode shape:

$$w(y,t) = \varphi(y)\sin(\omega t + \alpha) \tag{13}$$

where $\varphi(y)$ is a mode shape function chosen to satisfy as many boundary conditions as possible, ω is a frequency of vibration, t is time, and α is a phase angle.

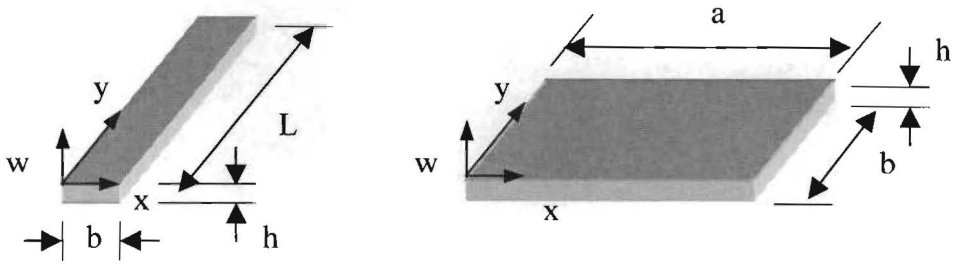

(a) **(b)**

Figure 44. Geometry of Structural Elements: (a) Beam; and (b) Plate

Strain energy for flexural deformation of a beam is defined as follows (Clough and Penzien 1993):

$$V = \frac{1}{2}\int_0^L EI(y)\left(v_{yy}\right)^2 dy \tag{14}$$

where *EI(y)* is the bending stiffness of the beam as a function of distance y, v_{yy} is the second partial derivative of an assumed mode shape function for the fundamental mode of vibration, and the length of beam is L.

For a beam element in the prototype soundwall, maximum strain energy is obtained by substituting $w(y,t)$ from Equation (13) into Equation (14) and maximizing the result as follows:

$$V_{\max} = \frac{1}{2}\int_0^L EI(y)\varphi_{yy}^2(y)dy \tag{15}$$

where E is the modulus of elasticity of the material, $I = bh^3/12$ is moment of inertia of the beam, and φ_{yy} is the second derivative of the mode shape function with respect to y.

Likewise, maximum kinetic energy of a beam element is given by (Clough and Penzien 1993):

$$T_{\max} = \frac{1}{2}\omega^2\int_0^L \rho A(y)\varphi^2(y)dy \tag{16}$$

where A is the area of the beam cross section and ρ is density of the material.

Since the total energy of the beam oscillates between kinetic and strain energy, the maximum of these two must be equal, or:

$$T_{\max} = V_{\max} \tag{17}$$

Equating maximum strain energy and kinetic energy from Equations (15) and (16) and solving for the frequency gives:

$$\omega^2 = \frac{V_{\max}}{\frac{1}{2}\int_0^L \rho A(y)\varphi^2(y)dy} \tag{18}$$

Next, consider the case of free-vibration of a thin plate that undergoes small transverse displacement (see Figure 44 [b]). Thickness of the plate, h, is taken to be constant, and material is assumed to be homogenous and isotropic. Moreover, the thin plate is assumed to have the following shape of transverse deformation:

$$w(x,y,t) = \varphi(x,y)\sin(\omega t + \alpha) \tag{19}$$

where x and y are rectangular Cartesian coordinates, $\varphi(x,y)$ is a mode shape function chosen to satisfy as many boundary conditions as possible, ω is the frequency of vibration, t is time, and α is a phase angle.

Strain energy of a plate element is:

$$V = \frac{D}{2}\int_0^b\int_0^a [(w_{xx})^2 + (w_{yy})^2 + 2\nu w_{xx}w_{yy} + 2(1-\nu)(w_{xy})^2]dxdy \tag{20}$$

where $D = Eh^3/12(1-\nu^2)$ is flexural rigidity of the plate, ν is Poisson's ratio, E is modulus of elasticity of the material, and h is the thickness of the plate. After substitution of Equation (19) into Equation (20), maximum strain energy of the plate, which occurs at the time of maximum deflection, can then be expressed as (Clark 1972):

$$V_{\max} = \frac{D}{2}\int_0^b\int_0^a [\varphi_{xx}^2(x,y) + \varphi_{yy}^2(x,y) + 2\nu\varphi_{xx}(x,y)\varphi_{yy}(x,y) + 2(1-\nu)\varphi_{xy}^2(x,y)]dxdy \tag{21}$$

where subscripts indicate partial differentiation with respect to the x-y Cartesian coordinate system.

Furthermore, kinetic energy of the plate is defined as (Clark 1972):

$$T = \rho\frac{h}{2}\iint \dot{w}^2 dxdy \tag{22}$$

where ρ is density of the material, h is thickness of the plate, and w is the assumed mode shape. The symbol, "˙", indicates differentiation with respect to time. Maximum kinetic energy occurs when the velocity is a maximum. After substitution of Equation (19) into Equation (22), maximum kinetic energy takes the form:

$$T_{\max} = \frac{1}{2}\rho h\omega^2\int_0^b\int_0^a \varphi^2(x,y)dxdy \tag{23}$$

Equating maximum strain energy and kinetic energy from Equations (21) and (23) and solving for frequency gives:

$$\omega^2 = \frac{V_{max}}{\frac{1}{2}\rho h \int_0^b \int_0^a \varphi^2 dxdy} \tag{24}$$

This completes presentation of equations for strain and kinetic energy for individual structural elements of beams and plates. In what follows, these formulae are applied to the prototype soundwall using the principle of superposition.

8.2.2 Fundamental Frequency of Transverse Vibration

As shown in Figure 45, an individual module in the soundwall is composed of horizontal and vertical beam elements that serve as support for plate elements that are attached on each exterior surface. Since energy is a scalar, it is possible to calculate the contribution of energy for each member in the module. Individual energy values can then be added to obtain total strain energy of the entire module and, subsequently, for the entire soundwall.

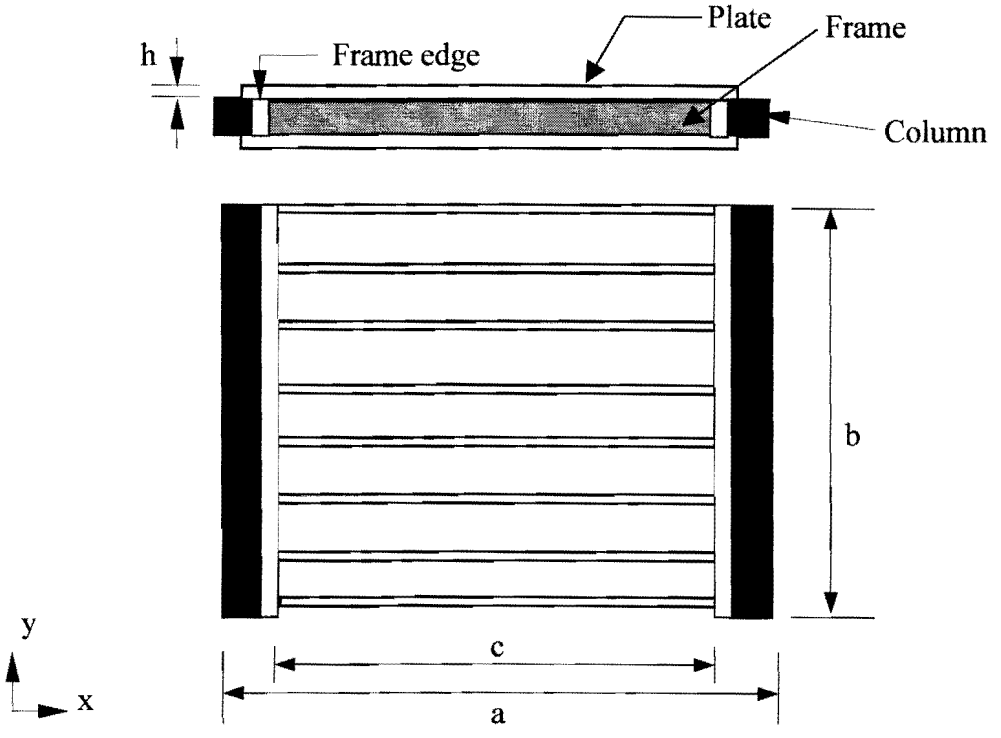

Figure 45. Schematic of Module and Adjacent Columns

In order to begin the analysis, the mode of vibration for a single module is assumed to be symmetrical about a plane that is perpendicular to the module and bisects its centerline. A function that appropriately describes the deflected shape of a single module is taken to have the general form:

$$\varphi(x,y) = 1 - \cos(\frac{\pi y}{2b}) + \beta \sin(\frac{\pi y}{2b})\left[1 - \cos(\frac{2\pi x}{a})\right] \tag{25}$$

where a is the length of the module, b is the height of the module, c is the width of horizontal members in the frame, and β is an unknown factor that is chosen to minimize the frequency.

One possible configuration of the deflected shape of the module and its two adjacent columns due to a simple transverse mode of vibration is shown in Figure 46. The bottom of the module is assumed to be pinned along the ground due to friction. Crossing members of the interior frame are rigidly fixed to vertical edges of the frame which are assumed to have the same deflected shape as the columns. By assuming continuity of deformation between both vertical edges of the module and the columns, the deflected shape of the columns is required to be:

$$\varphi(y) = 1 - \cos(\frac{\pi y}{2b}) \tag{26}$$

while a mode shape for horizontal members in the frame is as follows:

$$\varphi_i(x,y) = 1 - \cos(\frac{\pi y_i}{2b}) + \beta \sin(\frac{\pi y_i}{2b})\left[1 - \cos(\frac{2\pi x}{a})\right] \tag{27}$$

where y_i is the height coordinate along the y axis for the i^{th} member.

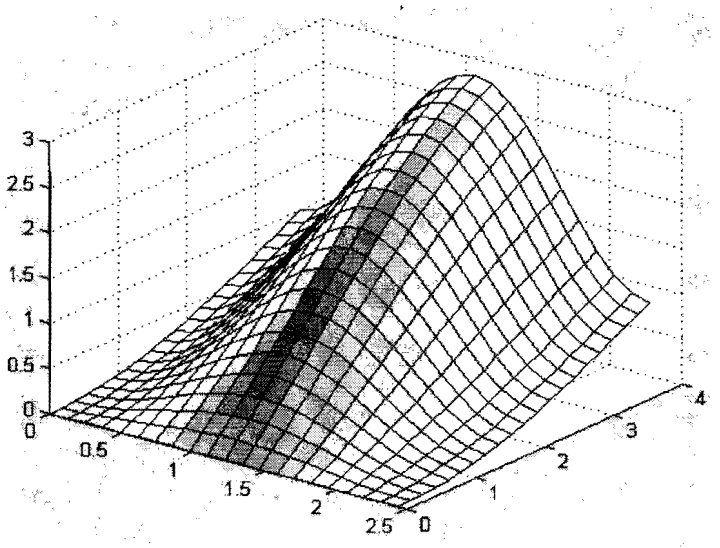

Figure 46. Assumed Symmetric Mode Shape for Module

Referring to Figure 45 for the limits of integration and using Equations (15), (21), and (25)-(45) leads to a set of equations that expresses the maximum strain energy for a column, plate, and horizontal frame members as follows:

$$V_{\max}^{c} = \frac{1}{2}\int_{0}^{h} E_c I_c \varphi_{yy}^2 dy = \frac{E_c I_c \pi^4}{64b^3} = c_1 \tag{28}$$

$$V_{\max}^{p} = \frac{D}{2}\int_{0}^{b}\int_{0}^{a}[\varphi_{xx}^2 + \varphi_{yy}^2 + 2\nu\varphi_{xx}\varphi_{yy} + 2(1-\nu)\varphi_{xy}^2]dxdy = c_2\beta^2 + c_3\beta + c_4 \tag{29}$$

$$V_{\max}^{b} = \sum_{i=1}^{8} V_{i\max}^{b} = \sum_{i=1}^{8} \frac{1}{2}\int_{0}^{c} E_b I_b \phi_{ixx}^2 dy = c_5\beta^2 \tag{30}$$

where c_i are constants related to element material properties and dimensions of a column, plate, or horizontal frame members, and the superscripts *c*, *p*, and *b* are symbolic references to column, plate, and, horizontal frame members, respectively. Strain energy for the column includes the contribution of the two vertical members of the frame. Definition of the constants, c_i, are shown in Appendix C under a MATLAB algorithm entitled **RAYLEIGH.m**.

Likewise, maximum kinetic energy formulae for a column, plate, and horizontal frame members follow from use of Equations (16), (23), and (25)-(45):

$$T_{\max}^{c} = \frac{1}{2}\rho_c A_c \omega^2 \int_0^b \varphi^2 dy = c_6 \omega^2 \tag{31}$$

$$T_{\max}^{p} = \frac{1}{2}\rho h \omega^2 \int_0^b \int_0^a \varphi^2 dx dy = (c_7 \beta^2 + c_8 \beta + c_9)\omega^2 \tag{32}$$

$$T_{\max}^{b} = \sum_0^8 T_{i\max}^{b} = \frac{1}{2}\rho_b A_b \omega^2 \int_0^c \varphi^2 dx = \omega^2 (c_{10}\beta^2 + c_{11}\beta + c_{12}) \tag{33}$$

By equating strain energy and kinetic energy, the following relation is obtained:

$$n(T_{\max}^{p} + T_{\max}^{b}) + (n+1)T_{\max}^{c} = n(V_{\max}^{p} + V_{\max}^{b}) + (n+1)V_{\max}^{c} \tag{34}$$

where n is the number of the modules in the entire wall. For the special case of a very long wall, $n \to +\infty$, $n \cong n+1$ and Equation (34) can be solved as follows:

$$\omega^2 = \frac{V_{\max}^{c} + V_{\max}^{p} + V_{\max}^{b}}{(T_{\max}^{c} + T_{\max}^{p} + T_{\max}^{b})/\omega^2} = \frac{(c_2 + c_5)\beta^2 + c_3\beta + (c_4 + c_1)}{(c_7 + c_{10})\beta^2 + (c_8 + c_{11})\beta + (c_9 + c_6 + c_{12})} \tag{35}$$

To obtain the minimum frequency, Equation (35) is differentiated with respect to the unknown parameter β and the result is set equal to zero:

$$\frac{d^2\omega}{d\beta^2} = 0 \tag{36}$$

Solving the result for β as a function of ω^2 yields the following expression:

$$\beta(\omega^2) = \frac{\omega^2(c_8 + c_{11}) - c_3}{2(c_2 + c_5 - \omega^2 c_7 - \omega^2 c_{10})} \tag{37}$$

An iterative numerical procedure can be invoked to solve Equations (35) and (37) simultaneously to obtain β and the minimum frequency.

Unlike sheet plastic modules, the exterior portion of a plastic lumber frame is composed of 11 narrow plates oriented vertically (see Figure 21). Since the width of these elements is small compared to the height (0.22 m versus 3.66 m, respectively), they behave more like a beam elements. In this case, an assumed shape function for each narrow plate is:

$$\varphi_i(x,y) = 1 - \cos(\frac{\pi y}{2b}) + \beta \sin(\frac{\pi y}{2b})\left[1 - \cos(\frac{2\pi x_i}{a})\right] \tag{38}$$

where x_i is the distance along the x axis of the ith narrow plate.

Maximum strain energy of both the front and back plates, each of which is composed of 11 narrow plates, is therefore:

$$V_{\max}^{p} = \sum_{i=1}^{22} V_{i\max}^{p} = \frac{1}{2}\int_0^b E_p I_p \varphi_{yy}{}^2 dy = c_{13}\beta^2 + c_{14}\beta + c_{15} \tag{39}$$

and the maximum kinetic energy becomes:

$$T_{\max}^{p} = \sum_{i=1}^{22} T_{i\max}^{p} = \frac{1}{2}\rho_p A_p \omega^2 \int_0^b \varphi^2 dy = \omega^2(c_{16}\beta^2 - c_{17}\beta + c_{18}) \tag{40}$$

Following the steps used for Equations (31)-(37) leads to the following expressions for ω and β for the case of narrow plates forming the fascia of the wall:

$$\omega^2 = \frac{V_{\max}^{c} + V_{\max}^{p} + V_{\max}^{b}}{(T_{\max}^{c} + T_{\max}^{p} + T_{\max}^{b})/\omega^2} = \frac{(c_{13}+c_5)\beta^2 + c_{14}\beta + (c_{15}+c_1)}{(c_{16}+c_{10})\beta^2 + (c_{11}-c_{17})\beta + (c_{11}+c_9+c_{18})} \tag{41}$$

$$\beta(\omega^2) = \frac{\omega^2(c_{11}-c_{17}) - c_{14}}{2(c_{13}+c_5-\omega^2 c_{16} - \omega^2 c_{10})} \tag{42}$$

An iterative numerical procedure is used to solve Equations (41) and (42) simultaneously to obtain the minimum frequency for the first transverse mode of a soundwall that is constructed of recycled plastic lumber.

8.2.3 Fundamental Frequency of Torsional Vibration

In order to investigate frequencies associated with torsional modes of vibration, the following two-dimensional function is assumed to represent the shape of the entire wall:

$$\varphi(x,y) = \left[1 - \cos(\frac{\pi y}{2b})\right]\cos(\frac{\pi x}{l_w}) \tag{43}$$

where l_w and b are length and height of the wall, respectively (see Figure 43). Equation (43) describes the mode shape for columns as well as modules. More explicitly,

specializing the notion for a column located at x_i and a plastic internal frame member located at a height y_i gives the following set of equations:

$$\varphi(y) = \left[1 - \cos(\frac{\pi y}{2b})\right]\cos(\frac{\pi x_i}{l_w}) \tag{44}$$

$$\varphi(x) = \left[1 - \cos(\frac{\pi y_i}{2b})\right]\cos(\frac{\pi x}{l_w}) \tag{45}$$

where x_i and y_i are column location and the height coordinate, respectively.

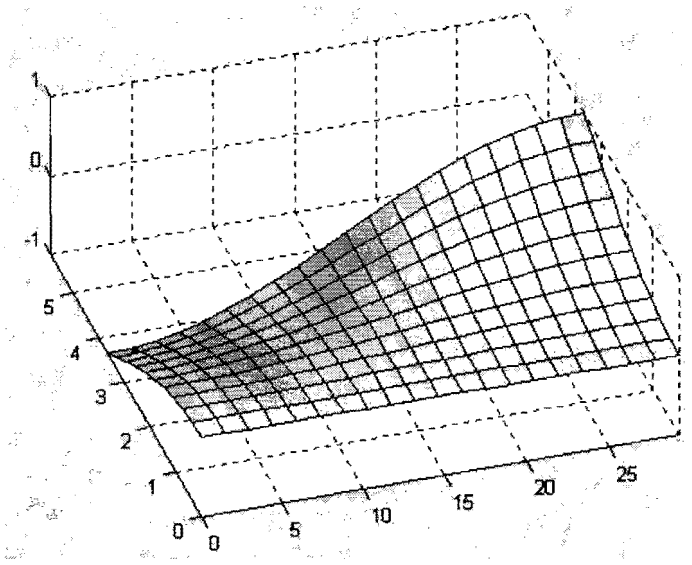

Figure 47. Assumed Torsional Mode Shape for Entire Wall

Substitution of Equations (44), (43), and (45) in Equations (15), (21), and (15), respectively, and using the principle of superposition leads to the following set of equations for the maximum strain energy in the columns, plates, and horizontal frame members:

$$V^c_{\max} = \sum_{i=1}^{13} V^c_{i\max} = \sum_{i=1}^{13} \frac{1}{2} \int_0^b E_c I_c \varphi^2_{yy}(y) dy \tag{47}$$

$$V^p_{\max} = D \int_0^b \int_0^{l_w} [\varphi^2_{xx}(x,y) + \varphi^2_{yy}(x,y) + 2\nu\varphi_{xx}(x,y)\varphi_{yy}(x,y) + 2(1-\nu)\varphi^2_{xy}(x,y)] dx dy \tag{48}$$

$$V^b_{\max} = \sum_{i=1}^{8} V^b_{i\max} = \sum_{i=1}^{8} \frac{1}{2} \int_0^{l_w} E_b I_b \varphi^2_{xx}(x) dx \tag{46}$$

Likewise, maximum kinetic energy formulas for a column, plate, and horizontal frame members excited by the first torsional mode are obtained from Equations (16), (23), and (16), respectively:

$$T^c_{\max} = \sum_{i=1}^{13} T^c_{i\max} = \sum_{i=1}^{13} \frac{1}{2} \rho_c A_c \omega^2 \int_0^b \varphi^2(y) dy \tag{49}$$

$$T^p_{\max} = ht\omega^2 \int_0^b \int_0^{l_w} \varphi^2(x,y) dx dy \tag{50}$$

$$T^b_{\max} = \sum_{i=1}^{8} T^b_{i\max} = \sum_{i=1}^{8} \frac{1}{2} \rho_b A_b \omega^2 \int_0^{l_w} \varphi^2(x) dx \tag{51}$$

By equating strain energy and kinetic energy, the following relation is found:

$$T^c_{\max} + T^p_{\max} + T^b_{\max} = V^c_{\max} + V^p_{\max} + V^b_{\max} \tag{52}$$

so that the frequency of the soundwall for the first torsional mode is found to be:

$$\omega^2 = \frac{V^c_{\max} + V^p_{\max} + V^b_{\max}}{(T^c_{\max} + T^p_{\max} + T^b_{\max})/\omega^2} \tag{53}$$

As for the first bending mode, when the plate attached to the frame is actually assembled from a series of vertical plates, a shape function for each plate is assumed to be (see Equation (44)):

$$\varphi(y) = \left[1 - \cos\left(\frac{\pi y}{2b}\right)\right] \cos\left(\frac{\pi x_i}{l_w}\right) \tag{54}$$

Maximum strain energy and kinetic energy of each narrow plate are as follows:

$$V^p_{i\max} = \frac{1}{2} \int_0^b E_p I_p \varphi_{yy}{}^2(y) dy \tag{55}$$

$$T^p_{i\max} = \frac{1}{2} \rho_p A_p \omega^2 \int_0^b \varphi^2(y) dy \tag{56}$$

Therefore, the frequency formula for the first torsional mode changes to:

$$\omega^2 = \frac{V_{\max}^c + 12 \times \sum_{i=1}^{22} V_{i\max}^p + V_{\max}^b}{(T_{\max}^c + 12 \times \sum_{i=1}^{22} T_{i\max}^p + T_{\max}^b)/\omega^2} \tag{57}$$

8.2.4 Analytical Results

The lowest fundamental frequencies corresponding to the first and second modes of vibration were determined for two cases of the prototype soundwall (see Table 10). The first case considers the prototype soundwall to be composed of 13 fiberglass-reinforced columns and 12 sheet plastic modules, while the second case considers the prototype soundwall as having 13 fiberglass-reinforced columns and 12 modules that are constructed with fiberglass-reinforced plastic lumber. The surface of each module is considered to be one large plate and 11 narrow plates for the first and second case, respectively.

The Rayleigh method of analytical analysis of dynamic properties is implemented using a MATLAB algorithm entitled **RAYLEIGH.m** (see Appendix C). As listed in Table 9, required input for the program includes density, Poisson's ratio, modulus of elasticity, and geometry of the entire wall. These are the same values that will be used in subsequent numerical analyses.

Table 9. Input for Rayleigh's Method

Property	Sheet Plastic Module	Plastic Lumber Module
ρ_{beam} (kg/m^3)	775	775
ρ_{plate} (kg/m^3)	775	775
ρ_{column} (kg/m^3)	775	775
E_{beam} (Pa)	3.11×10^9	3.11×10^9
E_{plate} (Pa	3.11×10^9	3.11×10^9
E_{column} (Pa)	3.11×10^9	3.11×10^9
a (m)	3.66	3.66
b (m)	2.44	0.22
c (m)	2.26	2.26
h (m)	0.013	0.051
ν	0.4	0.4

Table 10. Rayleigh's Method for Fundamental Frequencies

Soundwall Composition	1st Fundamental Frequency (Hz)	2nd Fundamental Frequency (Hz)
Sheet plastic modules	2.92	3.07
Plastic lumber modules	2.27	2.51

In short, reasonable values are predicted for both the 1st and 2nd fundamental frequencies. For a more comprehensive comparison of fundamental frequencies see Section 8.4.

To apply Rayleigh's method, it is necessary to use a shape function that satisfies the geometric and force boundary conditions while also satisfying equations of motion. It is not always possible to choose a function for the mode shape that satisfies both types of boundary conditions and therefore precedence is usually given to satisfaction of geometric boundary conditions. Due to extra constraints implied by the assumed mode shapes, Rayleigh's method always predicts higher values for fundamental frequencies of vibration. For example, a pinned connection is assumed between the bottom edge of the module and the ground for the mode shape of the 2nd fundamental frequency. By closely looking at the deformed shape, one finds that this antisymmetric mode shape holds for both the pinned and fixed boundary conditions. Therefore, the value of the 2nd frequency given by Rayleigh's method is actually greater than the one corresponding to only the fixed boundary condition as well as only the pinned connection. In conclusion, choosing a suitable shape function plays a crucial role in producing a close approximation.

For the current study, results for natural frequencies obtained from experimental testing are deemed to be more likely to be correct than those obtained from a closed-form solution even thought the two match reasonable well. A fourth alternative for obtaining dynamic characteristics of a structure, besides system identification, experimental testing, and the analytical solution, is numerical analysis which is described in the following section.

8.3 NUMERICAL ANALYSIS

The method of analytical analysis presented in Section 8.2 has been shown to predict reasonable values for dynamic properties of the prototype soundwall, but there are numerous limitations that are important to keep in mind. For example, materials are assumed to behave linearly, predicted results are only as accurate as the assumed mode shape functions, and nonorthogonal geometry adds complexity to derivation of strain and kinetic energy. As an alternative, numerical simulation through finite element modeling provides an easy, systematic technique for determining the response of a structural system to static, impulse, or cyclic loadings where none of these limitations apply. The technique can also be used to determine structural behavior of a system to fatigue, creep, or temperature fluctuations.

According to the finite element method, a geometrically complex domain is represented as a collection of simple subdomains, called finite elements. Continuous approximations, often polynomials, of the solution are formulated for each element in terms of nodal values. Equations for each element can then be assembled by imposing interelement continuity and by balancing interelement forces to obtain a final solution to a predefined differential equation that describes the behavior of the item under study.

8.3.1 Motivation

Plastics are not as stiff and are much more dense than wood. This combination of lower flexibility and increased mass leads to a lower fundamental frequency and increased period of oscillation in comparison with the response of a wall constructed from wood or other stiffer materials. In fact, the fundamental frequency of a soundwall along a highway may be low enough to overlap significant portions of the frequency spectrum associated with wind. In this case resonant behavior could ensue during a wind storm and the structure might undergo large motions that could disconcert motorists or residents living near the wall. As an extreme example, the Tacoma Narrows Bridge responded violently when 48 to 64 kmph (30 to 40 mph) winds induced vortex shedding. Many engineers believe this led to resonant behavior and, subsequently, catastrophic failure of the bridge.

For small structures, wind tunnels can be used to investigate response to large wind stimuli such as tornadoes, wind storms, and hurricanes. Testing of a soundwall in a wind tunnel is not feasible, but numerical simulation through finite element modeling provides an excellent alternative if the model has been calibrated.

From a calibrated model, predictions can be made with reasonable accuracy as to how the prototype soundwall will respond to static or dynamic loads. Deflections, stresses, and modal parameters, such as resonant frequencies and mode shapes, are only a few of the response characteristics that can be estimated. Parametric studies can also be performed to optimize dimensions, such as height or thickness, that would enable a soundwall to perform adequately in a wind storm or earthquake.

8.3.2 Construction of Finite Element Model

As shown in Figure 48, a finite element model of the recycled plastic soundwall was developed in conjunction with a commercial code named ABAQUS (1989). Pre- and post-graphics processing was performed using PATRAN® (1989).

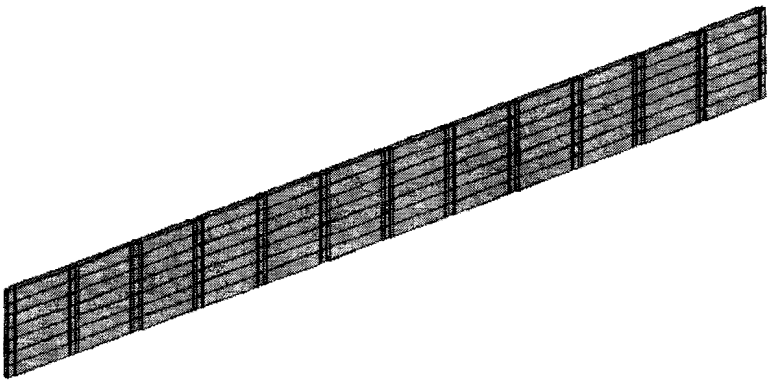

Figure 48. Finite Element Model of the Soundwall

As stated previously, a variety of materials and module configurations are incorporated into the prototype soundwall. To simplify development of a finite element model, it is assumed that the entire soundwall is constructed from modules made with fiberglass-reinforced plastic lumber and also fiberglass-reinforced columns. This material

is used in the simulation because it appears to have the highest potential for field implementation.

In what follows, both static and dynamic behavior of an individual column and an individual module are calibrated with experimental data. These two subcomponents are used to create a finite element model of the entire prototype soundwall. Results for deflections, natural frequencies, and accelerations obtained by the simulation are expected to vary from results obtained in the field due to the fact the numerical model is not an exact replica of the actual soundwall structure.

Two types of elements used in the numerical model include:

1. Solid elements (C3D20) - twenty-noded brick elements with three displacement components and no rotational degrees of freedom at each node. Each brick element provides quadratic interpolation along a given edge. Columns and vertical members in the frame of each module are constructed with C3D20 elements.

2. Shell elements (S8R5) - eight-noded doubly curved shell elements with reduced integration and quadratic interpolation. These elements have five degrees of freedom per node: three are displacement components and two are in-surface rotation components. Each element has a mathematical thickness, and a unit normal to the shell surface is formed so that cross-sectional behavior can be analyzed through numerical integration. Sheet plastic and horizontal members in the frames are modeled with S8R5 elements.

8.3.2.1 Simulation of a Column

Static and dynamic response of a fiberglass-reinforced column were modeled using C3D20 elements. Static behavior of the numerical model was calibrated by comparing simulated deflection to that of a closed-form solution (Boresi et al. 1993). A concentrated load of 500 N (112 lb) was applied at the top of a cantilever column with a fixed base. Deflection at this location is calculated to be 0.0185 m from a closed-form solution. The numerical simulation was made to match to this estimate by altering the number of hexahedral elements modeling the column (see Figure 49). By performing a convergence

study, it was found that a column composed of seven hexahedral elements (C3D20s) predicts maximum deflection at the top of 0.0185 m as shown in Figure 50.

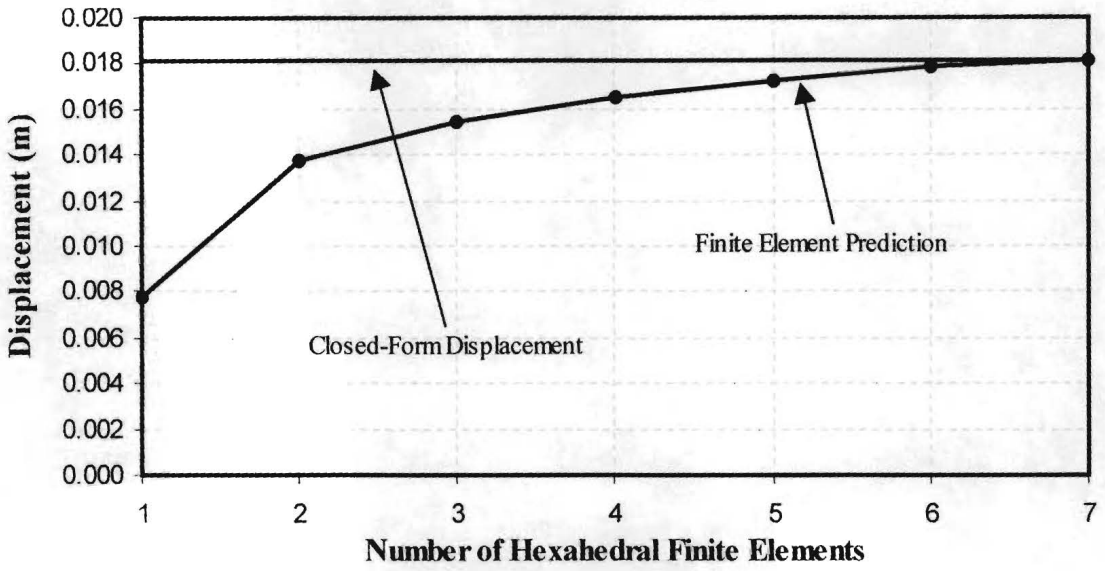

Figure 49. Convergence Study of Static Column Displacement

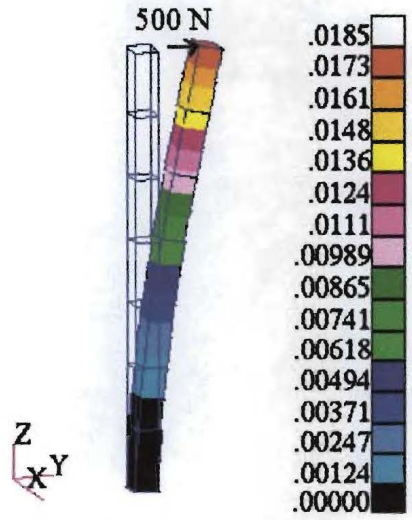

Note: Units in meters (m)

Figure 50. Finite Element Model of Column

To model dynamic behavior of the column, natural frequencies were calibrated to match frequencies obtained from an impact hammer excitation of a fiberglass-reinforced column. A set value for modulus of elasticity of the fiberglass-reinforced plastic column

was taken directly from brochures of the manufacturer; however, material density was shown to vary slightly in the brochures depending on the geometry of a particular member. Lack of a set value for density is most likely due to material inconsistencies, such as gaseous pores, that develop in a cross-section as the recycled plastic cools. Minor adjustment of this property changes fundamental frequencies predicted for the column, but it does not change simulated static behavior. Table 11 compares natural frequencies estimated by finite element analysis (FEA) of a column to those obtained through experimental testing (see Figure 38).

Table 11. Impact Test and FEA Predictions of Column Frequencies

Natural Frequency	Impact Test Frequency (Hz)	Simulation Frequency (Hz)	Percent Difference (%)
1st	4.88	4.88	0
2nd	30.03	30.38	1.2
3rd	81.79	81.82	0

Natural frequencies were successfully matched by setting density of the material equal to 775 kg/m^3 (48.3 lb/ft^3), Poisson's ratio to 0.4, material damping to 0.04, and the modulus of elasticity to 3.11×10^9 N/m^2 (450 ksi). A value for material damping was determined from experimental tests on a fiberglass-reinforced column (see Table 6).

8.3.2.2 Simulation of a Module

Static tests were performed in the field on five types of modules to determine stiffness in both the short and long span directions (see Section 6.3). A finite element model of a module was calibrated to match deflection in both the short and long-span directions of a fiberglass-reinforced plastic lumber module from the prototype soundwall (see Figure 28).

In a field test on a fiberglass-reinforced plastic lumber module, a load of 738 N (166 lb) deflected the center of the module 0.0030 m (0.120 in.) and 0.0015 m (0.060 in.) for supports along the short and long dimensions, respectively (see Figure 29). After calibration of the numerical model, simulated deflection was 0.0030 m (0.120 in.) and 0.0020 m (0.066 in.) along the short and long dimensions, respectively. Figures 51 (a) and

(b) show fringe plots of vertical deflection at the maximum load for each case. The simulation has 0% error in prediction of deflection in the long span case and 25% error in prediction of deflection when the short span is unsupported. Due to complexity of connections and uncertainty of material properties, this moderate amount of error in the short direction is considered to be acceptable. Also, global deflection of the tops of the columns and wall modules due to bending from lateral wind loads are of more concern than localized deflection from concentrated loads on each individual wall panel.

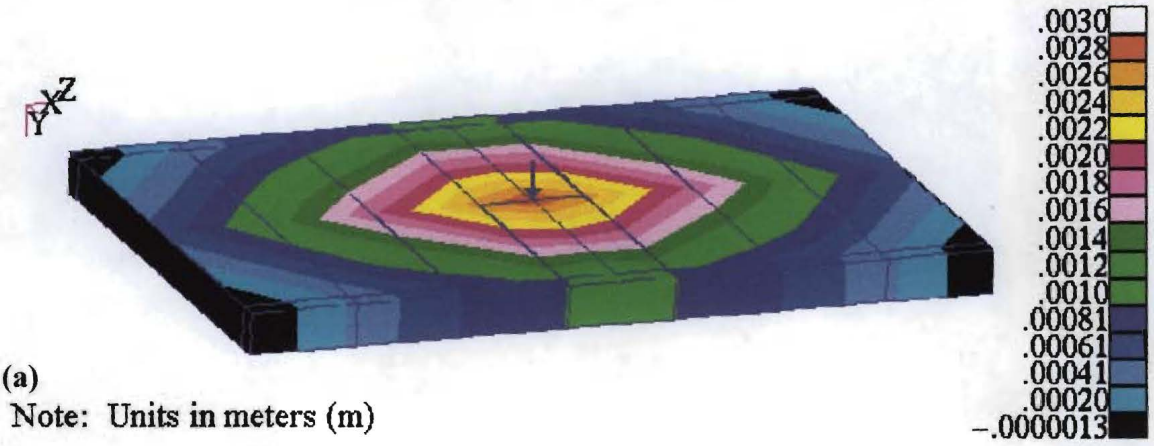

(a)
Note: Units in meters (m)

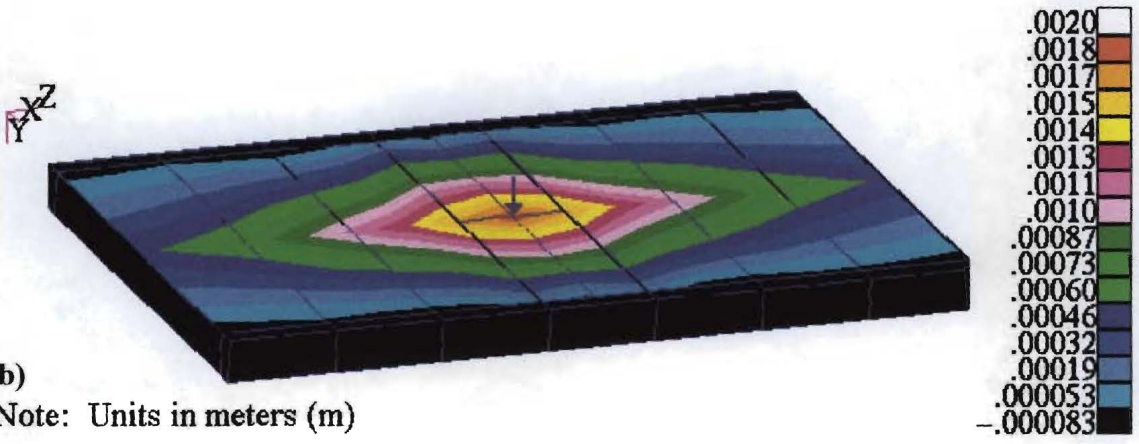

(b)
Note: Units in meters (m)

Figure 51. Deflection of a Simply Supported Module Due to Concentrated Load: (a) Long Span; and (b) Short Span

To calibrate dynamic behavior of a module, the first natural frequency that is determined through numerical simulation of a single module is adjusted to match to the first natural frequency of a fiberglass-reinforced plastic lumber module as determined through field tests. As shown in Figure 52, a fiberglass-reinforced plastic lumber module was placed flat on the ground with supports under the long edges. Two accelerometers were placed on the module: one on top near the middle of the module and the other at the edge and also near the middle of the long span. An impact hammer was used to strike the center of the module near the central accelerometer, and acceleration response time histories were acquired for the two accelerometers. Subsequently, an FFT of the time history data from each accelerometer transformed each set of data into the frequency domain (see Figure 53). Natural frequencies are recognized to occur at 8.32, 26.32, and 37.85 Hz.

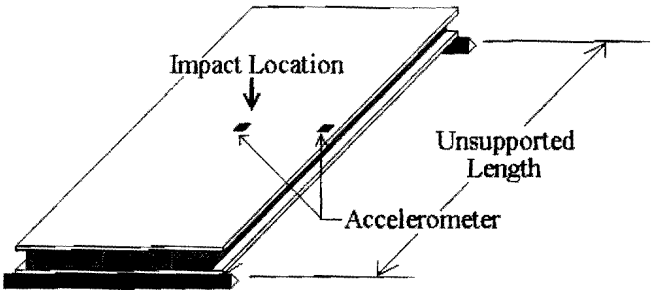

Figure 52. Location of Accelerometers on Module

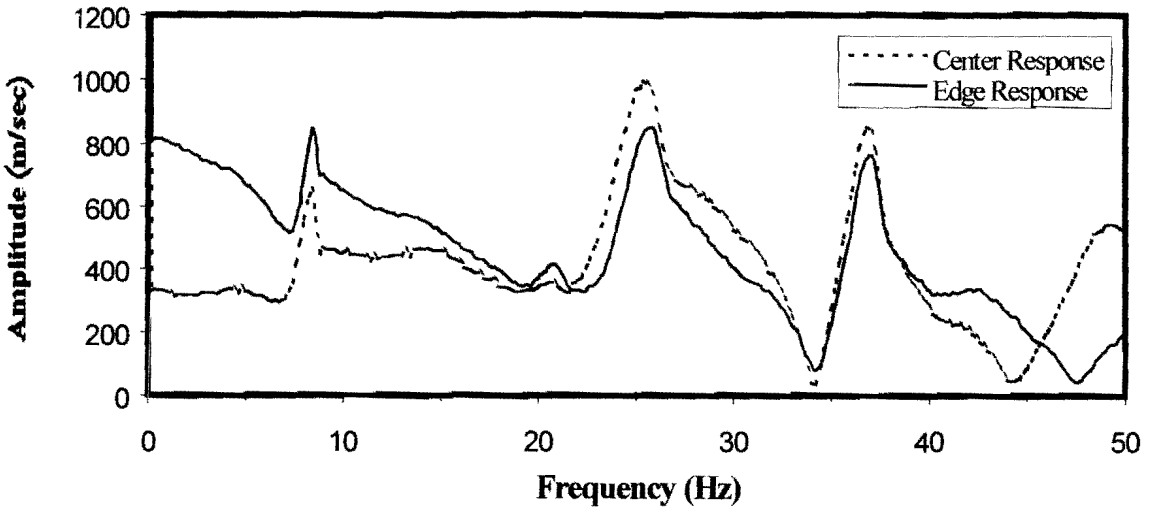

Figure 53. Frequency Response of Module to Impact Hammer Excitation

For purposes of calibrating dynamic behavior of the finite element model, only the first natural frequency (8.32 Hz) was matched since the lowest frequency is of primary concern. In the simulation of the module, it was necessary to enter material properties such as density, damping, and modulus of elasticity for three types of members: vertical spacers, horizontal boards, and exterior plastic lumber. Unlike the column, adjustment of density was unnecessary to match the first natural frequency for the module.

8.3.2.3 Simulation of the Soundwall

With the calibration of static and dynamic characteristics of a column and module now complete, 13 columns and 12 modules are combined in a finite element model to simulate behavior of the prototype soundwall (see Figure 48). Sample listings of input files for ABAQUS are given in Appendix D. The first three natural frequencies predicted by the numerical simulation are listed in Table 12, and mode shapes that correspond to each natural frequency are shown in Figures 54 (a), (b), and (c), respectively. From the simulation, it was determined that the mode shape corresponding to the first three natural frequencies involve pure bending (1st mode) as well as combined bending and torsion (2nd and 3rd modes).

Table 12. Frequency Results for the Soundwall

Mode of Vibration	Type of Motion	Simulation Frequency (Hz)
1	Transverse	2.31
2	Torsional	2.54
3	Torsional	3.07

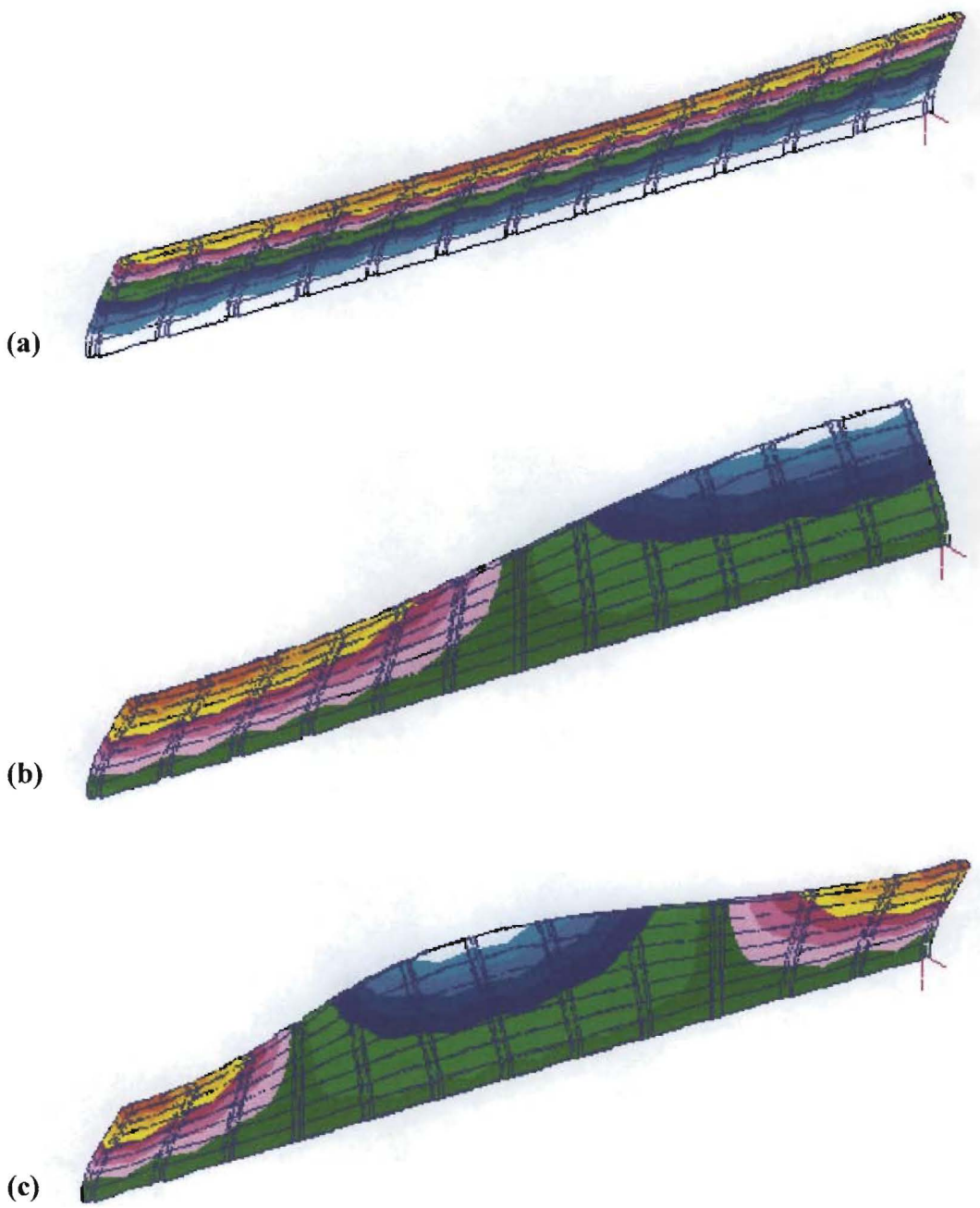

Figure 54. Modes of Vibration: (a) 1st Mode; (b) 2nd Mode; and (c) 3rd Mode

8.4 COMPARISON OF RESULTS

Results of the dynamic investigation of the entire soundwall for all methods are now condensed for comparison in Table 13. With exception of the 1st natural frequency that could not be identified through system identification, it is evident that system identification, experimental testing, analytical analysis, and numerical analysis all predict nearly the same

nearly the same 1st, 2nd, and 3rd natural frequencies of vibration (see Figure 54). Rayleigh's method predicts frequencies of 2.27 Hz and 2.51 Hz for the first transverse and first torsional modes, respectively, for a wall composed of plastic lumber modules. These modes correspond to the 1st and 2nd natural frequencies of the other methods. Note that the value for the 1st natural frequency obtained from the Rayleigh method (2.27 Hz) and FEA

Table 13. Summary of Frequencies for Each Method

Method	1st Natural Frequency (Hz)	2nd Natural Frequency (Hz)	3rd Natural Frequency (Hz)
Experimental Testing (Peak-Amplitude Method)	1.88	2.71	3.00
Analytical Analysis (Rayleigh Method)	2.27	2.51	--[a]
System Identification (SOCIT)	--[a]	2.73	3.20
Numerical Analysis (Finite Element Analysis)	2.31	2.54	3.07

Note: --[a] = Not Available

(2.31 Hz) are higher than the first natural frequency obtained by experimental testing (1.88 Hz). As mentioned earlier, an exact replica of the actual prototype soundwall was not modeled. Fiberglass-reinforced plastics are, in general, stiffer than unreinforced plastics; consequently, frequencies obtained by these two methods are greater since all structural members are fiberglass-reinforced. Another likely cause for a higher first natural frequency predicted by analytical and numerical analysis is that a majority of connections are modeled as being perfectly rigid; whereas, modules in the actual soundwall are not securely connected to adjacent columns. Therefore, added stiffness of adjacent modules is not realized to its fullest extent and the structure behaves in a less rigid fashion.

The preferred method of determining dynamic properties is through direct testing on the actual structure. System identification and a peak-amplitude method were successfully implemented to determine natural frequencies and damping of the soundwall. Experimental testing with the peak-amplitude method consistently produced desired

results, while system identification with SOCIT had difficulty determining the lowest frequency.

If a structure is not available for experimental testing, numerical simulation is an effective alternative that could be used to provide modal parameters and structural response. Here, the first three natural frequencies and their respective mode shapes were successfully determined through careful calibration of a finite element model. The components were then combined to form the complete structure.

In the following chapter, numerical simulation is used to predict acceleration and deflection response at the top of the complete soundwall when it is subjected to both a weak and strong wind pressure time history. Then, more refined analyses are performed for the strong wind using a probability-based method in an attempt to better characterize the random nature of wind excitation.

9. RANDOM VIBRATION DUE TO WIND

9.1 INTRODUCTION

Effects of strong winds on the prototype soundwall are discussed in this chapter. First, the frequency spectrum associated with anticipated wind events is developed and compared to natural frequencies of the prototype soundwall so that a general conclusion can be made regarding wind sensitivity of the barrier. Then, small and large scale wind events are applied to a finite element model of the soundwall to determine an upper bound estimate for deflection and acceleration response. In these two simulations, each wind pressure event is applied to the surface of the soundwall and response is calculated using modal superposition. Simulation of the small wind event is compared with field acceleration data. Finally, a probabilistic method based on the theory of random response is used to obtain the root mean square (RMS) of the deflection response. Dynamic behavior is predicted for a variety of wall heights and column stiffnesses using power spectral density and spatial correlation of wind velocity.

9.2 WIND EVENTS

In Section 9.5, numerical simulation by modal superposition is carried out for two wind events that are applied to the prototype soundwall. The first event, which was recorded at the Riverside Campus of Texas A&M University, is small in magnitude with a mean velocity of 4.0 m/sec (9 mph). A second, larger event is obtained by amplifying a wind speed time history (M15N541) that was recorded at the Wind Engineering Research Center (WERC) at Texas Tech University as part of the Texas Tech Field Experiment Data Package (see Figure 55). This original M15N541 wind velocity time history is used for purposes of developing a frequency spectrum of wind.

The Texas Tech data file contains wind speed time histories at elevations of 4, 10, 21, and 49 m (13, 33, 70, and 160 ft) above ground. Data were recorded using three-cup anemometers on a 49-m (160-ft) tall meteorological tower at a data acquisition rate of 10 Hz for 900 seconds and low-pass filtered at 8 Hz. Terrain surrounding the tower was both

flat and open which is consistent with ASCE 7-95 exposure category *C* and similar to topography at the site of the prototype soundwall. For purposes of this project, however, wind speed data recorded from the 4-m (13-ft) high anemometer were used due to their relative proximity in above-ground elevation to the height of the prototype soundwall. This wind event has been amplified to a mean velocity of 40.1 m/sec (90 mph), which is equivalent to what the structure might experience during a strong wind storm. The data were amplified by multiplying by a constant value. In this way, the same coefficient of variation between the original time history and amplified time history is maintained (Roschke et al. 1996). Statistical characteristics of the small wind event recorded at the Riverside Campus, the original M15N541 velocity time history, and the amplified M15N541 velocity time history are shown in Table 14.

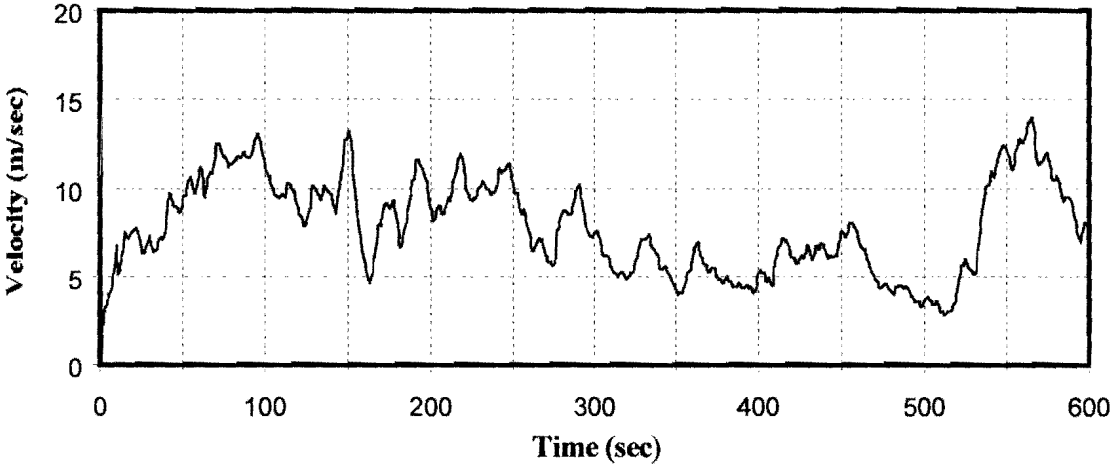

Figure 55. Original M15N541 Wind Velocity Time History

Table 14. Wind Speed Characteristics

Parameter	Riverside Campus	Original M15N541	Amplified M15N541
Mean Wind Speed (m/sec)	4.01	9.06	40.14
Standard Deviation (m/sec)	± 1.45	± 1.73	± 7.70
Coefficient of Variation (%)	36.2	19.1	19.2
Note: 1 m/sec = 2.24 mph			

9.3 PRESSURE

Dynamic excitation of the prototype soundwall is a result of fluctuating pressures applied to the surface of the structure. If the flow of a fluid such as air is assumed to be uniform and normal to the surface, the total drag force applied to a bluff body by that fluid may be expressed as (Blevins 1984):

$$F_D = \frac{1}{2}\rho A U^2 C_D \tag{58}$$

where ρ is the fluid density, U is velocity of the fluid, A is area of the surface on which the fluid acts, and C_D is a dimensionless drag coefficient. Here, it is assumed that lifting forces are negligible since the soundwall is relatively thin compared to its dimensions of width and height. In what follows, this drag force is converted into a pressure that is applied to the surface of the soundwall in a finite element model; it is first necessary, however, to approximate the distribution of pressure that acts on the face of the wall.

The surface of the earth exerts a horizontal friction force that retards the flow of wind. As shown in Figure 56, effects of this friction force decrease as the height above the ground increases. A commonly used mathematical descriptor of this behavior is the power law (Simiu and Scanlan 1986):

$$V(z) = V_H\left(\frac{z}{H}\right)^{\alpha} \tag{59}$$

where V_H is velocity at height H (arbitrarily taken here to be 100 m/sec at a height of 275 m), z is the height from the ground up to a point of interest, and α is an exponent dependent upon the roughness of the terrain (see Table 2.2.2 in Simiu and Scanlan 1986). For open terrain, a suitable value for α is 0.16.

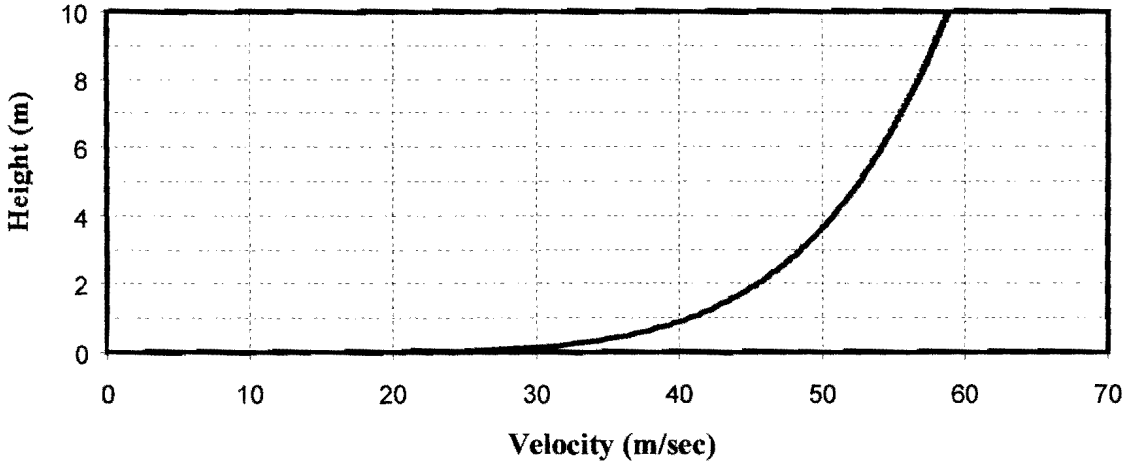

Figure 56. Wind Velocity Profile

To simplify numerical simulation of the response of the wall to the drag force as it acts normal to the surface of the wall, variation of the pressure is conservatively assumed to be zero near the ground and to increase linearly to the top of the 3.66-m (12-ft) wall. Pressure along the 30-m (96-ft) length of wall is assumed to be uniform as shown in Figure 57.

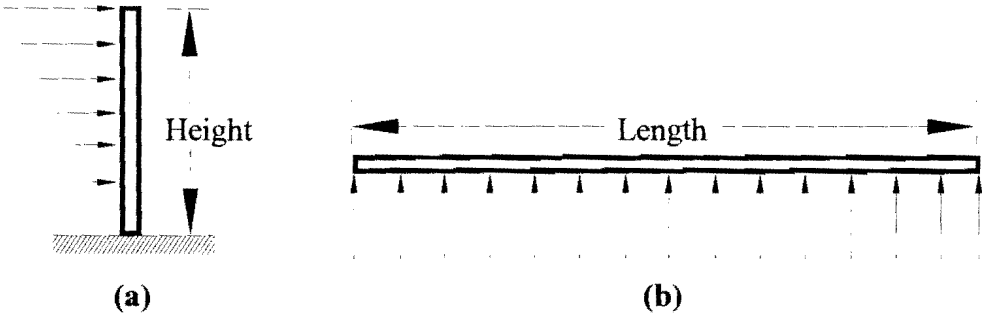

Figure 57. Assumed Wind Pressure Distribution on Soundwall: (a) Elevation View; and (b) Plan View

It is important to note that the deterministic finite element simulation applies a time history of wind pressure along the wall in a uniform fashion to the entire wall surface. For a long wall, an assumption of a uniform wind pressure along the structure is likely to be incorrect. As a consequence, the wall is exposed to a more severe load in the deterministic FEA than an actual wind event would impose. This approach results in an upper bound, or

conservative, prediction for deflection and acceleration response when the deterministic FEA is used.

Based on an assumed linear variation of wind pressure with elevation above ground, the total drag force calculated by Equation (58) can be used to calculate a pressure at the top of the wall for a wind flowing normal to the surface of the wall:

$$P_{\max} = \frac{\rho A U^2 C_D}{Height \times Length} \tag{60}$$

The drag coefficient, C_D, for a thin rectangular plate perpendicular to the flow of wind is a function of the aspect ratio (length/height) of the plate (see Figures 3 and 57). Values for this coefficient are readily available for a rectangular plate on the ground and normal to a smoothly flowing wind (see Table 4.6.1; Simiu and Scanlan 1986). The aspect ratio for the prototype soundwall is 8.0 since the wall has dimensions of 29.26 m × 3.66 m (96 ft × 12 ft); therefore, C_D is taken to be 1.177 and Equation (60) can be simplified to:

$$P_{\max} = 1.177 \rho U^2 \tag{61}$$

where ρ is 1.23 kg/m^3 (2.38 × 10^{-3} slug/ft^3) for air at 15 °C (59 °F).

Using Equation (61), the time history of wind speed for M15N541 (see Figure 55) is converted to a time history of wind pressure. Time histories of maximum wind pressure for the Riverside Campus event, the M15N541 event, and the amplified M15N541 event are shown in Figure 58. The Riverside Campus and amplified M15N541 maximum pressure data are applied to estimate deflection and acceleration response in the numerical simulation (see Section 9.4).

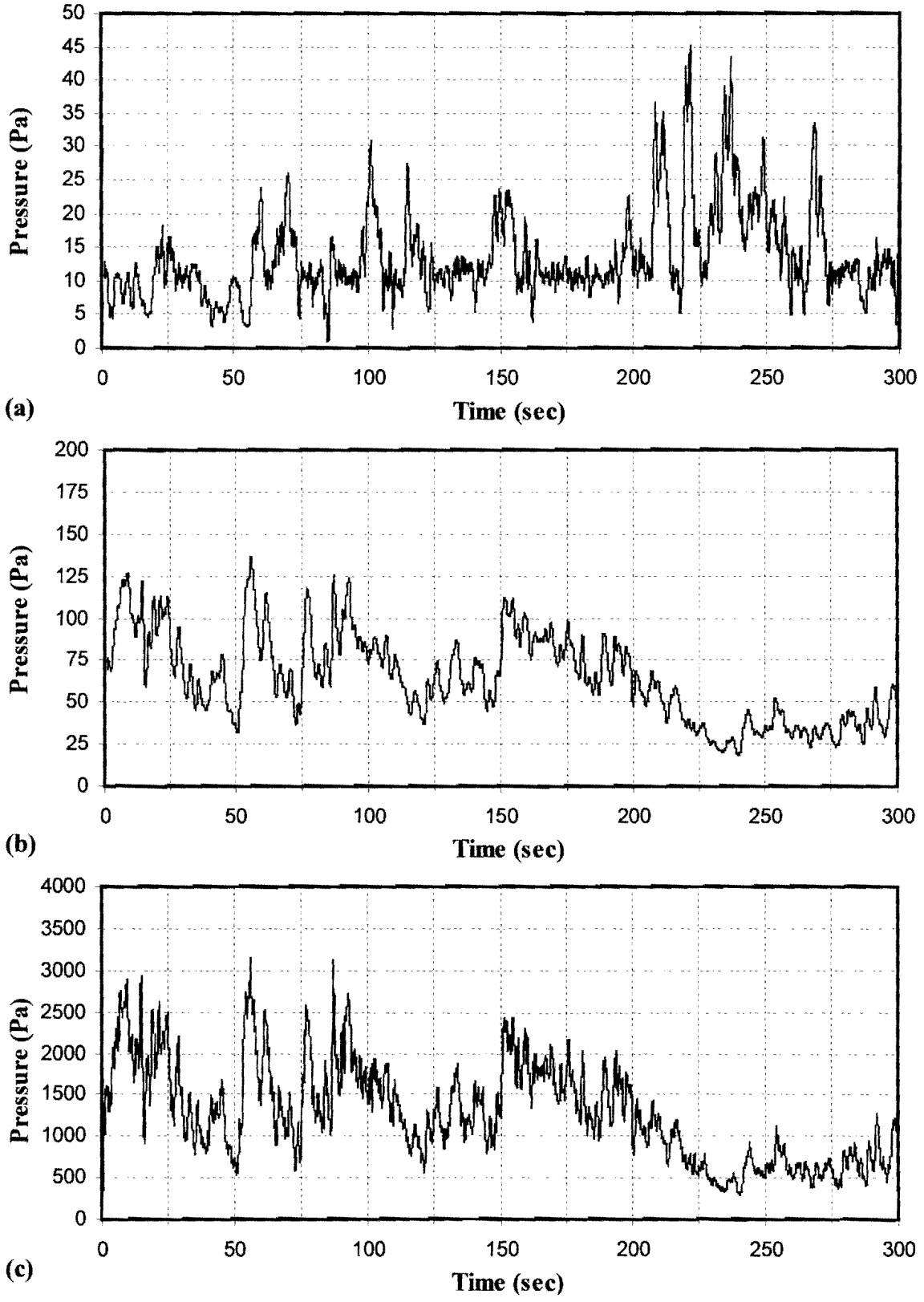

Figure 58. Time Histories of Maximum Wind Pressure: (a) Riverside Campus; (b) Original M15N541; and (c) Amplified M15N541

A semi-log plot of frequency of the fluctuating wind pressure for M15N541 is obtained through implementation of an FFT (see Figure 59). The first three natural frequencies of the prototype soundwall obtained from the system identification described earlier are also indicated on the graph for direct comparison.

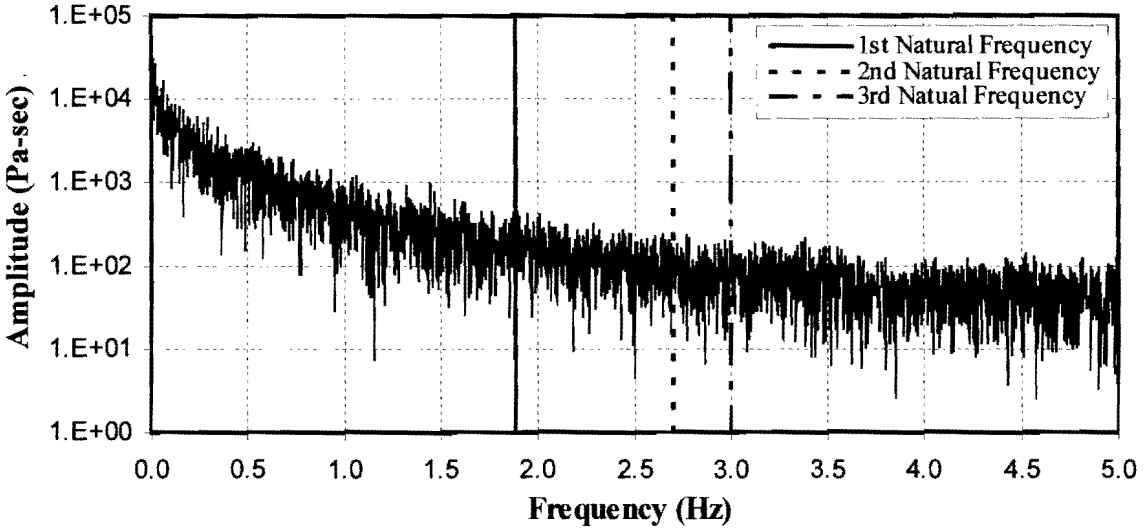

Figure 59. Frequency Spectrum of Original M15N541 Wind and Natural Frequencies of Prototype Soundwall

Primary energy of wind occurs mostly in the lower range of frequencies. As indicated, the first three natural frequencies of vibration of the prototype soundwall occur at 1.88, 2.71, and 3.00 Hz. For this reason, behavior of the prototype soundwall is checked for excess vibration due to wind excitation.

9.4 DYNAMIC RESPONSE

Discretization of the finite element mesh used in all dynamic analyses is shown in Figure 48. Two deterministic wind events are applied to the finite element model: a wind time history collected at the Riverside Campus that has a mean velocity of 4.0 m/sec (9 mph) and an amplified version of the M15N541 wind that has a mean velocity of 40.1 m/sec (90 mph). Three hundred seconds of wind pressure time history associated with each wind event are shown in Figure 58 (a) and (c), respectively.

9.4.1 Simulation Using Riverside Campus Wind Event

Deflection and acceleration of the prototype soundwall at the top and center of module 4 (refer to Figure 12) in the prototype soundwall is predicted by finite element simulation for 100 seconds of the Riverside Campus wind. The portion of the pressure time history applied to the model corresponds to a range in time from 200 to 300 seconds in Figure 58 (a) in order that maximum gust pressures are included in the numerical simulation.

As shown in Figures 60 and 61, maximum predictions of deflection and acceleration are 0.62 cm (0.24 in.) and 0.95 m/sec^2 (3.12 ft/sec^2), respectively. In comparison, maximum acceleration of 1.0 m/sec^2 (3.28 ft/sec^2) for the Riverside Campus wind was obtained from an accelerometer placed at the identical location on the prototype soundwall.

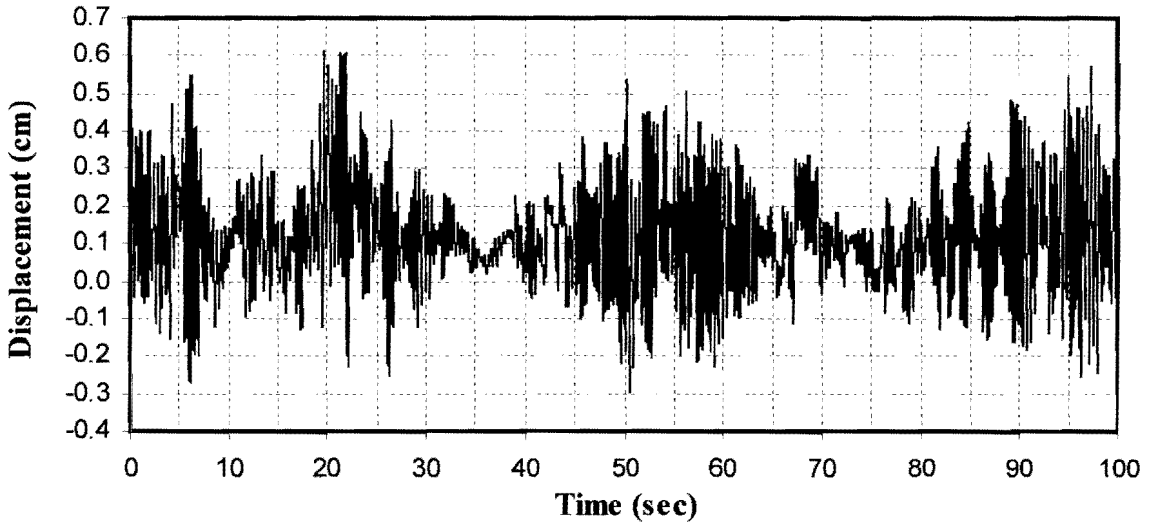

Figure 60. Time History of Deflection at the Top of the Wall Due to Riverside Campus Wind Event as Determined by Numerical Simulation

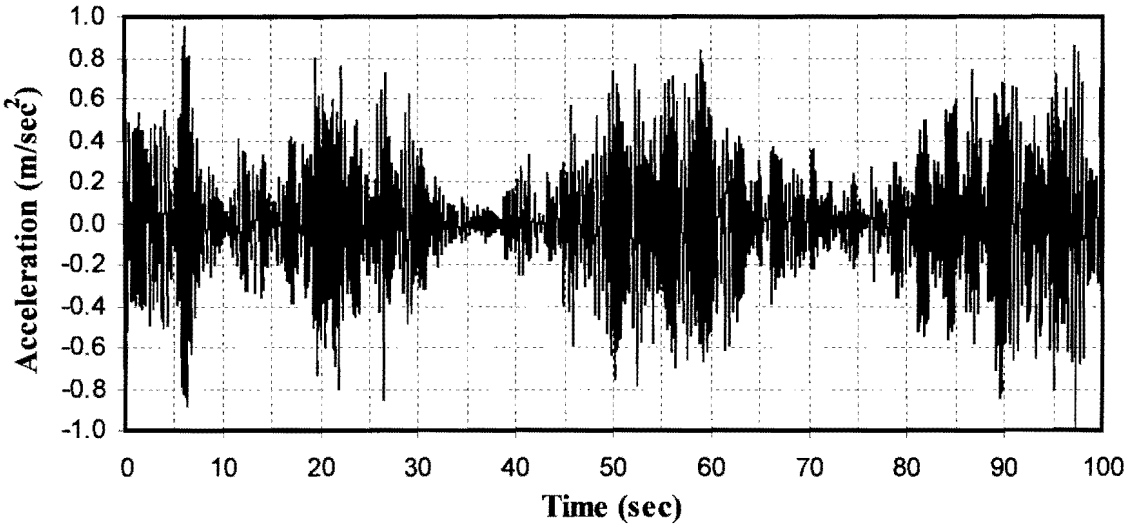

Figure 61. Time History of Acceleration at the Top of the Wall Due to Riverside Campus Wind Event as Determined by Numerical Simulation

If predicted and experimental acceleration data are transformed to the frequency domain through an FFT, frequency response of the numerical simulation matches reasonably well with the experimentally determined frequency for the first mode of the wall (see Figure 62). The frequencies corresponding to the peak numerical and experimental response occur at approximately 2.40 Hz and 2.00 Hz, respectively. As mentioned previously, the soundwall was not modeled exactly in the finite element simulation and, therefore, some differences in frequency response are not unexpected.

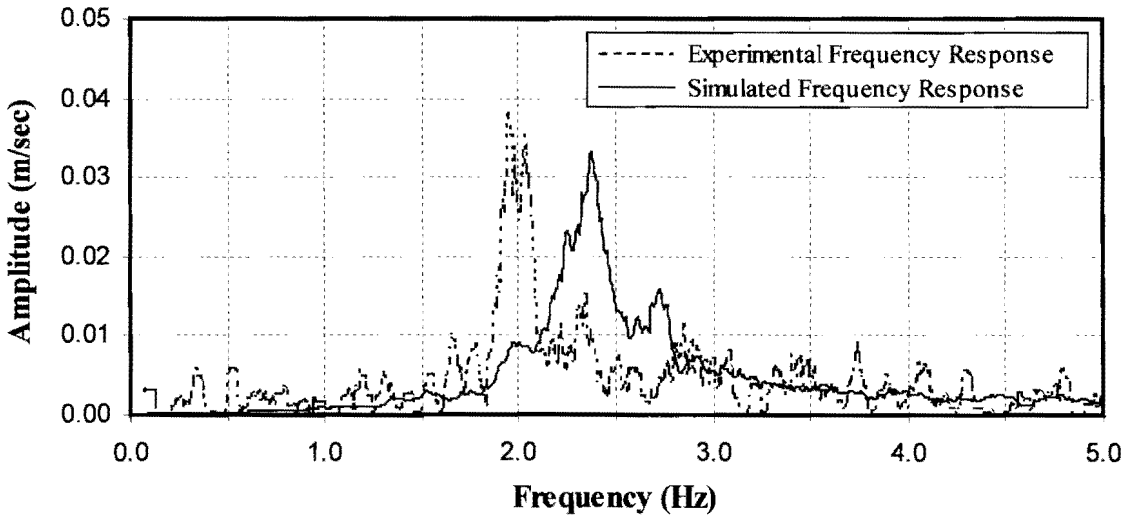

Figure 62. Experimental and Numerical Frequency Response to Riverside Campus Wind Event

Conservative estimates might be expected for maximum deflection and acceleration response in the simulation due to the fact that the applied pressure excites the structure uniformly along the entire length of the barrier. However, the numerical model is known to be stiffer than the actual soundwall structure (see Section 8.4) and, therefore, overly conservative estimates are avoided.

9.4.2 Simulation Using Amplified M15N541 Wind Event

Cross-sectional dimensions of columns in the prototype soundwall were chosen based on static load-deflection criteria that were established in the design phase of the project (see Section 4.3). However, with regard to dynamic behavior, it was necessary to investigate the response of the prototype soundwall to a strong wind event. Large deflection or oscillations of the wall structure could pose a hazard to those living or passing by the structure.

As shown in Figure 63, maximum transverse deflection predicted by FEA at the top-center of module 4 in the prototype soundwall due to a wind that has an average sustained velocity of 40.1 m/sec (90 mph) is 30.3 cm (11.9 in.). Maximum change in position for one cycle of oscillation is 23.0 cm (9.1 in.). Also, the top of the wall is predicted to have a maximum acceleration of 24.3 m/sec^2 (79.7 ft/sec^2) as shown in Figure 64.

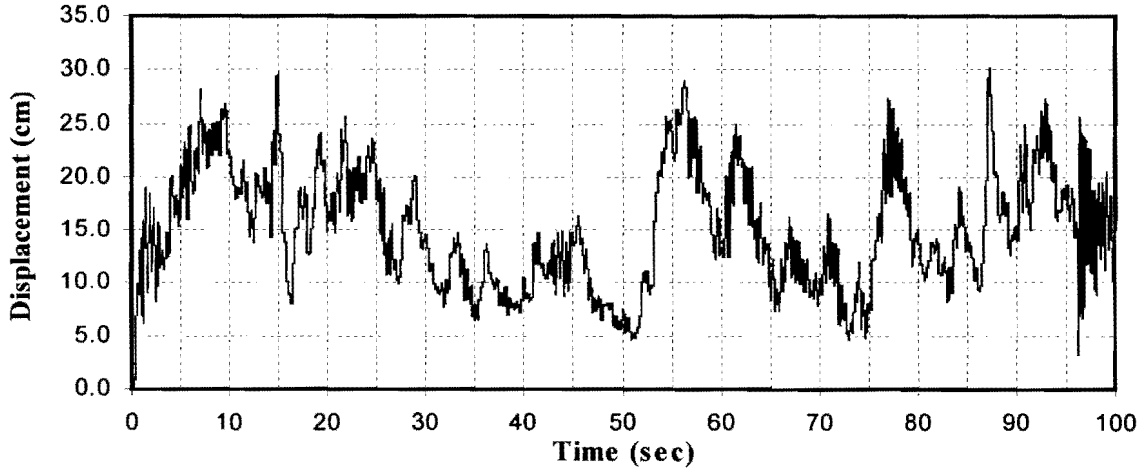

Figure 63. Time History of Deflection at the Top of the Wall Due to Amplified M15N541 Wind Event as Determined by Numerical Simulation

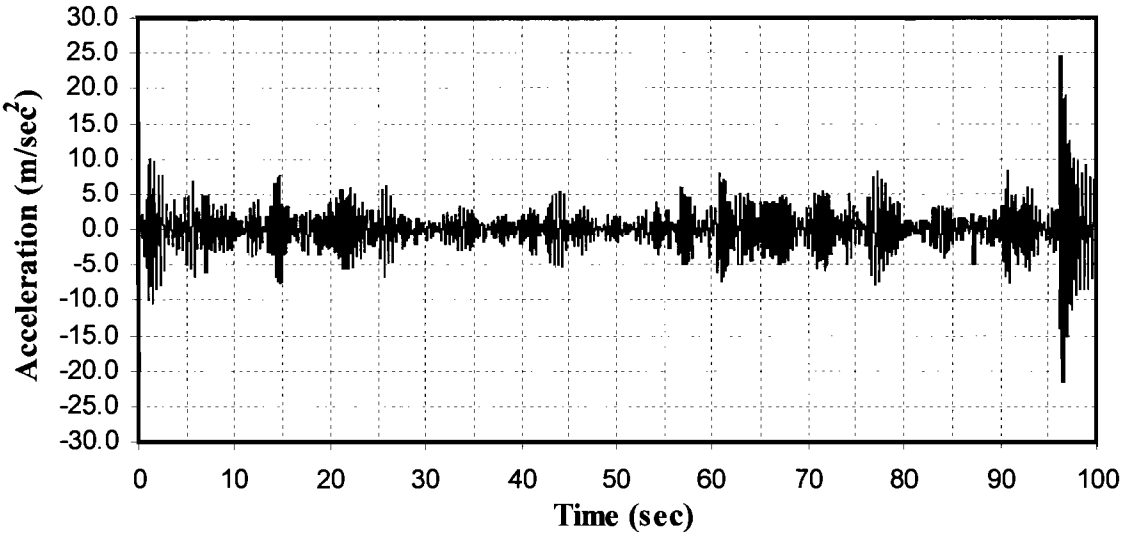

Figure 64. Time History of Acceleration at the Top of the Wall Due to Amplified M15N541 Wind Event as Determined by Numerical Simulation

Based on static load-deflection criteria discussed in Section 4.3.1 using the ASCE 7-95 (1995), deflection due to a 40 m/sec (90 mph) wind event is calculated to be 15.2 cm (6.0 in.). Therefore, the amplitude of the deflection response is predicted by FEA to be approximately 100% higher for the dynamically excited soundwall. While these levels of deflection and acceleration might be acceptable for such an extreme wind event, it is unknown as to whether or not the connections that hold the components of the wall together would be able to withstand the repeated loading and they could potentially fail in a fatigue mode.

Predicted acceleration output from the numerical simulation of this strong wind event is transformed to the frequency domain through an FFT. As shown in Figure 65, the primary frequency response of the amplified M15N541 wind load occurs at approximately 2.30 Hz. This value is less than the simulated frequency response produced by the Riverside Campus wind of 2.40 Hz, but it is still greater than the experimental frequency response of 2.00 Hz (see Figure 62).

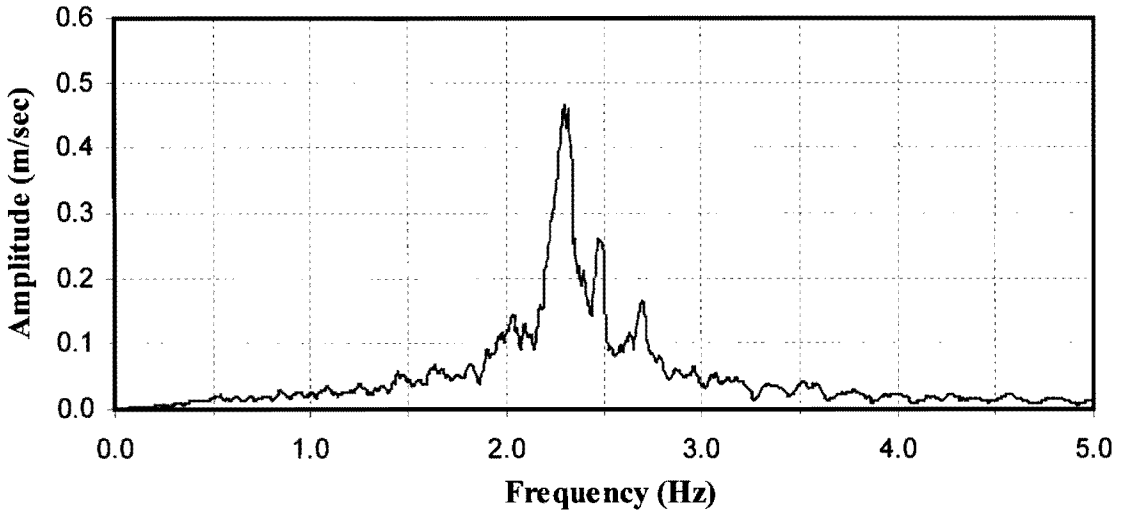

Figure 65. Frequency Response to Amplified M15N541 Wind Event

9.5 RANDOM RESPONSE

Finite element results for transverse deflection and acceleration were reported in the previous section for an actual wind event and a simulated time loading. Analysis of dynamic wind pressure was carried out using modal superposition. An important assumption was that the structure was excited with a pressure that varies linearly with height from the ground and is constant along the entire wall. In this section, a probabilistic method is utilized to predict dynamic response of the wall. A technique for using random response analysis leads to determination of a root mean square (RMS) value for maximum deflection. Additionally, a parametric study calculates this value for heights of the wall that range from 3.66 m (12 ft) to 5.21 m (17.1 ft). Comparison of a probabilistic RMS value of deflection for a 3.66-m (12-ft) high wall to an RMS value obtained using modal superposition and a deterministic time history of pressure leads to less conservative predictions.

9.5.1 Theory

According to the ABAQUS User's Manual (1995), random response analysis is used "to predict the response of a structure subjected to a nondeterministic continuous excitation that is expressed in a statistical sense by the combination of a power spectral

density (PSD) function and a correlation matrix." Since the loading is nondeterministic, it is characterized in a statistical sense and, therefore, several assumptions must be made. First, the excitation is taken to be a stationary process such that its statistical properties do not very with time. Secondly, the excitation must be ergodic. This means that, if one were to take several samples of excitation, then the time average of each sample would be the same regardless of the time origin. A wind signal, such as the one shown in Figure 58 (c), fits the description of a nondeterministic, continuous waveform and is assumed to satisfy requirements of being a stationary, ergodic process.

Some statistical characteristics that are used to describe random processes such as wind excitation include mean value, standard deviation, variance, and coefficient of variation (see Table 14). Other statistical properties that might be considered include probability density function, correlation, and power spectral density (PSD). Of primary interest in the current application are the mean value, correlation, and PSD of the amplified M15N541 wind event that is applied to the prototype soundwall through numerical simulation.

9.5.1.1 Power Spectral Density

Power spectral density is a measure of the energy of a stationary random process as a function of frequency. While a continuous PSD is a measure of the energy of the wind over a range of frequencies, a discrete equivalent is the average energy over a frequency interval (Miller 1994). If a Fourier transform is performed on a function $x(t)$ producing the complex data set $X(f)$, then the PSD over the range of frequencies $0 \le f < \infty$ is defined as follows:

$$\phi(f) = |X(f)|^2 + |X(-f)|^2 \tag{62}$$

When $x(t)$ is a real valued function such as arises from a wind event, the two terms are equal because $X(f)$ represents the complex conjugate of $X(-f)$. Therefore, Equation (62) reduces to the one-sided spectral density function and extends only over the positive frequency range:

$$\phi(f) = 2|X(f)|^2 \tag{63}$$

After subtracting the mean value of the amplified M15N541 wind event (see Figure 58 [c]), a one-sided PSD is calculated (see Figure 66) using an algorithm entitled **PSDD.m** (see Appendix C). As an alternative, a MATLAB® algorithm entitled PSD.m is capable of estimating a one-sided PSD using Welch's averaged periodogram method (MATLAB® 1992).

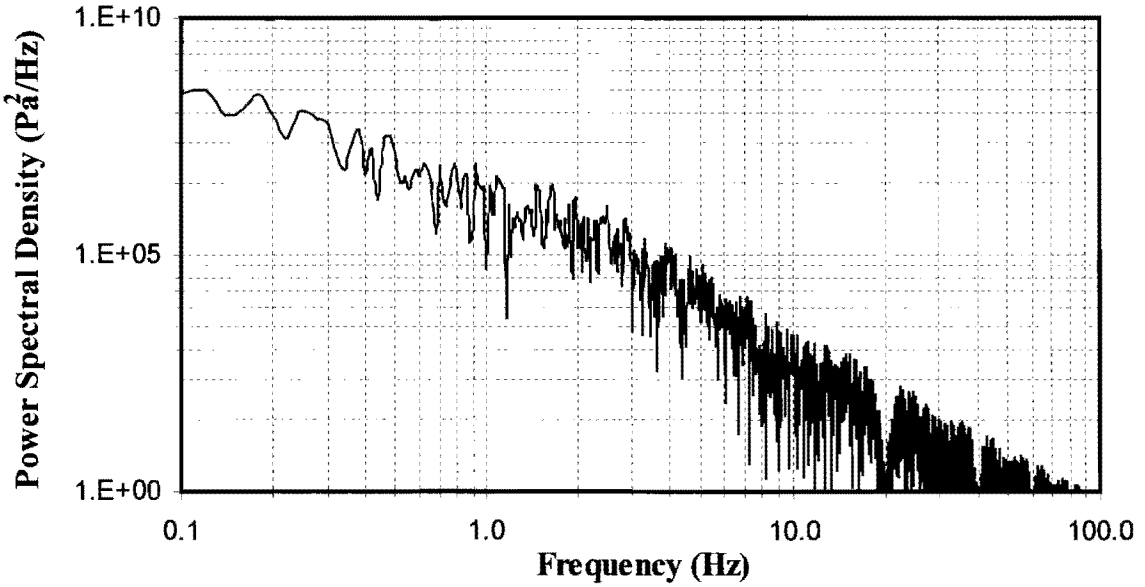

Figure 66. One-Sided Power Spectral Density of Amplified M15N541 Wind Event

Similar to a frequency spectrum associated with a given wind event (see Figure 59), the primary energy contribution of wind occurs in the lower range of frequencies and, therefore, the lowest modal frequencies of the structure are important indicators of the dynamic response.

9.5.1.2 Spatial Cross Correlation of Wind

Cross correlation is a statistical measure of the similarity between two time-dependent variables (Liu 1991). A cross correlation value of one indicates that two variables are perfectly correlated, while a value of zero indicates a complete lack of correlation. The following equation can be used to find the cross correlation between two time-dependent random variables, $X_1(t)$ and $X_2(t)$ (Liu 1991):

$$C = \frac{\overline{X_1' X_2'}}{\sqrt{\overline{X_1'^2}\,\overline{X_2'^2}}} \tag{64}$$

where C is the cross correlation coefficient, the primes denote fluctuating components (i.e. the mean has been subtracted to zero the function), and the bar above any quantity denotes the temporal average of each quantity.

To carry out a random response analysis using a finite element simulation, it is necessary to define cross correlation of wind pressure in the direction perpendicular to the flow of wind (lateral cross correlation) between all nodes in the mesh. This allows differences in wind pressure between any two points on the soundwall surface to be determined (see Figure 68).

Ideally, lateral cross correlation of wind pressure is determined by placing an array of anemometers perpendicular to the flow of wind at various heights in a free-field environment. Cross correlation coefficients between data can then be found using Equation (64). However, results will vary for different wind events. For this reason, a curve of correlation coefficients is developed from an average of 30 sets of experimental data (see Figure 67). These data were obtained from research performed at the Wind Engineering Research Center (WERC) at Texas Tech University. Data were collected from a series of anemometers that were spaced at 9.1 m (30 ft) intervals over 118.9 m (390 ft). Elevation of the anemometers was constant at 3.7 m (13 ft).

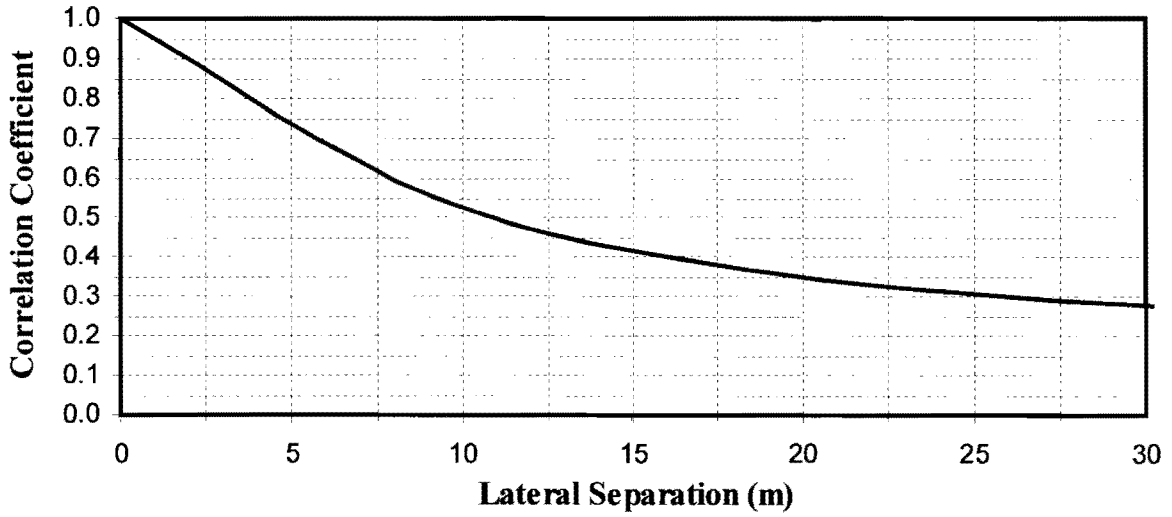

Figure 67. Spatial Correlation of Wind Velocity in Lateral Direction

Although correlation coefficients in Figure 67 were calculated for a number of stations located at a height of 3.7 m (13 ft), in what follows the coefficients are assumed to be valid for any two points on the wall that are separated by a distance *d* as shown in Figure 68.

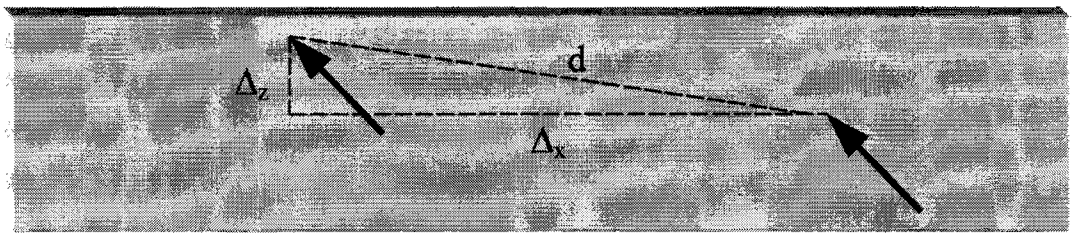

Figure 68. Diagram of Correlation Between Two Points on a Soundwall

Pressure is included in the numerical model by describing an envelope for a one-sided PSD and by specifying the surfaces to which the load is to be applied. In the numerical simulation, pressure loads are applied to finite element nodes using a tributary area approach. Also, it is necessary to define in the ABAQUS code a cross correlation coefficient between all nodes on the windward face of the wall through a user-supplied FORTRAN subroutine (see RANDOM RESPONSE in Appendix D).

This subroutine operates by determining coordinates and distances of separation between all nodes in the model. Using an equation obtained by curve-fitting the plot shown in Figure 67, cross correlation coefficients are determined using radial distances between nodes. A series of IF/THEN statements are also included for optimization purposes so that the subroutine iterates only through relevant combinations of nodes to calculate a large matrix of cross correlation coefficients.

9.5.2 RMS Deflection

Power spectral density is calculated for any dynamic event about a static equilibrium configuration (i.e. the mean value of the dynamic input is zero). In the current application, this is achieved by subtracting the mean from the pressure time history of the wind event shown in Figure 58 (c). Since pressure is a function of velocity that, in turn, is a function of elevation above ground, a distribution of pressure with respect to elevation

above ground must be assumed for the PSD function. To be conservative, a linear variation starting from zero at ground level up to a maximum value at the top of the wall is assumed for the PSD. In calculating total RMS response, it is necessary to add deflection resulting from application of the mean pressure obtained from a static analysis to the RMS deflection predicted from a random response analysis as follows:

$$\Delta RMS_{TOTAL} = \sqrt{(\bar{x})^2 + \frac{\sum_{i=1}^{N}(x_i - \bar{x})^2}{N}} = \sqrt{(\bar{x})^2 + (\sigma)^2} \tag{65}$$

where $\bar{x}$ is the mean static response and σ is standard deviation of the vibration.

A time history of wind pressure was applied to the soundwall in Section 9.4, and deflection response was determined using modal superposition. If the response shown in Figure 63 is subdivided into a time-varying excursion and a mean static deflection, then it is possible to calculate an RMS value using Equation (65). Therefore, a comparison can be made between the RMS deflection obtained via random response and the RMS deflection obtained from a time history analysis (modal superposition). The total RMS value estimated through random response should produce a result identical to a time history analysis if the cross correlation coefficients between all loads are set to one. However, if cross correlation coefficients are applied as suggested in Figure 67, a more realistic RMS response can be determined.

In what follows, total RMS deflection is predicted for a single location at the top of the wall. Walls having four different heights are simulated and results are shown in Table 15. All columns are given the same properties as a column reinforced with fiberglass (see Section 8.2.2.1). Output of RMS deflection was requested at six locations along the top of the soundwall; however, the location corresponding to module 9 of the actual soundwall (see Figure 12) gives the maximum predicted RMS deflection. Individual contributions of the static analysis and the random response analysis components to the overall RMS deflection are also listed along with the first three natural frequencies for each structure.

Table 15. RMS Deflection Due to Amplified M15N541 Wind Event

Wall Height (m)	Natural Frequencies 1st (Hz)	2nd (Hz)	3rd (Hz)	c (cm)	σ (cm)	ΔRMS_{TOTAL} (cm)
3.66	2.31	2.54	3.07	13.5	4.4	14.2
4.18	1.85	2.33	2.87	23.2	10.1	25.3
4.70	1.51	1.99	2.78	37.6	21.8	43.5
5.21	1.27	1.74	2.65	57.9	39.8	70.3

The value of 13.5 cm (5.3 in.) for static deflection of the 3.66-m (12-ft) high prototype soundwall is in good agreement with ASCE 7-95 load-deflection criteria that estimates deflection due to a 40 m/sec wind to be 15.2 cm (6.0 in.). As expected, magnitude of the deflection at the top of the wall is predicted to increase rapidly as the height of the wall increases (see Figure 69). Natural frequencies of the taller structures are relatively lower and, therefore, these structures are more readily excited by a wind event. Greater pressure must also be resisted by the taller structures due to the fact the wind pressure is assumed to increase linearly with elevation above the ground (see Figure 56).

The random response analysis predicts a total RMS deflection for the top of the 3.66 m (12 ft) wall to be 14.2 cm (5.6 in.) for the amplified M15N541 wind event. A deterministic analysis leads to an RMS deflection value of 14.6 cm (5.8 in.) calculated using Equation (65) where $\bar{x} = 13.5$ cm and $\sigma = 5.6$ cm. In this case, there is approximately a 3% reduction in total RMS response when cross correlation of wind is taken into account in numerical simulation; however, reduction in the dynamic component, σ, is approximately 27%. For wall heights of 4.18 m, 4.70 m, and 5.21 m, the reduction in total RMS response is 3%, 4%, and 6%, respectively. Similarly, reduction of only the dynamic component for these heights of wall is 17%, 16%, and 18%, respectively.

From this data, one can conclude that application of a deterministic pressure time history increasingly overestimates response as the height of the structure increases. There is also an overestimation of deflection due to the dynamic component of wind pressure, but the magnitude of this component is small in relation to the static deflection and, therefore, has less effect on overall response.

9.6 RANDOM RESPONSE WITH OTHER TYPES OF COLUMNS

In the previous section, RMS deflection was estimated through random response analysis for four different heights of the prototype soundwall. In this section, four columns with the same geometry but with different amounts of reinforcement are substituted in place of the fiberglass-reinforced columns. As before, the goal is to determine maximum RMS response for deflection at the top of the wall (see Figure 69). Correlation of wind pressure as suggested by Figure 67 is taken into account as is a linear variation of the PSD function versus elevation. Properties of these commercially available columns were supplied by Seaward International. The columns under study have different numbers and diameters of fiberglass rods and, thus, different bending stiffnesses as shown in Table 16. The stiffness and cost of the original fiberglass-reinforced columns in the prototype soundwall are also included in Table 16.

Table 16. Bending Stiffness and Cost of Fiberglass Reinforced Columns

Number and Type of Fiberglass Reinforcement	Bending Stiffness ($kN\text{-}m^2$)	Cost ($ per linear meter)
Fiberglass	441.0	57.80
4-2.5 cm (1 in.) rods	352.3	118.11
8-2.5 cm (1 in.) rods	493.0	--[a]
4-3.2 cm (1.5 in.) rods	862.4	126.31
8-3.2 cm (1.25 in.) rods	1264.4	--[a]

Note: --[a] = Not Available

Columns with fiberglass rods are expensive in comparison with those that utilize fiberglass or steel rebar (see Table 4). Also, it is pointed out that columns with eight fiberglass rods have these rods evenly distributed around their cross section (i.e. a total of three on each side), while columns with four fiberglass rods have one in each corner.

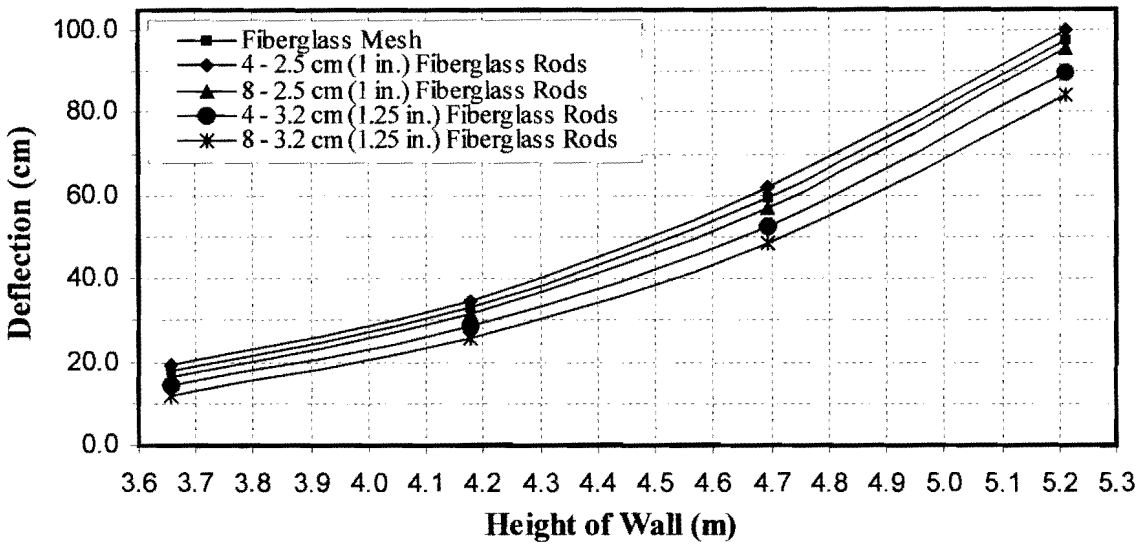

Figure 69. Maximum RMS Deflection at the Top of the Soundwall Due to Amplified M15N51 Wind Event for Different Columns and Wall Heights

Figure 69 provides a useful design tool for choosing an appropriate type of column for a specified wall height. For a wall height of 3.66 m (12 ft), only a few centimeters of deflection are prevented by using the stiffest column. However, in a 40 m/sec (90 mph) wind storm, it is expected that use of the stiffest column will result in approximately 10 cm (3.9 in.) less deflection for a wall height of 5.2 m (17.1 ft). Of course, total RMS deflection of 85 cm (33 in.) for a wall of this height might be considered to be unreasonable. Interestingly, the column reinforced with fiberglass particles performs better at all heights than the column with four 2.5 cm (1 in.) fiberglass rods. Also, the fiberglass-reinforced column is available at a significant reduction in cost.

9.7 SUMMARY

Deterministic simulations have been used to predict an upper bound response for deflection and acceleration at the top of the soundwall due to application of a small- and a large-scale wind event. Of primary interest is the fact that actual prototype soundwall is predicted to deflect a maximum distance of 30.3 cm (12 in.) in a 40.1-m/sec (90-mph) wind when a fully correlated, deterministic time history of pressure is applied. Through use of subsequent random response analyses, it is estimated that there is a 3% reduction in RMS deflection response when lateral cross correlation of wind is considered and a resulting amelioration of response of the wall is experienced. Therefore, a more accurate

value for deflection is estimated to be 29.4 cm (11 in.). A decision needs to be made as to whether or not this magnitude of deflection is acceptable for a wall that is 3.66 m (12 ft) in height.

Vulnerability to large deflections and accelerations can be reduced through use of stiffer columns as suggested in Section 9.7. Alternatively, the geometry of the wall could be redesigned so that the top edge is more aerodynamic. A third option to reduce sensitivity of the wall to wind would be to insert "crumb" rubber into the modules and thereby increase the mass of the structure. As noted previously, there is concern about leaching of toxic chemicals from shredded tire material; however, if this is found not to be the case, this method would increase damping of the soundwall structure and volume of recycled materials used in the wall. At the same time, natural frequencies of the soundwall would be reduced and the low-frequency content of the wind would have a larger effect on the structure. Therefore, the overall effect of this third option is unknown.

10. ACOUSTICS

10.1 INTRODUCTION

Previous chapters have focused on construction and structural behavior of the prototype sound barrier. Clearly, a soundwall must not only be able to withstand environmental loads such as wind and a range of temperatures, but it is to function primarily as a means of reducing noise along a highway or corridor.

"Guidelines for the Analysis and Abatement of Highway Traffic Noise" by the Texas Department of Transportation states that compliance with Title 23 of the Code of Federal Regulations - Part 772 (23 CFR 772) and FHWA's "Highway Traffic Noise Analysis and Abatement Policy and Guidance" is a prerequisite for granting federal-aid highway funds for construction, or reconstruction of a highway in the state of Texas. The 23 CFR 772 asserts that "All highway projects which are developed in conformance with this regulation shall be deemed to be in conformance with the Federal Highway Administration (FHWA) noise standards."

To comply with these guidelines, this chapter focuses on measurement of sound insertion loss of the recycled plastic soundwall by both an experimental and analytical method. Insertion loss is defined as the actual benefit derived from the construction of a noise barrier. A measured insertion loss is obtained through a field testing procedure that follows "Measurement of Highway-Related Noise" (Lee and Fleming 1996). A calculated insertion loss is estimated through computer simulation with the STAMINA 2.0 software package (March 1982 version). The simulation utilizes principles developed by Fresnel diffraction theory. According to this theory, loss of sound results from an increase in the path of sound as it travels around a sound barrier before it reaches the receiver (Klingner et al. 1996).

Two other acoustic descriptors of a noise barrier are often considered. The Noise Reduction Coefficient (NRC) is not determined for this soundwall due to the variety of surface materials used in construction of the wall. NRC ranges from zero to one and indicates a barrier that absorbs all incident sound versus one that reflects all incident sound.

The prototype soundwall is rather reflective due to the smooth, hard recycled plastic material on the surface. This fact suggests an NRC for the prototype wall that is very low, but as stated previously, no NRC was measured.

A Sound Transmission Class (STC) is also used to indicate the amount of noise a barrier transmits. The Mass Law states "that a panel which has a surface through-weight of 9.8 kg/m^2 (2 lb/sf) or more has sufficient mass to prevent transmission of noise through the panel which is higher than that which is diffracted over the top or around the ends of the wall" ("Value-engineered Features and Benefits of Monowall™ Approved for Florida DOT Qualified Products List" 1997). The recycled plastic composing the surface of the prototype barrier has an estimated through-weight of at least 2.1 N/m^2 (5 lbs/sf); therefore, the minimum requirement of the Mass Law is greatly exceeded.

10.2 APPROACH TO DETERMINE INSERTION LOSS

In performing a test to determine the insertion loss, an "indirect" BEFORE method is used (Lee and Fleming 1996) where noise levels are taken at the soundwall site to determine AFTER levels, while BEFORE levels are taken at an equivalent site. A site is deemed to be equivalent if geometric, atmospheric, and traffic conditions are practically identical at both locations. The unique layout of the soundwall at the Riverside Campus makes this determination possible (see Section 10.3).

Noise levels are recorded in decibels with an A-weighting bias. Insertion loss is then "determined by subtracting the difference in the adjusted reference and receiver levels for the BEFORE case from the difference in adjusted and receiver levels for the AFTER case" (Lee and Fleming 1996):

$$IL_i = (L_{A_{ref}} + L_{edge} - L_{A_{rec}}) - (L_{B_{ref}} - L_{B_{rec}}) \tag{66}$$

where IL_i is insertion loss at the ith receiver, L_{edge} is an edge diffraction correction factor, $L_{A_{ref}}$ is an AFTER adjusted reference level, $L_{A_{rec}}$ is an AFTER adjusted source level at the ith receiver, $L_{B_{ref}}$ is a BEFORE adjusted reference level, and $L_{B_{rec}}$ is a BEFORE adjusted source level at the ith receiver.

10.3 SITE AND BARRIER CHARACTERISTICS

The Riverside Campus at Texas A&M University is a renovated military base with many airplane runways. As shown in Figures 24 and 71, the location of the soundwall is ideal for the acoustic testing because it is relatively flat with few tall objects that would impede propagation of sound. A concrete runway is aligned parallel to the soundwall, and the surrounding area is a large pasture with mown vegetation.

An equivalent site to test BEFORE noise levels is located approximately 50 m (164 ft) down the runway from the prototype soundwall. Since the test for insertion loss occurred over a short period of time, atmospheric conditions were approximately the same for BEFORE and AFTER measurements.

The sound barrier is a continuous structure with no apertures between members. For the most part, the wall consists of front and back panel surfaces with an air expanse in between. A small gap does exists between the wall and the ground for purposes of water drainage. Other characteristics of the noise barrier are listed in Table 17.

Figure 70. Location of Soundwall at Riverside Campus Prior to Construction

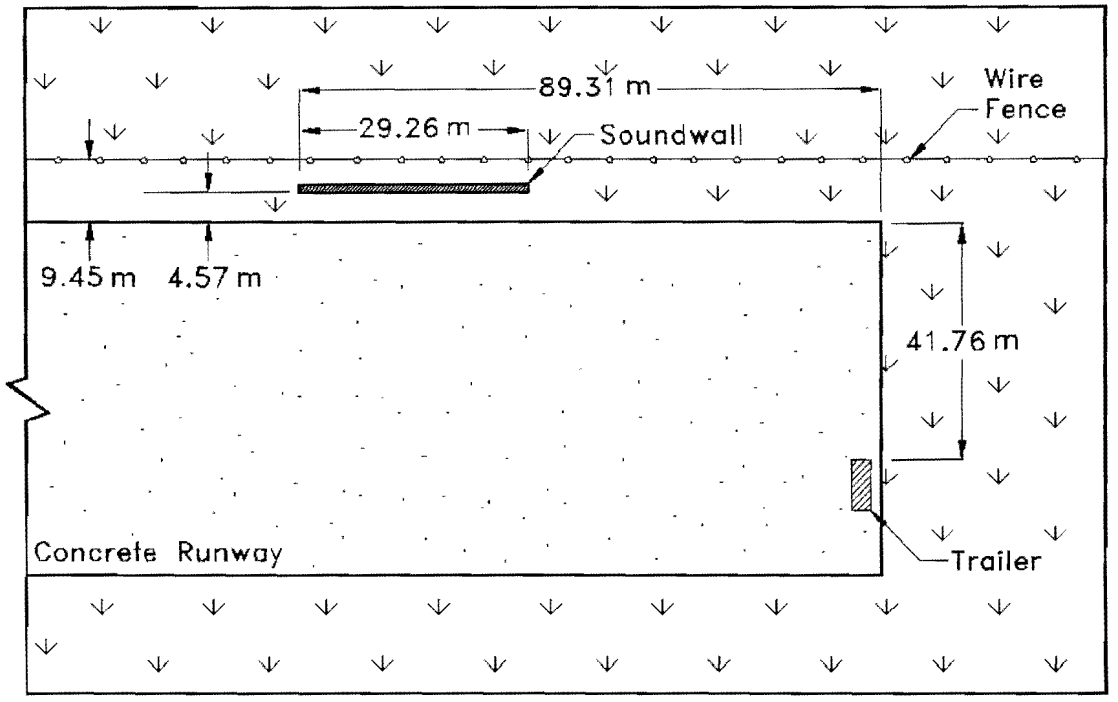

Figure 71. Plan View of Site

Table 17. Barrier Characteristics for Acoustics

Property	Value
Length	29.26 m (96 ft)
Height	3.66 m (12 ft)
Overall Thickness	0.31 m (1 ft)
Effective Thickness	Plastic lumber: 0.102 m (0.333 ft); Sheet plastic: 0.025 m (0.083 ft)
Material	Plastic lumber: FLDPE * Sheet plastic: HDPE **
NRC and STC	See note below
Method of Noise Reduction	Reflection
Tilt Angle	None

Note: Estimates for the NRC and STC are given for the following: Carsonite® International (NRC-0.15 to 0.85, STC-36), Quilite® International (NRC-0.64, STC-25), and Sound Fighter® Systems (NRC-1.0, STC-31). These systems utilize fiberglass-reinforced polyethylene with a rubber core, polycarbonate, and high-density polyethylene, respectively (Freudenrich 1996).
Notation: * FLDPE = fiberglass-reinforced low-density polyethylene
** HDPE = high-density polyethylene

10.4 SOUND EQUIPMENT

Quest Electronics Precision Integrating Sound Level Meters – Model 1800, which meet all ANSI standards, are used to record sound pressure levels in decibels (dBA). They

are set on tripods 1.5 m high at an incidence grazing angle of 45° to the sound source as shown in Figure 72.

In conjunction with the sound level meters, commercial software obtained from National Instruments™ was used to perform an octave-band analysis of the sound source. The software package, named the Third Octave Analysis Toolkit, displays sound intensity at several frequencies as taken from a Philmore CM-56 electret condenser microphone (LabVIEW® 1995). The microphone, which was wired directly to a data card, is known for its low electrical noise characteristics, high sensitivity, high stability, and excellent response at high frequencies (Lee and Fleming 1996).

All recorded sound levels are checked with a 1565-B General Radio Company Permissible Sound Level Meter. This meter was calibrated with a 1567 General Radio Company Sound Level Calibrator.

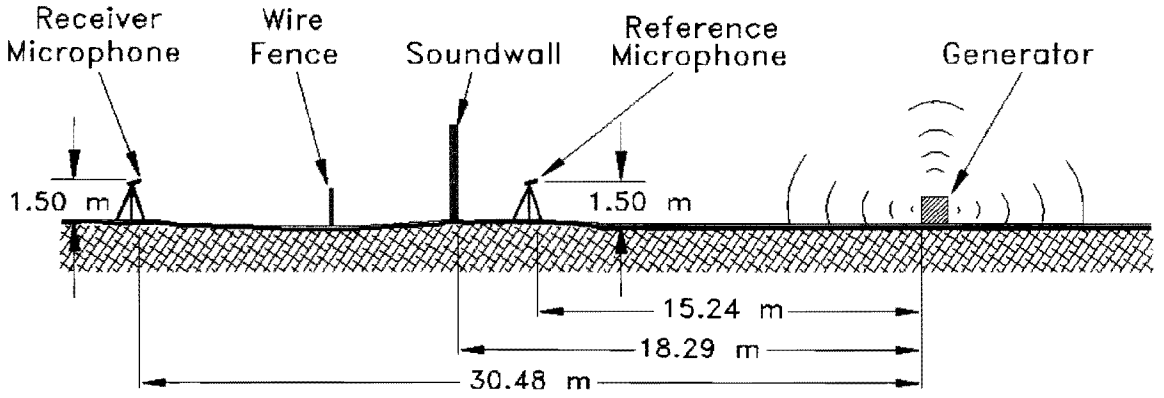

Figure 72. Elevation View of Setup for Insertion Loss

10.5 NOISE SOURCE

A power generator was used to produce noise at the soundwall site because no traffic passes by the wall. As an alternative, noise could have been produced by driving vehicles past the wall, but it was anticipated that noise would go around the ends of the relatively short wall thus making this option less advantageous.

The power generator produces constant, stationary sound; therefore, it is an excellent candidate to be classified as a point source. Intensity of the sound produced by

the generator is a function of distance from the point source ("Highway Noise Fundamentals" 1980):

$$I = \frac{W}{A} = \frac{W}{4\pi r^2} \propto {p_{rms}}^2 \tag{67}$$

where I is sound intensity at receiver (Pa), A is an area through which sound power passes (m^2), W is sound power passing through area A (Pa/m^2), r is a distance between source and receiver (m), and p_{rms} is sound pressure (Pa).

It is known that noise radiates spherically from a point source. Doubling of distance from the point source quadruples the area of the sphere through which sound power passes, thus reducing sound intensity by a factor of four. This phenomenon is referred to as the "inverse-square law."

To put the change in sound intensity in terms of a change of sound pressure level, the following relationship is known ("Highway Noise Fundamentals" 1980):

$$\Delta L = 10\log\left[\frac{{r_o}^2}{{r_i}^2}\right] \tag{68}$$

where ΔL is a change in sound pressure level (dB), r_o is the distance of a reference microphone from the point source (m), and r_i is the distance of a receiver microphone from the point source in meters.

Theoretically, the sound level decreases by six decibels if the location of the receiver position is twice that of the reference position. This scenario is referred to as "six decibel per distance doubling." As shown in Figure 72, there is a doubling of distance between the receiver and reference microphones for the field test of insertion loss; for this reason, one would expect a loss of six decibels over this distance even without a sound barrier. The loss will be slightly different due to surface conditions of the ground and weather conditions such as variable winds.

10.6 RESULTS OF INSERTION LOSS

On a warm summer day, a power generating motor was set up at the soundwall and sound measurements were recorded in front of and behind the soundwall at distances specified in Figure 72. The test setup was moved further down the runway and an identical test was performed without the presence of the soundwall. Table 18 shows averages of BEFORE and AFTER A-weighted sound levels taken during three consecutive tests.

Table 18. Recorded Sound Levels

Microphone Location	BEFORE Level (dBA)	AFTER Level (dBA)
Reference (@ 15.24 m)	76.3	77.4
Receiver (@ 30.48 m)	66.0	50.0
Insertion Loss = (77.4 + 0.0 – 50.0) – (76.3 – 66.0) = 17.1 dBA		

Insertion loss was determined to be 17.1 dBA using the "indirect" BEFORE method given by Equation (66). Generally, a barrier that breaks the line of sight between the source and the receiver provides the minimum 5.0 dBA of insertion loss that is required by many states. Table 19 relates the effectiveness of a sound barrier to its insertion loss ("Traffic Noise Analysis Seminar" 1995).

Table 19. Effectiveness of Insertion Loss

Insertion Loss (dBA)	Energy Loss (%)	Loudness	Comment
6	75	Noticeable	Typical noise barrier reduction
10	90	One-half as loud	Usually highest achievable reduction
15	95	One-third as loud	Difficult to obtain
20	99	One-fourth as loud	Barrier would be too tall to consider

By these standards, the noise reduction capability of this barrier is more than adequate. The predicted drop of six decibels due to distance doubling at the location without the soundwall is measured to be 10.3 dBA. Probable causes for this unexpectedly large reduction in the level of A-weighted sound might include shifting winds and soft ground effects such as tall grass.

As shown in Figure 73, an octave band analysis was performed on the stationary sound source (i.e. the power generator) that had an overall sound level of 77 dBA. For comparison, a hypothetical octave band spectrum is shown for moving truck noise with an overall sound level of 82 dBA as calculated from a mixture of its three principal sources of noise: tires, exhaust, and engine ("Highway Noise Fundamentals" 1980). Contributions to overall sound intensity are shown for frequencies ranging from 20 to 20,000 Hz which corresponds to the frequency range of human hearing. These data are important because the wavelength of sound and the distance it travels is characterized by its frequency content.

Octave band analysis is often used to identify the dominant sub-sources of noise (i.e., exhaust stack, engine, tires) so that specific noise control measures for various sub-sources can be implemented. Here, comparison of the two spectrums shows that a higher range of frequencies of sound are excited by the power generator than those by truck noise. Based on comparisons such as the one shown in Figure 73, decisions can be made by experienced acoustical engineers as to whether or not a power generator provides an alternative means for testing insertion loss of sound barriers.

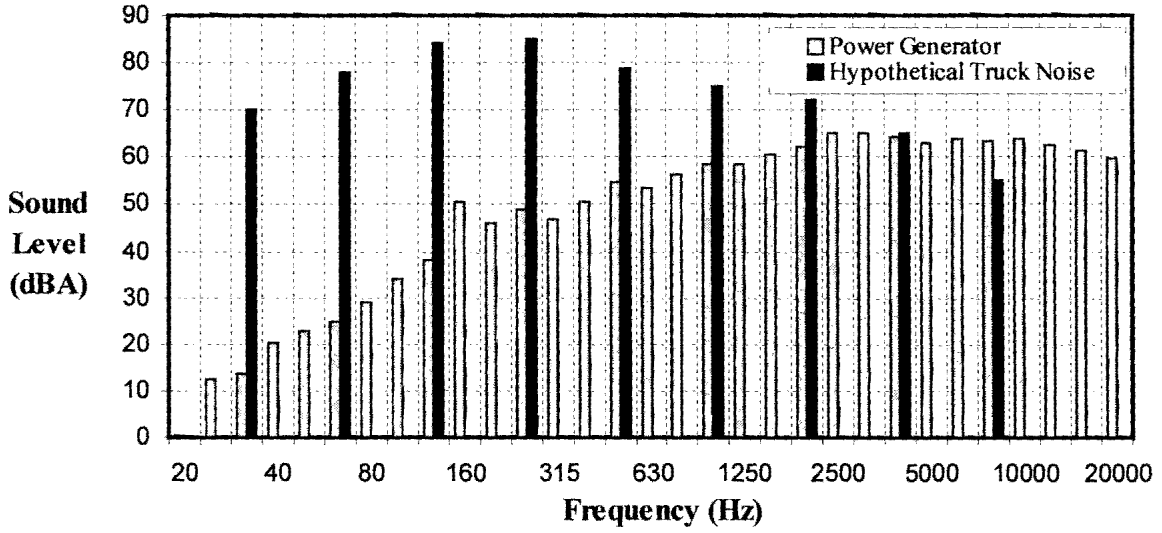

Figure 73. Octave Analysis Comparison of Noise Sources

10.7 NUMERICAL SIMULATION OF INSERTION LOSS

STAMINA requires that the number and types of vehicles be specified as input. Due to the fact that a power generator was used in the field test on the prototype soundwall, an equivalent number of vehicles that would produce the same sound level was specified. The generator emitted 75.5 dBA in field tests at a distance of 15.24 m from the reference microphone. As shown in Appendix B, a traffic flow of 7,000 cars/hour, 400 heavy trucks/hour, and 400 medium trucks/hour that are placed the same distance from the receiver will generate an equivalent sound level of 75.1 dBA in STAMINA.

Another input for STAMINA is the length of the roadway. To account for the fact that the stationary power generator emits noise as a point source, length of roadway is set to a small value of 6.10 m (20 ft), as shown in Figure 74. The short stretch of roadway also keeps vehicle noise from traveling around the ends of the small soundwall in the simulation. Error is obviously introduced into the model by this technique because sound from a point source radiates differently than that from a line source, and STAMINA treats the short stretch of roadway as a line source.

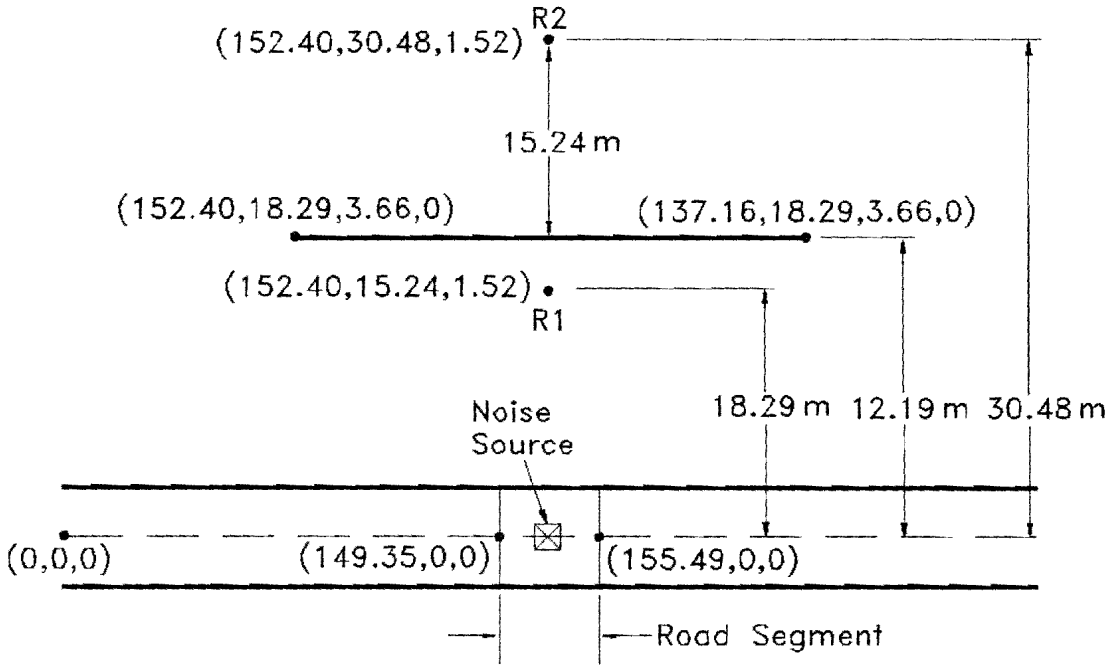

Figure 74. Plan View of Geometry for STAMINA 2.0 Simulation

Two other input values are also worth mentioning. An alpha factor was chosen as 0.5 for "soft ground" since a majority of the site is covered by grass, and a shielding factor was taken to be 0.0 since there are no tall sound hindrances near the wall.

Once all of the values were entered into STAMINA, the program was executed and an insertion loss of 12.2 dBA was predicted. This value is conservative in comparison with the measured insertion loss of 17.1 dBA.

10.8 SUMMARY

Use of a stationary power generator for production of noise greatly simplifies the testing of insertion loss. While STAMINA estimates the insertion loss to be 12.2 dBA, the measured insertion loss is 17.1 dBA. Discrepancy in results is most likely related to the use of the stationary noise source and how it is modeled in STAMINA. Overall, the sound barrier proved to possess excellent characteristics of acoustic reduction and should be acoustically suitable for installations along highways.

11. CONCLUSIONS

11.1 MATERIAL DURABILITY

Manufacturers of recycled materials, such as Plastic Pilings, Inc., often have 50-year warranties against material defects. In reality, it is difficult to determine whether structures made from a combination of recycled plastic materials will degrade over a long period of time. Today, recycled plastics appear to possess more durability than previous recycled materials. For example, they can withstand prolonged exposure to ultraviolet radiation due to UV retardant additives. In addition, composite melding with steels and fiberglass, advances in polymer technology, and improvements in manufacturing techniques are enhancing the strength and quality of the materials.

Both exemplary and unacceptable behavior of recycled materials was witnessed in the course of this study on the prototype soundwall. While the structure was exposed to extreme weather for a period of nearly one year, several plastic sheets manifested localized warping. In contrast, plastic lumber boards showed few detrimental effects from weathering and exposure to ultraviolet radiation. It was expected that the unreinforced plastic lumber boards might also warp based on initial observations (see Chapter 3); however, no bowing was manifested because the internal frame of each module supported the boards sufficiently. Also, there was no noticeable deformation of the soundwall indicating that the internal framework is capable of withstanding long-term thermal and wind loadings. It is suggested that future applications for soundwall structures employ materials with fiberglass-reinforcement since fiberglass adds substantially to stiffness and facilitates construction of good connections between members. In conclusion, recycled plastics used in the prototype soundwall performed acceptably well over a period of approximately one year.

11.2 CONSTRUCTABILITY AND STRUCTURAL INTEGRITY

The entire prototype soundwall was constructed in approximately three months by four people. Fabrication of modules progressed smoothly after a procedure was developed for constructing sheet plastic modules and plastic lumber modules (see Chapter 5). It was quickly learned that columns need to be carefully aligned and evenly spaced in the field

before the modules are inserted. One column was misaligned resulting in the prototype soundwall not being perfectly straight. In a second case, a module was also constructed with a width slightly greater than the span between columns which made insertion difficult. Other than for this module there was little difficulty using a forklift to insert the modules between the columns. In future applications, modules could be inserted more quickly with a hoist or crane.

Structurally, all modules in the prototype soundwall maintained their integrity over the course of approximately one year. An exception, mostly aesthetic, is the warping of some sheet plastic panels. As described in Chapter 6, plastic lumber modules proved to have higher rigidity in both the long and short span directions compared to the sheet plastic modules. Higher rigidity of the plastic lumber module in the long direction is mostly due to use of fiberglass reinforced lumber; therefore, future installations would do well to continue to incorporate the inner frame of plastic lumber modules.

As for connections, only minor difficulties were encountered with screws, nails, or bolts coming loose. Screws seemed to work best in connecting structural members together, but ring-shank nails are economically and aesthetically appealing making this a viable alternative.

11.3 DYNAMIC BEHAVIOR

After intense investigation of dynamic characteristics of the soundwall for purposes of determining the degree of wind sensitivity, it was found that the prototype barrier is mildly susceptible to resonant response due to wind loading (see Chapters 8, 9, and 10). A large scale wind event was applied to a finite element model of the soundwall and maximum deflection was predicted to be 30.3 cm (11.9 in) at the top of the wall for a wind with a mean velocity of 40.1 m/sec (90 mph). Subsequent analyses accounting for cross correlation of wind resulted in reduction of maximum deflection to a value of 29.4 cm (11.6 in.). A decision needs to be made as to whether or not this magnitude of deflection is acceptable for wall that is 3.66 m (12 ft) in height. No abnormal behavior or vibration was detected for the prototype soundwall, but it was exposed only to moderate winds at the Riverside Campus of Texas A&M University.

For taller plastic soundwalls, wind sensitivity is even a greater concern. Since stiffness of the prototype barrier is provided for the most part by the columns, sensitivity to wind loadings could be reduced by increasing column size or increasing steel or fiberglass reinforcement within each column (see Section 9.6). Increased natural frequencies of the system due to higher stiffnesses would reduce susceptibility to wind by moving the natural frequencies away from the frequency spectrum associated with wind.

11.4 ACOUSTIC PERFORMANCE

With a measured insertion loss of 17.1 dBA, future installations of this type of soundwall should easily meet or exceed the required minimum insertion loss of 5.0 dBA (see Chapter 10). Since no regular traffic passes the barrier, a power generator was successfully used to produce noise. Although STAMINA 2.0 predicts a 12.1 dBA insertion loss, many assumptions were made to model the noise source in the simulation; therefore, some discrepancy is expected between results of the field insertion loss test and the simulation.

In light of the fact that there was no mention of sound production for a sound barrier by alternative means in any of the journals relating to sound analysis fundamentals, this subject is open to further debate by experienced acoustic engineers.

11.5 COST

According to information on noise barrier costs, average unit costs (in 1995 dollars) for earth berm barriers are $43 per square meter, concrete barriers average $202 per square meter, and brick averages $206 per square meter (Armstrong 1996). Average costs per square meter for wood, metal, and combination barriers are approximately $145, $137, and $152, respectively. Lower life-cycle costs associated with use of recycled plastic materials is economically favorable and environmentally beneficial. Many types of recycled plastic materials were incorporated into the full-scale prototype soundwall. Table 20 summarizes all costs associated with construction of the full-scale soundwall.

Table 20. Actual Soundwall Cost

Item	Quantity	Unit Price ($)	Total Item Cost ($)
Columns			
#8 steel-reinforced plastic	4	411.30	1,645.20
#4 steel-reinforced plastic	4	360.00	1,440.00
Fiberglass-reinforced plastic	5	316.80	1,584.00
Tongue-and-groove plastic lumber			
Fiberglass-reinforced plastic	88	37.32	3,284.16
Unreinforced plastic	44	28.08	1,235.52
Plastic sheets			
1.27-cm (1/2-in.) thick	20	200.00	4,000.00
1.91-cm (3/4-in.) thick	4	295.00	1,180.00
Vertical spacers			
Unreinforced plastic	30	86.76	2,602.80
Horizontal boards			
Fiberglass-reinforced plastic	96	15.54	1,491.84
Connections			
Bolts	48	2.00	96.00
Screws (per box)	5	10.00	50.00
Nails (per bag)	5	2.50	12.50
Labor			
Construction (per person-hour)	150	5.00	750.00
Installation (per person-hour)	40	5.00	200.00
Shipping and handling of materials			
Plastic lumber module and adjacent column	6	125.00	750.00
Plastic sheet module and adjacent column	6	100.00	600.00
Foundation			
Holes, concrete, steel (per column)	13	50.00	650.00
		Total Costs ($) =	21,572.02
		Surface Area of Wall (m^2) =	107.02
		Cost per Square Meter ($/$m^2$) =	201.57

With an approximate cost of $201.57 per square meter, the recycled plastic soundwall provides a viable alternative to conventional building materials. Two of the most promising components in the prototype soundwall are fiberglass-reinforced plastic lumber modules and fiberglass-reinforced plastic columns. It is expected that future soundwall installations would use a combination of these two components. Therefore, Table 21 shows an amended cost estimate for this scenario in which the columns are less expensive, but larger a number of more expensive plastic lumber is required. Shipping costs are also reduced in anticipation of procurement of materials from an in-state manufacturer.

Table 21. Estimated Future Cost

Item	Quantity	Unit Price ($)	Total Item Cost ($)
Columns			
Fiberglass-reinforced plastic	13	316.80	4,118.40
Tongue-and-groove plastic lumber			
Fiberglass-reinforced plastic	264	37.32	9,852.48
Vertical spacers			
Unreinforced plastic	24	86.76	2,082.24
Horizontal boards			
Fiberglass-reinforced plastic	96	15.54	1,491.84
Connections			
Screws (per box)	12	10.00	120.00
Labor			
Construction (per person-hour)	120	5.00	600.00
Installation (per person-hour)	40	5.00	200.00
Shipping and handling of materials			
Plastic lumber module and adjacent column	12	100.00	1,200.00
Foundation			
Holes, concrete, steel (per column)	13	50.00	650.00
		Total Costs ($) =	17,616.96
		Surface Area of Wall (m^2) =	107.02
		Cost per Square Meter ($/$m^2$) =	164.61

The estimated cost of the all-fiberglass-reinforced soundwall is approximately $164.61 per square meter. This is much less expensive than the actual cost per square meter of the prototype soundwall. The savings when compared to $202 per square meter and $206 per square meter for concrete and brick sound barriers, respectively, would be quite significant for a large soundwall installation.

11.6 PROJECT SUMMARY

Several topics related to use and construction of a sound barrier with recycled plastics have been thoroughly addressed. These subjects include durability of recycled plastics, constructability, structural integrity, dynamic performance, acoustic effectiveness, and aesthetic appeal. With knowledge gained from experimentation with recycled plastics in construction of the prototype soundwall, the researchers believe an effective sound barrier system can be developed for use in Texas.

REFERENCES

AASHTO. (1989). "Guide Specifications for Structural Design of Sound Barriers." Washington, D.C.

AASHTO. (1975). "Standard Specifications for Structural Supports for Highway Signs, Luminaries, and Traffic Signals." Washington, D.C.

AASHTO. (1994). "Standard Specifications for Structural Supports for Highway Signs, Luminaries, and Traffic Signals." Washington, D.C.

ABAQUS. (1995). "ABAQUS User's Manual." Hibbitt, Karlson, & Sorenson, Inc., version 5.5, Pawtucket, RI.

Anderson, G., Regan J., Fleming, G., and Menge, C. (1978). "Federal Highway Traffic Noise Prediction Model." Federal Highway Administration, Washington, D.C.

Armstrong, R. (1996). "Highway Traffic Noise Barrier Construction Trends." *The Wall Journal*, v. 6, no. 27, pp. 6-9, Lehigh Acres, FL.

Armstrong, R. (1997). "Summary of Noise Barriers Constructed by End of 1995." *The Wall Journal*, v. 5, no. 26, pp. 12-19, Lehigh Acres, FL.

ASCE 7-95. (1995). "Minimum Design Loads for Buildings and Other Structures." American Society of Civil Engineers, New York, NY.

Barry, T. and Regan, J. (1978). "FHWA Highway Traffic Noise Prediction Model." *Report No. FHWA-RD-77-108*, Washington, D.C.

Basu, S. and Akhter, G. (1985). "Review of Structural Design Criteria for Noise Walls." Analysis Group, Inc., Washington, D.C.

Bendtsen, H. and Schou, K. (1991). "Noise Barriers - A Catalogue of Ideas." Denmark Ministry of Transport, Road Directorate, Road Data Laboratory, Copenhagen, Denmark.

Blevins, R. (1984). *Applied Fluid Dynamics Handbook*, Van Nostrand Reinhold Co., New York, NY.

Bligh, R., Alberson, D., and Butler, B. (1995). "Applications of Recycled Materials in Roadside Safety Devices." *Research Study No. 1458-1*, Texas Transportation Institute, Texas A&M University, College Station, TX.

Boresi, A., Schmidt, R., and Sidebottom, O. (1993). *Advanced Mechanics of Materials*, 5th edition, John Wiley & Sons, Inc., New York, NY.

Bowlby, W. (1981). "Sound Procedures for Measuring Highway Noise: Final Report." FHWA - Demonstration Project Division, Arlington, VA.

Chopra, A. (1995). *Dynamics of Structures*, Prentice-Hall Co., Englewood Cliffs, NJ.

Clark, S. (1972). *Dynamics of Continuous Elements*, Prentice-Hall, Inc., Englewood Cliffs, NJ.

Clough, R. and Penzien, J. (1993). *Dynamics of Structures*, 2nd edition, McGraw-Hill, Inc., New York, NY.

Cohn, L. (1981). "Synthesis of Highway Practice 87 - Highway Noise Barriers." Transportation Research Board, National Cooperative Highway Research Program, National Research Council, Federal Highway Administration, AASHTO, Washington, D.C.

Cohn, L. and Harris, R. (1993). "Special Noise Barrier Applications." U.S. Department of Transportation, Federal Highway Administration, Washington, D.C.

Ewins, D. (1984). *Modal Testing: Theory & Practice*, John Wiley and Sons, Inc., New York, NY.

Farnham, J. and Beimborn, E. (1990). "Noise Barrier Design Guidelines." Center for Urban Transportation Studies for University of Wisconsin, Milwaukee, WI.

Freudenrich, D. (1996). "Noise Wall Materials Comparison Matrix - Updated." *The Wall Journal*, v. 5, no. 23, pp. 10-13, Lehigh Acres, FL.

Fyfe, K. and Harrison, C. (1995). "Insertion Loss Performance of Road Noise Barriers." *The Wall Journal*, v. 4, no. 17, pp. 10-11, Lehigh Acres, FL.

"Guidelines for Analysis and Abatement of Highway Traffic Noise." (1996). Texas Department of Transportation, Environmental Affairs Division, Austin, TX.

"Guidelines for Evaluating the Performance of Highway Sound Barriers." (1996). Civil Engineering Research Foundation, Highway Innovative Technology Evaluation Center, Federal Highway Administration, Washington, D.C.

Hag-Elsafi, O., Elwell, D., Glath, G., and Hiris, M. (1996). "Development of Standards for Noise Barriers Using Recycled Plastic Lumber." *Research Report 167*, New York Department of Transportation, Albany, NY.

"Highway Noise Fundamentals." (1980). United States Department of Transportation, Federal Highway Administration, Washington, D.C.

"Highway Traffic Noise Analysis and Abatement." (1995). United States Department of Transportation, Federal Highway Administration, Office of Environment and Air Quality Branch, Washington, D.C.

Hunt, E. (1993). "Recycled Plastics in Highway Construction and Maintenance – Construction Report." Oregon Department of Transportation, Salem, OR.

Juang, J., Horta, L., and Phan, M. (1996). "SOCIT Guide." NASA Langley Research Center, Hampton, VA.

Juang, J. and Pappa, R. (1988). "A Comparative Overview of Modal Testing and System Identification for Control of Structures." *Shock and Vibration Digest*, v. 20, no. 5, pp. 4-15.

Juang, J. (1994). *Applied System Identification*, PTR Prentice-Hall, Inc., Englewood Cliffs, NJ.

Juang, J. (1997). "State-Space System Realization with Input- and Output-Data Correlation." NASA Technical Paper 3622, Langely Research Center, Hampton, VA.

Klingner, R., Busch-Vishniac, I., McNerney, M., Ho, S., and Peron, R. (1996). "Effective Noise Barrier Solutions for TxDOT: A First-Year Progress Report." *Research Report 0-1471*, Texas Department of Transportation, Center for Transportation Research, The University of Texas System, Austin, TX.

LabVIEW®. (1995). "Third-Octave Analysis Toolkit Reference Manual." National Instruments Corporation, Austin, TX.

Lee, C. and Fleming, G. (1996). "Measurement of Highway-Related Noise." Federal Highway Administration, U.S. Department of Transportation, Research and Special Programs Center, Cambridge, MA.

Liu, H. (1991). *Wind Engineering: A Handbook for Structural Engineers*, Prentice-Hall, Inc., Englewood Cliffs, NJ.

Lutes, L. and Sarkani, S. (1997). *Stochastic Analysis of Structural and Mechanical Vibrations*, Prentice-Hall Co., Englewood Cliffs, NJ.

MATLAB®. (1992) "Reference Guide." The MathWorks, Inc., Natick, MA.

Manual of Steel Construction, Load and Resistance Factor Design (AISC-LRFD). (1994). American Institute of Steel Construction Inc., 2nd edition, Chicago, IL.

Mota, S., Boyd, S., and Quaile, A. (1993). "Development of Specifications for Plastic Lumber for Use in Highway Applications - Phase I." The Research and Development Branch, Ontario Ministry of Transportation, Newmarket, Ontario, Canada.

Pappa, R. and Ibrahim, S. (1981). "A Parametric Study of the Ibrahim Time Domain Modal Identification Algorithm." *Shock and Vibration Bulletin*, 51 (3).

Pappa, R., Woodard, S., and Juang, J. (1997). "The Development of Autonomous Structural Modal Identification." *Shock and Vibration Digest*, vol. 31, no. 8, pp. 18-23.

PATRAN®. (1989) "PATRAN™ Plus User Manual." A Division of PDA Engineering, version 5.0, publication no. 2191025., Costa Mesa, CA.

"Plans of Proposed State Highway Improvement." (1995). Texas Department of Transportation, *Project No. 3256-1-70*, Harris County, Houston, TX.

"Recycle Texas: A Reuse and Recycling Directory." (1995). Texas Natural Resource Conservation Commission, RG-79 *(formerly LP 91-09)*, Austin, TX.

Reddy, J. (1993). *An Introduction to the Finite Element Method.* McGraw-Hill, Inc., 2nd edition, New York, NY.

"Roadside Noise Abatement." (1995). OECD Scientific Expert Group, Organization for Economic and Cooperation and Development, Paris, France.

Roschke, P., Harrison, B., and Benson, F. (1996). "Recycled Content Sign Blanks." *Research Study No. 1338-1*, Texas Transportation Institute, Texas A&M University, College Station, TX.

Roschke, P., Bligh, R., and Pruski, K. (1995). "Commingled Plastic Guardrail Post." *ASCE Journal of Transportation Engineering*, v. 121, no. 2, pp. 201-213.

Saadegghvaziri, A. and MacBain, K. (1998) "Sound Barrier Applications of Recycled Plastics." Department of Civil Engineering, New Jersey Institute of Technology, Newark, NJ.

Simiu, E. and Scanlan, R. (1986). *Wind Effects on Structures*, John Wiley & Sons, Inc., New York, NY.

Simpson, M. (1976). "Noise Barrier Design Handbook." Department of Transportation, Federal Highway Administration, Washington, D.C.

Storey, B. and Godfrey, S. (1994). "Highway Noise Abatement Measures: 1994 Survey of Practice." *Research Study No. 1994-4*, Texas Transportation Institute, Texas A&M University, College Station, TX.

Tang, T. and Lindeman, W. (1996). "Noise Abatement Wall Basics." *The Wall Journal*, v. 5, no. 24, pp. 8-9, Lehigh Acres, FL.

Title 23, Code of Federal Regulations, Part 772. (1982). Federal Aid Policy Guide. Washington, D.C.

"Traffic Noise Analysis Seminar." April 10-14, 1995. Presented by Cohn, L. and Harris, A., The University of Louisville - Speed Scientific School, Louisville, KY.

"Value-engineered Feature and Benefits of Monowall™ Approved for Florida DOT Qualified Products List." (1997). *The Wall Journal*, v. 6, no. 29, pp. 8-9, Lehigh Acres, FL.

Vold, H., Kundrat, J., Rocklin, G., and Russell, R. (1982). "A Multi-Input Modal Estimation Algorithm for Mini-Computers." SAE International Congress and Exposition, Detroit, MI.

Yang, C. (1986). *Random Vibration of Structures*, John Wiley and Sons, Inc., New York, NY.

BIBLIOGRAPHY

Bowlby, W. (1992). "Synthesis of Highway Practice 181: In-Service Experience with Traffic Noise Barriers." Transportation Research Board, National Cooperative Highway Research Program, Washington, D.C.

Carsonite International, Inc. (1994). "Product Specification for Sound Barrier." Carson City, NV.

Figallo, G. (1996). "To Absorb or Not to Absorb." *The Wall Journal*, v. 5, no. 22, pp. 12-13, Lehigh Acres, FL.

Gharabegian, A. (1996). "Improving the Performance of Highway Soundwalls." *Sound and Vibration*, v. 30, no. 7, pp. 30-33, Bay Village, OH.

Quilite® International. (1996). "Report: Sound Transmission Loss Test No. TL95-101." Los Angeles, CA.

Seaward International, Inc. (1995). "Seatimber™ Composite Marine Timber Typical Performance Characteristics." Clearbrook, VA.

Sound Fighter® Systems, Inc. (1995). "Materials and Testing Section." Shreveport, LA.

APPENDIX A – AASHTO CALCULATIONS

1989 AASHTO specifications for soundwalls:

Equation

$P = .00256\,(1.3V)^2\,C_d\,C_c$

Note: English units are used on this page and converted to metric units on the next page.

P = wind pressure in pounds per square foot

V = wind speed (mph) based upon 50 year mean recurrence interval

(1.3V) = gust speed, 30%

C_d = drag coefficient (1.2 for sound barriers)

C_c = combined height, exposure, and location coefficient

C_c categories

B1 - Urban and suburban areas with numerous closely spaced obstructions having the size of single-family dwellings or larger that prevail in upwind direction from the sound barrier for a distance of at least 1500 ft (0.37 for 0-14 ft centroid)
B2 - Urban and suburban areas with more open terrain not meeting the requirements of B1 (0.59 for 0-14 ft centroid)

V from Figure 1-2.1.2.A is found to be 70 mph for central Texas

Cd =	1.2
Cc=	0.37
V=	70
P=	9.41252

Cd =	1.2
Cc=	0.59
V=	70
P=	15.0091

Cd =	1.2
Cc=	0.37
V=	80
P=	12.2939

Cd =	1.2
Cc=	0.59
V=	80
P=	19.6038

Cd =	1.2
Cc=	0.37
V=	90
P=	15.5595

Cd =	1.2
Cc=	0.59
V=	90
P=	24.811

Cd =	1.2
Cc=	0.37
V=	100
P=	19.2092

Cd =	1.2
Cc=	0.59
V=	100
P=	30.6309

Minimum Pressures from Tables 1-2.1.2.B and 1-2.1.2.C for indicated wind velocity

	70	80	90	100	110	velocity (mph)
Case B1						
0-14 ft centroid	9	12	16	19	23	pressure (psf)
Case B2						
0-14 ft centroid	15	20	25	31	37	pressure (psf)

Case B1					
I =	0.000142	m^4	I =	0.00015	m^4
E = 300,000 psi =	3.1E+09	N/m^2	E = 400,000 psi	2.8E+09	N/m^2
$M_{max} = w_o h^2/3$ =	19783.99	N*m	$M_{max} = w_o h^2/3$ =	19784	N*m
$s_{max} = M_{max}$ y/I =	28295931	N/m^2	$s_{max} = M_{max}$ y/I =	2.7E+07	N/m^2
$D_{max} = 11 w_o h^4/120EI$ =	0.165	m	$D_{max} = 11 w_o h^4/120EI$ =	0.176	m
I =	0.00015	m^4			
E = 500,000 psi	3.45E+09	N/m^2			
$M_{max} = w_o h^2/3$ =	32279.14	N*m			
$s_{max} = M_{max}$ y/I =	43727474	N/m^2			
$D_{max} = 11 w_o h^4/120EI$ =	0.141	m			

Case B2					
I =	0.000142	m^4	I =	0.00015	m^4
E = 300,000 psi =	3.1E+09	N/m^2	E = 400,000 psi	2.8E+09	N/m^2
$M_{max} = w_o h^2/3$ =	32279.14	N*m	$M_{max} = w_o h^2/3$ =	32279.1	N*m
$s_{max} = M_{max}$ y/I =	46167045	N/m^2	$s_{max} = M_{max}$ y/I =	4.4E+07	N/m^2
$D_{max} = wh^4/8EI$ =	0.269	m	$D_{max} = 11 w_o h^4/120EI$ =	0.287	m
I =	0.00015	m^4			
E = 500,000 psi	3.45E+09	N/m^2			
$M_{max} = w_o h^2/3$ =	32279.14	N*m			
$s_{max} = M_{max}$ y/I =	43727474	N/m^2			
$D_{max} = 11 w_o h^4/120EI$ =	0.230	m			

APPENDIX B – STAMINA OUTPUT

STAMINA 2.0 output with soundwall:

```
                    STAMINA 2.0/BCR
                FHWA VERSION (MARCH 1982)
              TRAFFIC NOISE PREDICTION MODEL
             DEVELOPED UNDER CONTRACT BY BBN

     INPUT UNITS-     E    I, OUTPUT UNITS-     E    I)


 MODIFIED BY THE MINNESOTA DEPT. OF TRANSPORTATION
 FOR OPERATION ON A MS-DOS PERSONAL COMPUTER, 1985

 Rivrwall
0PROGRAM INITIALIZATION PARAMETERS

      HEIGHT       CODE            DESCRIPTION
         .00          1              R              A        N
        1.00          2              A        E     A        N
         .00          3              H        D     T        S        C
        8.00          4              H        D     T        A        K
        2.30          5              H        D     T        D        C


0ROADWAY    1      runway

                        VEHICLE TYPE    VEHICLES/HOUR      SPEED
                             CARS             7000.          65.
                             HT                400.          65.
                             MT                400.          65.
                           ------------COORDINATES-------------
                                 X              Y              Z      GRADE
 1                               490.            0.             0.       0
 2                               510.            0.             0.       0
1BARRIER    1    TYPE(R)      BARRIER 1
0             ---------COORDINATES----------
                    X          Y          Z          Z0       DELZ          P
 1                450.       60.        12.          0.         1.          1
 2                550.       60.        12.          0.


 BARRIER LENGTH BY SECTION
    100.00
1RECEIVERS
0                          ------------COORDINATES------------
                                 X              Y              Z
 1                               500.           50.            5.
 2                               500.          100.            5.
1  ALPHA FACTORS - ROADWAY DOWN, RECEIVER ACROSS

  1 *  .5  .5
1 SHIELDING FACTORS - ROADWAY DOWN, RECEIVER ACROSS

  1 *  .0  .0
1Rivrwall
0  ?EIVER     LEQ(H)     SIG    L10     L50     L90

 1              75.1      6.8    78.5    69.8    61.0
 2              56.5      7.5    59.6    50.1    40.5
```

STAMINA 2.0 output without soundwall:

```
                    STAMINA 2.0/BCR
                FHWA VERSION (MARCH 1982)
              TRAFFIC NOISE PREDICTION MODEL
             DEVELOPED UNDER CONTRACT BY BBN

    (INPUT UNITS-     E    I, OUTPUT UNITS-     E    I)


 MODIFIED BY THE MINNESOTA DEPT. OF TRANSPORTATION
 FOR OPERATION ON A MS-DOS PERSONAL COMPUTER, 1985

 Rivrwall
0PROGRAM INITIALIZATION PARAMETERS

      HEIGHT       CODE          DESCRIPTION
         .00          1            R              A       N
        1.00          2            A       E              N
         .00          3            H       D      T       S       C
        8.00          4            H       D      T       A       K
        2.30          5            H       D      T       D       C


0ROADWAY    1      runway

                        VEHICLE TYPE    VEHICLES/HOUR      SPEED
                             CARS             7000.          65.
                             HT                400.          65.
                             MT                400.          65.
                          ----------COORDINATES----------
                                X              Y             Z      GRADE
 1                             490.            0.            0.       0
 2                             510.            0.            0.       0
1RECEIVERS
0                         ----------COORDINATES----------
                                X              Y             Z
 1                             500.           50.           5.
 2                             500.          100.           5.
1  ALPHA FACTORS - ROADWAY DOWN, RECEIVER ACROSS

  1 *  .5  .5
1 SHIELDING FACTORS - ROADWAY DOWN, RECEIVER ACROSS

  1 *  .0  .0
1Rivrwall
0RECEIVER     LEQ(H)    SIG    L10     L50     L90

 1             75.1     6.8    78.5    69.8    61.0
 2             67.7     6.8    71.1    62.3    53.6
```

APPENDIX C – MATLAB FILES

Six MATLAB® algorithms are included in this section: **FFT.m**, **FILTER.m**, **MODEL.m.**, **PSDD.m**, **RAYLEIGH.m**, **TRANSFER.m**, and **SRIM.m**.

The following file is titled **FFT.m**. The algorithm implements a fast Fourier transform (FFT) on a time history of acceleration response data.

```
%=========================================================================
clear;
load c:\Soundwall\Data\Impact_Hits_Wall\trial.asc;          % read in the data file
points=input('How many points do you want to consider: ');
channel=input('Please input the channel:');
m=trial(:,channel);
n=m(1:points);
cal=input('Please enter calibration: ');                    % calibration
o=n*cal;
p=fft(o);
t=0:(points-1);
t=t./(points*0.002);
plot(t,abs(p));                                             % plots the fft
axis([0 5 0 20]);                                           % sets the x and y axes
angle=[];
for i=1:points                                              % this calculates phase which
        y=phase(p(i));
        angle=[angle,y];
end;
frequency=t';
fft=abs(p);
%real_angle=angle/pi*180;
%plot(t,real_angle');                                       % phase could be plotted
%axis([0 100 -190 190]);
save c:\Temp\freq.asc frequency -ascii                      % send output to files
save c:\Temp\fft.asc fft -ascii
%=========================================================================
```

The following file is titled **FILTER.m**. The algorithm serves as a low-pass digital data filter.

```
%=============================================================================
xn=input('Enter the input data :');
N=input('Enter the filter order :');
T=input('Enter the sample time interval :');
w1=input('Enter the lowpass freq (Hz): ');
%calculate the Wn
 fn=1/2/T;
 f1n=w1/fn;
 [B1,A1]=butter(N,f1n);
 [H1, wT]=freqz(B1,A1,200);
 hertz=wT/(2*pi*T);
 plot(hertz,abs(H1))
 title('Lowpass Filter'),...
   xlabel('Hz'),ylabel('Magnitude'),grid
yn=filter(B1,A1,xn);
disp('Output data is in array yn');
%=============================================================================
```

The following file is titled **MODEL.m**. The algorithm extracts natural frequencies, damping, and mode shapes for given acceleration and impact force time-histories; it determines these characteristics through implementation of the peak-amplitude method.

```
%==========================================================================
% This m-file will conduct the traditional modal analysis.
% The time history of the input date will be shown. The Frequency
% Response Function(FRF) between each pair of output and input
% signals, natural frequencies and corresponding mode shape and
% damping ratio will be calculated and returned. The input is the matrix:
%
%       z=[y u]--y are output accel signals, u is impact signal.
%
% Output will have four matrices:
%
%       nfreq--contain natural freq.
%       mode---2D matrix contain mode shape. Row for each input
%            index, column for each mode.
%       lag--Same as mode, contain the phase angle.
%       damp--contain damping ratio.
%==========================================================================
zz=input('Please input the data file [y u] :');
deltt=input('Input the sampling time interval(s) :');
[row col]=size(zz);
disp('*****Removing the mean of the output date*****')
for i=1:col-1
zz(:,i)=dtrend(zz(:,i));
end
disp('*****Plotting the time history*****')
time=0:deltt:deltt*(row-1);
figure(1)
clf
subplot(211)
plot(time,zz(:,col)),....
ylabel('Force amplitude'),....
title('Impact hammer signal')
subplot(212)
for i=1:col-1
hold on
plot(time,zz(:,i))
end
title('Accel output signal'),....
xlabel('Time (sec)'),....
ylabel('Accel level')
flag=0;
flag=input('------Enter 1 to print the plot : ');
if flag==1
print
end
disp('Press any key to continue')
pause
```

```
disp('*****Caculate and plot the FRF*****')
length=0;
length=input('Give the number of points for FFT (power of 2 better):');
if length>=0
zz=zz(1:length,:);
end
[row,col]=size(zz);

impft=fft(zz(:,col));                          % do the FFT of impact input
accelft=[];                                    % do the FFT of accel outputs
for i=1:col-1
accelft=[accelft fft(zz(:,i))];
end

for i=1:col-1                                  % form the transform function
tf(1:row,i)=accelft(1:row,i)./impft;
end

clear impft accelft                            % calculate the magnitude and
for i=1:col-1                                  % phase of the RFT
mag(1:row,i)=abs(tf(1:row,i));
phase(1:row,i)=angle(tf(1:row,i))*180/pi;
end
[row,col]=size(tf);                            % plot the RFT
maxl=floor(row/2);
deltf=1/(row*deltt);
freq=0:maxl;
freq=freq*deltf;
figure(2)
clf
subplot(211)
for i=1:col
plot(freq',mag(1:maxl+1,i))
hold on
end
title('The responses of the transfer functions')
ylabel('Amplitude')
subplot(212)
for i=1:col
plot(freq', phase(1:maxl+1,i))
hold on
end
xlabel('Freq. (Hz)'),....
ylabel('Angle')
disp('Press any key to continue')
pause
disp('*****Do mode parameter analysis*****')
nmode=input('Enter the number of mode of interest :');
flag=1;
for i=1:nmode
disp('******Begin search for a new mode*******')
disp('-----Please give a narrow band around the peak-----')
while flag;
freql=input('Enter the low limit of freq. (hz) :');
freqh=input('Enter the high limit of freq. (hz):');
```

```
indl=floor(freql/deltf)+1;
indh=floor(freqh/deltf)+1;
figure(2)
clf
subplot(211)
for k=1:col
plot(freq(indl:indh)',mag(indl:indh,k))
hold on
end
title('The responses of the transfor functions')
ylabel('Amplitude')
subplot(212)
for k=1:col
plot(freq(indl:indh)', phase(indl:indh,k))
hold on
end
xlabel('Freq. (Hz)');
ylabel('Phase angle');
flag=input('Enter 1 to change the freq. range;ortherwise: press enter:');
end
flag=input('Enter 1 to print the plot: ');
if flag==1;
print
end
indfreq=0;
for k=1:col
[ym,nf]=max(mag(indl:indh,k));
indfreq=indfreq+nf;
end
indfreq=floor(indfreq/col)+indl-1;
nfreq(i)=freq(indfreq);

for k=1:col                                    % output for natural frequencies
mode(k,i)=mag(indfreq,k);                      % find the peak value of each FRF
 end
 for k=1:col
 lag(k,i)=phase(indfreq,k);                    % find the phase angle
 end
 flag=1;
        %the following part will find
%the damping ratio the damping will be
        %calculated from the curve which
        %has the biggest amplitude
 [ym,ind]=max(mode(:,i));                      % search the biggest peak
 hpp=ym/1.414;                                 % for search half power points
 [ym,nf]=max(mag(indl:indh,ind));
 indfreq=nf+indl-1;
 for k=indl:indfreq;                           % make the array
 if mag(k,ind)>mag(k+1,ind)                    % monotonously increase
    change=mag(k,ind);
    mag(k,ind)=mag(k+1,ind);
    mag(k+1,ind)=change;
 end
 end
                                               % make the array
```

```
for k=indfreq:indh                                          % monotonously decrease
if mag(k,ind)<mag(k+1,ind)
   change=mag(k,ind);
   mag(k,ind)=mag(k+1,ind);
   mag(k+1,ind)=change;
end
end
bandf=floor((indfreq-indl));
bandb=floor((indh-indfreq));                                % they can be removed
f1=table1([mag(indfreq-bandf:indfreq,ind),....
        freq(indfreq-bandf:indfreq)'],hpp);                 % half power point
f2=table1([mag((indfreq):indfreq+bandb,ind),...
        freq(indfreq:indfreq+bandb)'],hpp);                 % half power point
damp(i)=nfreq(i)*(f2-f1)/(2*f1*f2);                         % output for damping ratio
mode(:,i)=mode(:,i).*lag(:,i)./abs(lag(:,i));               % output for mode shape
end
%=============================================================================
```

The following file is titled **PSDD.m**. The algorithm calculates a power spectral density (PSD) of a time history. Units of a PSD are the units of the input time history squared and divided by Hertz.

```
%=========================================================================
load mph90PSD.txt;
sr=input('What is the sampling rate');
channel=input('Which channel is of interest:');
X=mph90PSD(:,channel);
disp('There are this many points:')
length(X)
N=input('How many points to use:');
Y=fft(X,N)/N;
p=2*Y.*conj(Y)/(N*sr);
t=0:N-1;
t=t./(0.0125*N);
p_vector=abs(p(1:N/2));
y=max(p_vector)
loglog(t,abs(p));
axis([0 5 0 y]);
%=========================================================================
```

The following file is titled **TRANSFER.m**. The algorithm plots the transfer function in the frequency domain when both an input and output time histories are given. It is also capable of calculating and plotting the phase angle of the transfer function versus frequency.

```
%=================================================================
clear;
load c:\Soundwall\Holding\Wall_Data\trial.asc;          % read in the data file
points=3450;                                            % how many points to consider
channel1=input('Which is the acceleration column:');
channel2=input('Which is the impact column:');

a=trial(:,channel1);
b=a(1:points);
c=(b/0.2)*9.807;                                        % calibration
d=fft(c);

m=trial(:,channel2);
n=m(1:points);
o=n*5414.6;                                             % calibration
p=fft(o);
tf=d./p;

t=0:(points-1);
t=t./(points*0.002);
plot(t,abs(tf));                                        % plots the transfer function
axis([1.5 3.5 0 0.02]);                                 % sets the x and y axes

angle=[];                                               % this calculates phase which
for i=1:points                                          % could also easily be plotted
        y=phase(tf(i));
        angle=[angle,y];
end;
real_angle=angle/pi*180;

transfer_function=abs(tf);
phase_angle=real_angle';
frequency=t';

save c:\Temp\freq.asc frequency -ascii                  % send output to files
save c:\Temp\transfer.asc transfer_function -ascii
save c:\Temp\phase.asc pahse_angle -ascii
%=================================================================
```

The following file is titled **RAYLEIGH.m**. The algorithm calculates the transverse and torsional vibration frequency for the prototype soundwall using Rayleigh's (energy) method. The wall is assumed to be composed of 12 fiberglass-reinforced lumber modules and 13 fiberglass-reinforced plastic columns.

```
%=========================================================================
% input the geometry and material properties
        a=input('Enter the module length a= :');
        b=input('Enter the module height b= :');
        mu=input('Enter the Poissons ratio mu= :');
        Es=input('Enter the modulus for sheet Es= :');
        Ep=input('Enter the modulus for lumber plate Ep= :');
        Ec=input('Enter the modulus for column Ec= :');
        Eb=input('Enter the modulus for cross member Eb= :');
        rhos=input('Enter the density for sheet rhos= :');
        rhop=input('Enter the density for lumber plate rhop= :');
        rhoc=input('Enter the density for column rhoc= :');
        rhob=input('Enter the density for cross menber rhob= :');
%Calculate the areas and stiffnesses
        t=0.0127;                   % sheet thickness
        D=Es*t^3/12/(1-mu^2)*2;     % double the sheet stiffness
        rhos=rhos*2;                % double the sheet density
        Ic=0.2032^3*0.26/12;        % moment of inertia of the column and vertical member
        Ib=0.0381*0.2032^3/12;      % moment of inertia of the crossing member
        Ac=0.2032*0.26;             % column area
        Ab=0.0381*0.2032;           % crossing member area
        Ip=0.22*0.0508^3/12;        % moment of inertia of the lumber plate
        Ap=0.22*0.0508;             % lumber plate area
% Form the coefficients
d1=pi*(256*b^4+3*a^4+32*a^2*b^2);
d2=-8*a^4;
d3=2*a^4*pi^2;
d4=0;
d5=3*pi^2;
d6=8*pi;
d7=6*pi^2-16*pi;
d8=0;
d9=0;
d10=0;
d11=0;
d12=0;

 for i=0:3.66/7:3.66
 d4=d4+4*sin(pi*i/2/b);
 d8=d8+3*sin(pi*i/2/b)^2;
 d9=d9+4*sin(pi*i/2/b)*(1-cos(pi*i/2/b));
 d10=d10+2*(1-cos(pi*i/2/b))^2;
 end

 for i=0.11:2.2167/10:2.2167
 d11=d11+8*pi*(1-cos(pi*i/a)^2)^2;
 d12=d12+16*(cos(pi*i/a)^2-1);
```

```
end
        c1=Ec*Ic*pi^4/64/b^3;
        c2=D*pi^2/(128*a^3*b^3)*d1;
        c3=D*pi^2/(128*a^3*b^3)*d2;
        c4=D*pi^2/(128*a^3*b^3)*d3;
        c5=Eb*Ib*pi^4*beta^2*d4/a^3;
        c6=b*rhoc*Ac*(3*pi-8)/(4*pi);
        c7=rhos*t*a*b*d5/(8*pi^2);
        c8=rhos*t*a*b*d6/(8*pi^2);
        c9=rhos*t*a*b*d7/(8*pi^2);
        c10=rhob*Ab*a*d8/4;
        c11=rhob*Ab*a*d9/4;
        c12=rhob*Ab*a*d10/4;
        c13=Ep*Ip*pi^3/(64*b^3)*d11;
        c14=Ep*Ip*pi^3/(64*b^3)*d12;
        c15=Ep*Ip*pi^3/(64*b^3)*pi*22;
        c16=rhop*Ap*b*d11/4/pi;
        c17=rhop*Ap*b*d12/4/pi;
        c18=rhop*Ap*b*(3*pi-8)*22/4/pi;
%=========================================================================
% Calculation of transverse vibration fundamental freq.
% Mode shape: phi(x,y)=1-cos(pi*y/2b)+beta*sin(pi*y/2b)*(1-cos(2*pi*x/a)
%     beta: the parameter to be minimized
%       a: length of one module
%       b: height of the module
% initialization
        judge=1;
        beta=1;
% start the loop to minimize the freq.
        while(judge)
% strain energy in the column
        vc=c1;
% strain energy in the plate
        vp=c13*beta^2+c14*beta+c15;
% strain energy in the cross member
        vb=c5*beta^2;
% kinetic energy in the column
        Tc=c6;
% kinetic energy in the plate
        Tp=c16*beta^2-c17*beta+c18;
% kinetic energy in the crossings (total)
        Tb=c10*beta^2+c11*beta+c12;
        omiga=(vc+vb+vp)/(Tp+Tc+Tb);
        beta1=(omiga*(c11-c17)-c14)/2/(c13+c5-omiga*c16-omiga*c10);
        if(abs(beta1-beta)<=eps)
        judge=0;
        disp(' ---------- Weis 2nd shape function ---------- ');
        disp('Transverse foundamental freq. for Lumber plates case:')
        omiga=sqrt(omiga)/2/pi
        else
        beta=beta1;
        end
        end
%=========================================================================
% Calculation of the torsional vibration natural freq.
```

```
% Mode shape: phi(x,y)=(1-cos(pi*y/2b))*cos(pi*x/a)
%        a: length of one module
%        b: height of the module
% strain energy in the plate
        vp=Ep*Ip*pi^4*c2/64/b^3;
% strain energy in the column
        vc=Ec*Ic*pi^4/64/b^3*c4;
% strain energy in the crossings (total)
        vb=Eb*Ib*pi^4*c0/4/a^3;
% kinetic energy in the plate
        Tp=rhop*Ap*b*c3*c2;
% kinetic energy in the column
        Tc=b*rhoc*Ac*c3*c4;
% kinetic energy in the crossings (total)
        Tb=rhob*Ab*a*c0/4;
        omiga=(vc+vb+vp)/(Tp+Tc+Tb);
        disp(' ---------- Weis shape function ---------- ');
        disp('2nd foundamental freq. for discrete lumber plate case:');
        omiga=sqrt(omiga)/2/pi
%=========================================================================
```

The following file is titled **SRIM.m** and was written by Jer-Nan Juang of NASA Langley Research Center. It appears here in its unaltered form. The algorithm may call upon other m-files that are not shown. Description of operations performed by the file are included in initial comments of the code.

```
%=========================================================================
function [a,b,c,d,x0]=srim(u,y,fg,n,p,dt);
%
%    Function srim identifies a discrete model directly from
%    arbitrary input and output data. Input and output data correlation
%    matrices are used to compute an observability matrix for
%    realization of system matrices. This is an extension of eradc.
%
%    [a,b,c,d]=srim(u,y,fg,n,p,dt);
%
% INPUT PARAMETERS
%
% u  : input histories stacked by columns
% y  : output data stacked by columns
% fg  : 0 or any number will do regular id work or any vector shorter than 3.
%      fg(1) > 1 desired size of system model obtained by modal truncation
%            = 1 user's interaction required to determine the size of reduced model
%      fg(2)=1 full decomposition method used for determining a & c;
%            otherwise partial decomposition method used for computing a & c
%      fg(3)=1 direction method used for computing b & d (time consuming)
%         =2 output-error minimization method used for computing b & d
%            (very time comsuming)
%            otherwise indirect method for computing b & d
% n  : desired model order obtained by singular values truncation
%      n=0 interactive
% p  : an integer (assumed number of states=p*no. of outputs)
% dt : sample time (sec)
%
% OUTPUT PARAMETERS
%
% a  : state matrix
% b  : input matrix
% c  : output matrix
% d  : direct transmission matrix
% x0  : initial condition

%        J. N. Juang 8-23-95
%        NASA Structural Dynamics Branch
format short e; format compact
if isempty(fg)==1 | length(fg)<3;
  fg=[fg zeros(1,3-length(fg))];
end;
flagera=1; if n==0; flagera=0; n=10000; end;
[nd,m]=size(y); [nd,r]=size(u);
nd2=sqrt(nd);
%
% Compute correlation matrices
```

```
p=p+1;
vvt=vcorr([u/nd2 y/nd2],p);
 mid=p*(r+m)+r+1:(p+1)*(r+m);
 rid=p*(r+m)+1:p*(r+m)+r;;
 idy=[];idu=[];
 for k=1:p;
  mid=mid-(r+m); rid=rid-(r+m);
        idy=[idy mid]; idu=[idu rid];
 end;
UoR=vvt(idy,idu)*pinv(vvt(idu,idu));
rhh=vvt(idy,idy)-UoR*vvt(idy,idu)';clear vvt;
%
% Perform Singular Value decomposition for identification of
% observability matrix
%
if fg(2)~=1;
  disp(['The partial decomposition method is used for computing A & C'])
  [U,xs,V]=svd(rhh(:,1:(p-1)*m)); clear rhh V;
   xs=diag(xs); sigcont=sum(xs);
        nmax=length(xs);
else;
  disp(['The full decomposition method is used for computing A & C'])
  [U,xs,V]=svd(rhh); clear rhh V;
   xs=diag(xs);
        nmax=length(xs)-m;xs=xs(1:nmax); sigcont=sum(xs);
end;
        if n>nmax | n<0; n=nmax; end;
   disp(['Maximum Hankel singular value = ' sprintf('%e',max(xs))])
   disp(['Minimum Hankel singular value = ' sprintf('%e',min(xs))])
   n_index=length(find(xs>0.00000001));
%
% Determine the order of the system
%
  if flagera==0; clg;
      if fg(1)==1; subplot(211); end;
          semilogy([xs],'*');
    xlabel(' Number');ylabel('SV Magnitude');
    title(' Hankel Singular Values (HSV)');pause;
    disp([' '])
    disp(['The HSV plot allows you to determine a desired model size.'])
   else;
     if n>n_index;
      disp(['The initial order is set to ' num2str(n) '.'])
      disp(['It is now set to ' num2str(n_index) '.'])
      n=n_index;
     end;
   end;
while n > 0;
  if flagera==0;
     n=input(['Desired Model Order (See HSV plot) (0=stop)=: ']);
     if isempty(n)==1 | n==0; break; end;
     if n>nmax | n<0; n=nmax; end;
     sigkpt=sprintf('%g',100*sum(xs(1:n))/sigcont);
     disp([' Model Describes ' sigkpt ' (%) of Test Data'])
  end;
```

```
% Determine A and C
%
  Oi=pinv(U(1:(p-1)*m,1:n));
  a=Oi*U(m+1:p*m,1:n);
  c=U(1:m,1:n);
%
% Determine B and D
%
%
%     Direct method is used for computing B and D
%
 if fg(3)==1;
  disp(['The direct method is used for computing B & D'])
          q=p-1;
   qm=q*m;
          OpA=zeros((q+1)*n,n+m);
          OOp=Oi(:,m+1:qm)*U(1:(q-1)*m,1:n);
          OpA(1:n,1:n+m)=[-a*Oi(:,1:m) eye(n)-a*OOp];
   for k=2:q-1;
             OOp1=Oi(:,k*m+1:qm)*U(1:(q-k)*m,1:n);
             OpA((k-1)*n+1:k*n,:)=[Oi(:,(k-2)*m+1:(k-1)*m)-a*Oi(:,(k-1)*m+1:k*m) ...
                    OOp-a*OOp1];
                    OOp=OOp1;
 end;
             OpA((q-1)*n+1:q*n,:)=[Oi(:,(q-2)*m+1:(q-1)*m)-a*Oi(:,(q-1)*m+1:q*m) OOp];
          clear OOp OOp1;
          OpA(q*n+1:(q+1)*n,1:m)=Oi(:,(q-1)*m+1:qm);
          OpG=Oi*UoR(m+1:(q+1)*m,:)-a*Oi*UoR(1:q*m,:); clear Oi;
          OpG=block_tr(n,q+1,r,OpG,1);
          b=pinv(OpA)*OpG; clear OpA OpG;
          d=b(1:m,:);
          b=b(m+1:n+m,:);
          x0=zeros(n,1);
 else;
%
%     Output-error minimization method is used for computing B and D
 if fg(3)==2;
  disp(['The output-error minimization method is used for computing B & D'])
    [b,d,x0]=ac2bd(u,y,a,c);
 else;

%     Indirect method is used for computing B and D
%
  disp(['The indirect method is used for computing B & D'])
    pm=p*m;
%         io=n+1:pm; no=length(io); % The last m columns of U are used
          io=(p-1)*m+1:pm; no=m;    % All the truncated columns of U are used.
          Uon=zeros(p*no,n+m);
          ki=-m+1:0;
    for k=1:p-1;
             ki=ki+m;
             Uon((k-1)*no+1:k*no,:)=[U(ki,io)' U(k*m+1:pm,io)'*U(1:(p-k)*m,1:n)];
          end;
          Uon((p-1)*no+1:p*no,1:m)=U(ki+m,io)';
          UoT=U(:,io)'*UoR;
```

```
        UoT=block_tr(no,p,r,UoT,1);
        b=pinv(Uon)*UoT;
        d=b(1:m,:);
        b=b(m+1:n+m,:);
        x0=zeros(n,1);
 end;
 end;
%
% Solve for eigenvalues and eigenvectors
%
  [phi,lambda]=eig(a);
  lambda=diag(lambda);
%
%  Calculate the singular values of modal participation to
%  the pulse response samples
%
  if fg(1)==1; subplot(212); end;
  [lambda,bm,cm,msv,index]=svpm(lambda,phi\b,c*phi,fg(1));
   xt=deg2hz(lambda,dt);
   xt=[xt(:,1:2) msv];
    disp('  Damping(%)    Freq(HZ)      Mode SV');
          disp(xt);
  if flagera==1; n=0; end;
end;
%
% Reduce the system model and put in the block-diagonal form
%
  if length(a(:,1))>length(index);
    x0=phi\x0;x0=x0(index,:);
    [a,b,c]=bk_diag(lambda,[x0 bm],cm);
          x0=b(:,1);
          b=b(:,2:r+1);
  end;
%=========================================================================
```

APPENDIX D – ABAQUS FILES

Portions of two ABAQUS files are included in this section. The first input file simulates dynamic behavior of the prototype soundwall through application of a time history of wind pressure. Response is calculated in this program using modal superposition. The second input file performs random response analysis of wind pressure that is applied to the surface of the soundwall in the form of power spectral density (PSD). Correlation is also introduced in the input file by a FORTRAN subroutine.

In what follows, the main body of code that is used to create nodes and elements and define material properties of the full-scale soundwall is detailed. Afterwards, specific steps that were included to perform the two types of analysis are introduced. Several portions of the code have been removed and comments have been added in parenthesis for convenience of those who wish to reference this source.

```
**********************************************************************************
*HEADING
*PREPRINT, HISTORY=NO, MODEL=NO, ECHO=NO          (Reduce the output file size)
*NODE                                             (Define the nodes in the model)
     1,        0.,         0.
     2,     0.1016,         0.
.
.
.
  5615,     29.464,     0.2032,      -0.15
  5616,     29.464,         0.,      -0.15
*ELEMENT, TYPE=C3D20, ELSET=COL_PROP              (Define the column elements)
     1,     1,     3,     8,     6,    13,    15,    20,
    18,     2,     5,     7,     4,    14,    17,    19,
    16,     9,    10,    12,    11
     2,    13,    15,    20,    18,    25,    27,    32,
    30,    14,    17,    19,    16,    26,    29,    31,
    28,    21,    22,    24,    23
.
.
.
   135,  1537,  1539,  1544,  1542,  1549,  1551,  1556,
  1554,  1538,  1541,  1543,  1540,  1550,  1553,  1555,
  1552,  1545,  1546,  1548,  1547
   136,  1549,  1551,  1556,  1554,  1561,  1563,  1568,
  1566,  1550,  1553,  1555,  1552,  1562,  1565,  1567,
  1564,  1557,  1558,  1560,  1559
*ELEMENT, TYPE=C3D20, ELSET=VERT_PRO              (Define the vertical elements)
    15,   185,   187,   192,   190,   197,   199,   204,
   202,   186,   189,   191,   188,   198,   201,   203,
   200,   193,   194,   196,   195
.
.
```

```
  289,  3513,  3515,  3520,  3518,  3525,  3527,  3532,
 3530,  3514,  3517,  3519,  3516,  3526,  3529,  3531,
 3528,  3521,  3522,  3524,  3523
  290,  3501,  3503,  3508,  3506,  3513,  3515,  3520,
 3518,  3502,  3505,  3507,  3504,  3514,  3517,  3519,
 3516,  3509,  3510,  3512,  3511
*ELEMENT, TYPE=S8R5, ELSET=HOR_PROP                    (Define the horizontal elements)
   29,   271,   276,   366,   361,   273,   373,
  364,   372
   30,   259,   264,   354,   349,   261,   381,
  352,   380
.
.
.
  377,  3423,  3428,  3518,  3513,  3425,  4285,
 3516,  4284
  378,  3411,  3416,  3506,  3501,  3413,  4293,
 3504,  4292
*ELEMENT, TYPE=S8R5, ELSET=PANEL1_P                    (Define the front panel elements)
   37,   271,   361,   349,   259,   434,   437,
  439,   436
   38,   259,   349,   337,   247,   439,   445,
  447,   444
.
.
.
  542,  3435,  3525,  3513,  3423,  5455,  5461,
 5463,  5460
  543,  3423,  3513,  3501,  3411,  5463,  5469,
 5471,  5468
*ELEMENT, TYPE=S8R5, ELSET=PANEL2_P                    (Define the back panel elements)
   44,   276,   366,   354,   264,   490,   493,
  495,   492
   45,   264,   354,   342,   252,   495,   501,
  503,   500
.
.
.
  540,  3440,  3530,  3518,  3428,  5511,  5517,
 5519,  5516
  541,  3428,  3518,  3506,  3416,  5519,  5525,
 5527,  5524
** col_prop
*ORIENTATION, SYSTEM=R, NAME=OID1                      (Define various properties)
      1.,       0.,       0.,       0.,       1.,       0.
    3.,       0.
*SOLID SECTION, ELSET=COL_PROP, MATERIAL=COLUMN_M, ORIENTATION=OID1
      1.,
** vert_prop
*SOLID SECTION, ELSET=VERT_PRO, MATERIAL=VERTICAL, ORIENTATION=OID1
      1.,
** hor_prop
*SHELL SECTION, ELSET=HOR_PROP, MATERIAL=HORIZONT, ORIENTATION=OID1
   0.0381,     5
** panel1_p
```

```
*ORIENTATION, SYSTEM=R, NAME=OID2
      1.,       0.,       0.,       0.,       0.,      -1.
    3,       0.
*SHELL SECTION, ELSET=PANEL1_P, MATERIAL=PANEL_MA, ORIENTATION=OID2
   0.0508,     5
** panel2_p
*SHELL SECTION, ELSET=PANEL2_P, MATERIAL=PANEL_MA, ORIENTATION=OID2
   0.0508,     5
*NSET, NSET=TOP
3724
**********************************************************************************
** column_material                                        (Define column materials)
*MATERIAL, NAME=COLUMN_M
*DENSITY
     750.,
*ELASTIC, TYPE=ISO
  3.2E+9,       0.4
*DAMPING, COMPOSITE=0.04
**********************************************************************************
** vertical_material                                      (Define vertical materials)
*MATERIAL, NAME=VERTICAL
*DENSITY
     750.,
*ELASTIC, TYPE=ISO
  3.2E+9,       0.4
*DAMPING, COMPOSITE=0.04
**********************************************************************************
** horizontal_material                                    (Define horizontal materials)
*MATERIAL, NAME=HORIZONT
*DENSITY
     750.,
*ELASTIC, TYPE=ISO
  3.2E+9,       0.4
*DAMPING, COMPOSITE=0.04
**********************************************************************************
** panel_material                                         (Define panel materials)
*MATERIAL, NAME=PANEL_MA
*DENSITY
     750.,
*ELASTIC, TYPE=ISO
  3.2E+9,       0.4
*DAMPING, COMPOSITE=0.04
**********************************************************************************
STEP                                                     (Perform a frequency analysis)
*FREQUENCY
15,20.0,2.0,30
[[[Include BCs here]]]
*END STEP
**********************************************************************************
```

MODAL SUPERPOSITION ANALYSIS

The following commands must be included in a separate job step to estimate response using modal superposition in conjunction with a time history of wind pressure:

```
**********************************************************************************
*AMPLITUDE,DEFINITION=TABULAR,NAME=WIND,INPUT=mph90.txt
        (This line should appear after material definitions and prior to any analysis steps in the code)
**********************************************************************************
*STEP                                                    (Perform a frequency analysis)
*FREQUENCY
[[[include required parameters]]]
*END STEP
**********************************************************************************
*STEP
*MODAL DYNAMIC
0.01,100  (Calls for modal superposition analysis for 100 second at a time increment of 0.01 seconds)
*DLOAD,AMPLITUDE=WIND
37,P,1.857                                              (Define the pressure distribution)
38,P,1.571                                              (P applies a pressure to a shell)
.
.
.
282,P3,0.429                                            (P3 applies a pressure to a solid)
283,P3,0.143
**
*MODAL DAMPING, MODAL=COMPOSITE                         (Include damping)
*EL FILE, FREQUENCY=0
*EL PRINT, FREQUENCY=0                                  (Don't include element results)
*NODE FILE,NSET=TOP,MODE=1,LASTMODE=15,FREQUENCY=1
U
(Ask for displacement at node 3724 ... it was set equal to NSET=TOP in the main body of the program)
*NODE PRINT,NSET=TOP,MODE=1,LASTMODE=15,FREQUENCY=0
[[[Include BCs here]]]
*END STEP
**********************************************************************************
```

A time history of pressure file should appear in the same directory and be prepared in an eight column format that alternates between time and amplitude as follows:

```
0.10,0.00,0.20,5.00,0.30,9.71,0.40,11.39,
0.50,11.99,0.60,14.32,0.70,18.82,0.80,25.75,
0.90,34.11,1.00,19.68,1.10,21.64,1.20,25.99,
1.30,35.38,1.40,42.11,1.50,39.76,1.60,38.41,
1.70,40.23,1.80,42.11,1.90,43.08,2.00,43.56,
.
.
.
```

RANDOM RESPONSE ANALYSIS

The following commands must be included in a separate job step to implement random response analyses using power spectral density and correlation,:

```
**********************************************************************************
*PSD-DEFINITION,NAME=WIND,TYPE=FORCE,G=9.807          (Define the PSD by points)
8.0,0.0,0.0001                                       (White noise spectrum)
8.0,0.0,5.0
**********************************************************************************
*USER SUBROUTINES                                     (Define correlation)
      SUBROUTINE UCORR(PSD,CORRR,CORRI,KSTEP,LCASE,JNOD1,JDOF1,
     JNOD2,JDOF2,COOR1,COOR2)
      INCLUDE 'ABA_PARAM.INC'
      DIMENSION PSDT(1),COOR1(3),COOR2(3)
      DATA PSDT/8HPSD1    /
      OPEN(UNIT=16,FILE='/tmp/ste4087/',STATUS='NEW'
      IF(COOR1(2).EQ.0 .AND. COOR2(2).EQ.0) THEN
      DISTANCE=(((COOR1(1)-COOR2(1))**2)+((COOR1(2)-COOR2(2))**2)+
     +                ((COOR1(3)-COOR2(3))**2))**0.5
      CORRR=(-0.00003*(DISTANCE**3)+(0.0022*(DISTANCE**2))+(-0.066*(DISTANCE))+1
      ELSE
      CORRR=0.0
      WRITE(16,40) CORRR,JNOD1,JDOF1,JNOD2,JDOF2
   40 FORMAT('',F7.5,3x,F7.5,3x,F7.5,3x,F7.5,3x,F7.5)
      RETURN
      CLOSE(16)
      END
**********************************************************************************
*STEP                                                 (Perform a frequency analysis)
*FREQUENCY
[[[Include required parameters]]]
*END STEP
**********************************************************************************
*STEP
*RANDOM RESPONSE                                      (Call for random response analysis)
0.001,5,50,,1          (Low freq., high freq., increments between low and high freqs., linear plots)
*MODAL DAMPING,MODAL=COMPOSITE                        (Include damping)
*DLOAD,LOAD CASE=1
37,P,1.857
38,P,1.571                                           (P applies a pressure to a shell)
.
.
.
870,P,3.001                                          (P3 applies a pressure to a solid)
872,P,3.001
**
*CORRELATION,PSD=WIND,USER
1
*NODE PRINT,NSET=TOP,MODE=1,LASTMODE=15,FREQ=0
*NODE FILE,NSET=TOP,MODE=1,LASTMODE=15,FREQ=10       (Ask for total RMS of node 3724)
RTU
[[[Include BCs here]]]
*END STEP
**********************************************************************************
```

APPENDIX E – GRAPHIC DESIGNS

The following designs were considered for etching into smooth plastic wall panels or plastic lumber modules of the prototype soundwall: